GENETIC CHARACTERIZATION AND ENGINEERING OF DISEASE RESISTANCE TO SPOT FORM NET BLOTCH AND FUSARIUM HEAD BLIGHT IN BARLEY

A Dissertation
Submitted to the Graduate Faculty
of the
North Dakota State University
of Agriculture and Applied Science

By

Abdullah Fahad Alhashel

In Partial Fulfillment of the Requirements
for the Degree of
DOCTOR OF PHILOSOPHY

Major Department:
Plant Pathology

November 2022

Fargo, North Dakota

North Dakota State University
Graduate School

Title

GENETIC CHARACTERIZATION AND ENGINEERING OF DISEASE RESISTANCE TO SPOT FORM NET BLOTCH AND FUSARIUM HEAD BLIGHT IN BARLEY

By

Abdullah Fahad Alhashel

The Supervisory Committee certifies that this ***disquisition*** complies with North Dakota State University's regulations and meets the accepted standards for the degree of

DOCTOR OF PHILOSOPHY

SUPERVISORY COMMITTEE:

Dr. Thomas Baldwin
Chair

Dr. Shengming Yang

Dr. Timothy L. Friesen

Dr. Luis Del Rio Mendoza

Dr. Elias Elias

Approved:

11-17-2022	Dr. Jack Rasmussen
Date	Department Chair

ABSTRACT

Barley spot form net blotch (SFNB) caused by *Pyrenophora teres* f. *maculata* (*Ptm*) and Fusarium head blight (FHB) caused by *Fusarium graminearum* are devastating diseases of barley requiring advanced molecular breeding tools for disease management. I used genetic mapping and host-induced gene silencing (HIGS) to identify novel host genes and target existing pathogen genes to improve disease resistance in barley. Barley resistance to SFNB is often isolate specific and the Idaho isolate 13MI8.3 has a unique virulence profile. Two recombinant inbred mapping populations were utilized to characterize and map 13IM8.3 resistance. Quantitative trait loci (QTL) analysis revealed 10 significant resistance/susceptibility loci, including a previously unidentified QTL on chromosome 5H and the *Rpt4* locus on chromosome 7H containing a dominant susceptibility gene (*Sptm1*) for broad-spectrum susceptibility to SFNB. Fine mapping of the *Rpt4* locus in a $F_{2:3}$ population derived from the cross Tradition (S) × PI 67381 (R) anchored the *Sptm1* gene to a 400 kb region on chromosome 7H, and a putative cold-responsive protein kinase gene (*HORVU.MOREX.r3.7HG0735560*) was identified as a strong candidate and potential target for gene editing. As for the FHB management, HIGS was employed to silence the fungal gene *FgGCN5* using the barley line Golden Promise. The *FgGCN5* gene encodes a histone acetyltransferase which is essential for the *F. graminearum* growth. Despite demonstrated production of *FgGCN5* small-interfering RNAs in the transgenic barley; the disease severity, DON accumulation, and fungal biomass showed no difference from wild-type. This research allows for more in depth analysis for the use of HIGS against FHB. Use of genetic maps, QTL, molecular markers, and transgenic technology in this research will benefit barley breeders, growers, and the industry in developing resistance to these important diseases.

ACKNOWLEDGEMENTS

I would like to begin by expressing my sincere appreciation to my major advisor Dr. Shengming Yang for his consistent support, guidance, and encouragement throughout my graduate studies. Your immense knowledge and patience made my research and dissertation preparation possible in every respect. Also, I wish to express my gratitude to the remaining committee members, Dr. Thomas Baldwin and Dr. Timothy L. Friesen for their assistance with materials, facilities, and information related to the study, as well as Dr. Luis Del Rio Mendoza and Dr. Elias Elias for their time and suggestions that helped to improve my dissertation. I would like to acknowledge my former advisor Dr. Robert Brueggeman for his assistance and direction. Additionally, I thank my lab members Xiaohong Jiang, Megan Overlander, Madison Skadberg, Dr. Ruiying Liu, Mitchell Ritzinger, Manila Karki, Abby D'Eustachio that have had significant influence on my scientific development and projects. Moreover, I am grateful to Dr. Roshan Poudel for his constant support and expertise in data analysis. I would like to acknowledge all research collaborators Dr. Craig Carlson, Dr. Jason Fiedler, and Dr. Raja Nandety for their assistance with data analysis. Dr. Sandesh Dangi and Abbeah Navasca who shared their skills in qPCR analysis. Wail Alsolami, Rayan Skiba, Patrick Gross, and Tom Gross for their help in the green house and the lab work. Also, I thank all members of the Plant Pathology Department especially Dr. Jack Rasmussen, who have been so supportive and welcoming. Furthermore, I would like to thank the government of Saudi Arabia and King Saud University for sponsoring my education in the US. Finally, I owe my deepest gratitude to my parents, brother, and sister, who have supported, encouraged, and cared for me throughout my life and as a student in the US. I also want to thank my dearest wife, Wafa, who has always been there for me especially at the most challenging times and has loved and supported me unconditionally.

DEDICATION

This dissertation is dedicated to my beloved family. Dad Fahad Abdullah Alhashel, Mom Monirah Mohammed Alturki, Sister Mashael Fahad Alhashel, Brother Abdulaziz Fahad Alhashel, Wife Wafa Ibrahim Aljasser and Son Fahad Abdullah Alhashel. Thank you so much for your love, trust, and guidance.

TABLE OF CONTENTS

LIST OF TABLES

LIST OF FIGURES

LIST OF APPENDIX TABLES

LIST OF APPENDIX FIGURES

CHAPTER 1: LITERATURE REVIEW

Barley

Global and Local Barley Production

Barley (*Hordeum vulgare* L.) is one of the earliest and the most important cultivated cereal crops globally. In 2022, the United States produced 3.80 million tons of barley, ranking 9th behind the European Union, Russia, Australia, Canada, Turkey, the United Kingdom, Ukraine, and Argentina (USDA-FAS, 2022). After corn, wheat, and rice, barley is the fourth most-produced cereal crop in the United States. North Dakota (ND), along with Idaho (ID) and Montana (MT), is a leading producer and ranks second in barley production. North Dakota produced 48.18 million bushels of barley in 2022, while the total US yield was 174.33 million bushels (NASS, 2022). In the US, barley is primarily produced for malting, with minor uses as animal fodder and human consumption (Poehlman, 1994). Recently, the use of barley in the production of pet food has emerged as a new market for North Dakota and Minnesota barley growers, accounting for up to 30% of total barley production (Bailey, 2022). In other countries, approximately 75% of barley is used for animal feed, 20% for malting, and 5% for food consumption (IBGSC, 2012). Barley is an essential source of food in areas such as the Middle East, North Africa, Asia, and North and Eastern Europe. It contains 65 to 68% starch, 10 to 17% protein, 4 to 6% β-glucan, 2 to 3% free lipids, 1.5 to 2.5% minerals, and 11 to 34% total fibers (Fastnaught, 2001; Quinde et al., 2004). There are two types of barley produced: two-rowed and six-rowed barley. The florets of the six-row type are all fertile, whereas only the central florets of the two-row type are fertile. Moreover, six-row varieties were more widely planted and preferred by farmers, particularly in the malting industry during the 20th century in the US. However, modern malting industries prefer two-row varieties due to their advantageous malting

characteristics, such as a more robust malt flavor in beers and an increase in malting extract production (Knutson, 2020; Mathre).

History of Barley Production in the USA

In 1494, the second voyage of Christopher Columbus brought barley to North America (Newman and Newman, 2006). Though, production began in 1602 in New England due to increased European settlement using English two-row landraces that were poorly adapted to the region (Schwarz et al., 2011). In the 1700s, production increased and expanded westward into New York, following the Scottish six-row landraces that were more suitable for the region. Until the late 19th century, New York remained a leading producer of barley (Schwarz et al., 2011). In the late eighteenth century, the Spanish Missions contributed to the development of barley production in California, which was a major producer of barley until the 1970s, with production increasing during the mid-19th century gold rush. The coastal barley varieties of California are descended from North African six-row varieties that were brought from Spain (Schwarz et al., 2011). Barley would continue its westward migration from the East to the Midwest of the US with the Manchurian Oderbrucker line, and then to the western seaboard, including the Pacific Northwest (Schwarz et al., 2011; Slafer et al., 2002). North Dakota became a major producer of barley in the early 1900s, followed by Idaho and Montana in the mid-1950s (Schwarz et al., 2011).

Evolution of Barley

Within the Pooideae, the monophyletic Triticeae tribe contains 400-500 species, including wheat, barley, and rye (Middleton et al., 2014). Barley separated from wheat and rye 9.2 million years ago (Middleton et al., 2014; Brassac and Blattner, 2015); as a result, the genomes of these three species are highly syntenic (Moore et al., 1995). There are 33

hybridizable species within the *Hordeum* genus, which comprises diploid (2n = 2x = 14), tetraploid (2n = 4x = 28), and hexaploid (2n = 6x = 42) (Brassac and Blattner, 2015). The wild subspecies progenitor (*H. vulgare* ssp. *spontaneum*, *Hsp*) is the ancestor of domesticated barley (*H. vulgare* ssp. *vulgare*) (Pourkheirandish and Komatsuda, 2007). A second barley species (*H. bulbosum*) is the most closely related *Hordeum* species to domesticated barley diverged 4 Mya (Brassac and Blattner, 2015). There are four types of *Hordeum* genome: H, Xu, Xa and I. Both *H. vulgare* and *H. bulbosum* share a basic H genome. The wild barley and *H. bulbosum* (also known as bulbous barley), have been used as genetic sources in breeding programs to establish disease resistance and other desirable traits in cultivated barley (Jouve et al., 2018).

Domestication of Barley

The earliest evidence of barley grain collection dates back to 23 thousand years ago (KYA) on the shores of the Sea of Galilee (Pourkheirandish et al., 2015). Archaeological evidences of beer fermentation occurred 13 KYA indicate the beginning of cereal domestication (Liu et al., 2018). Approximately 10-12 KYA, the domestication of barley from its wild ancestor began at the emergence of Neolithic agriculture, (IBGSC, 2012; Paterson et al., 2003; Wang et al., 2019). Seed size, ear rachis stiffness, and seed release are the three primary physical traits that distinguish wild cereals from domesticated cereals (Salamini et al., 2002). Barley domestication resulted in wider leaves, shorter stems, shorter smooth awns, reduced seed dormancy, semi-brittle rachis if harvested before full maturity (Pourkheirandish and Komatsuda, 2007; Salamini et al., 2002), and white/yellow grain (Pourkheirandish and Komatsuda, 2007; Salamini et al., 2002; Jia et al., 2017). In addition, the winter and spring growth habits, two- and six-row spikelets, hulled and hulless variants, and semi-dwarf types are four major post-

domestication characteristics, but they are not fixed in all barley classes of current barley cultivars (Pourkheirandish and Komatsuda, 2007; Xu et al., 2017).

The brittle rachis and rough awns permit the ear to shatter and aid in seed dispersal (Pourkheirandish and Komatsuda, 2007). Two dominant complementary genes (*Btr1* and *Btr2*) that are closely linked (100kb apart) on the short arm of chromosome 3H (3HS) govern the Brittle rachis trait of wild barley (Civáň and Brown, 2017). The non-brittle rachis was caused by a loss-of-function mutation resulting from a 1-bp deletion or single point mutation in *Btr1* or an 11bp deletion in *Btr2* (Civáň and Brown, 2017). The development of naked/hulless barley, which makes it easier to remove the husk, occurred after the selection of non-brittle rachis. The prevalence of naked barley in Asian may indicate the origin of the trait (Pourkheirandish and Komatsuda, 2007). One recessive gene, *nud*, located within a 17 kb deletion on the long arm of chromosome 7H (7HL), is responsible for the characteristic (Sang, 2009). This gene encodes an ethylene response factor (ERF) controlling the caryopsis covered/naked phenotype. Homolog of this gene identified in Arabidopsis encodes the WIN1/SHN1 transcription factor, which is presumed to regulate a lipid biosynthesis pathway. Thus, staining with a lipophilic dye (Sudan black B) revealed a lipid layer on the pericarp epidermis only in barley with covered caryopsis (Taketa et al., 2008). Hulless barley is often used for human consumption only, while hulled or covered types are used as animal feed and malting kinds (Sang, 2009).

The temporary inability of a viable seed to germinate under optimal environmental conditions is controlled by seed dormancy. For wild types to endure challenging circumstances or to propagate across a larger area, seed dormancy was necessary (Pourkheirandish and Komatsuda, 2007). A delicate balance between non-dormant seed and resistance to pre-harvest sprouting is desired in modern agriculture, notably for the malting barley (Pourkheirandish and

Komatsuda, 2007). Seed dormancy is a quantitative feature that is heavily influenced by the environment. On chromosome 5H, two seed dormancy loci, *SD1* and *SD2*, have been found thus far (Li et al., 2004).

The presence of the two-rowed phenotype in wild barley suggests that the two-rowed spike is the ancestral form, which was transformed into a six-rowed spike during domestication (Pourkheirandish and Komatsuda, 2007). Due to the reduced tillering (basal branching) and rachis node number, cultivated six-rowed barleys do not produce three times as much grain as their potential (Kirby and Riggs, 1978; Lundqvist et al., 1997). In addition, lateral rows produce smaller and lighter grains than their central counterparts, resulting in less uniform grain size or weight in six-rowed spikes (Gupta et al., 2010; Lang et al., 2013). Two-row and six-row types of barley are determined by the *Vrs1.b* and *vrs1.a* alleles of the *Vrs1* gene on chromosome 2HL, respectively (Komatsuda et al., 2007). In addition, allelic variation at this locus *(vrs1.a*, *Vrs1.b*, *vrs1.c*, *Vrs1.p*, *Vrs1.t*) has been demonstrated to partially affect awn length (Komatsuda et al., 2007; Liller et al., 2017). Additional *Vrs1* alleles are designated according to the mutations present, such as *vrs1.a1*, *vrs1.a2*, *vrs1.a3*, and *vrs1.a4*. Four additional row-type determining genes have been found, *Vrs2*, *Vrs3*, *Vrs4*, and *Vrs5* on 5HL, 1HL, 3HS, and 4HS, respectively (Pourkheirandish and Komatsuda, 2007).

The molecular identities of the five major row-type genes were revealed. The highly conserved *Vrs5* (*Int-c*) gene was a cloned as an inhibitor of lateral branching which is an architecture comparable to a six-row spike (Ramsay et al., 2011; de Souza Moraes et al., 2021). *VRS1* encodes a homeodomain-leucine zipper class I (HD-ZIP1) protein orthologous to maize *grassy tillers1* (*gt1*) which inhibits tiller bud outgrowth at the downstream of *teosinte branched1* (*Tb1*), another major domestication locus controlling tillering and lateral

branching (Komatsuda et al., 2007; Whipple et al., 2011). *VRS2* is a homolog of the *Arabidopsis SHORT INTERNODES* gene, the loss of which causes hormonal imbalances between auxin and cytokinin in the spike (Youssef et al., 2017). *VRS3* encodes a possible Jumonji C-type (JMJC) H3K9me2/3 histone demethylase (Bull et al., 2017; van Esse et al., 2017), which is orthologous to the rice gene *OsJMJ706* controlling rice spikelet morphology (Sun and Zhou, 2008). According to comparative transcriptomics, *VRS3* promotes the expression of other *VRS* genes (Bull et al., 2017; van Esse et al., 2017). *VRS4* encodes a transcription factor that prevents ectopic branching in maize ears and tassels and is orthologous to the maize *ramosa2* gene (Koppolu et al., 2013). *VRS5* encodes a class II TCP transcription factor, and its orthologs suppress tiller bud outgrowth to promote apical dominance in maize, rice, wheat, and *Arabidopsis* (Ramsay et al., 2011; Dixon et al., 2018).

Vernalization is the process by which a plant transitions from a vegetative to a reproductive state by requiring a period of low temperature. The vernalization pathway genes prevent flower development during the winter, protecting floral organs from cold (Pourkheirandish and Komatsuda, 2007). Apart from a few strains that are considered hybrids with spring cultivars, almost all wild barleys grow in the winter. Three genes are responsible for vernalization: *sgh1*, *Sgh2*, and *Sgh3* on 4H, 5H, and 7H, respectively (Pourkheirandish and Komatsuda, 2007). The dominant mutation from *sgh2* to *Sgh2* is considered to have occurred first, with alleles *Sgh2I* and *Sgh2II* demonstrating a gradation of vernalization requirements (Pourkheirandish and Komatsuda, 2007).

Finally, compared to landraces and previous non-semi-dwarf cultivars, the average yield of semi-dwarf barley types carrying the *uzu1* gene is increased by 4.7-fold (Xu et al., 2017). There are more than 30 varieties of dwarf barley, but the three most important semi-dwarf

mutations in cultivars cultivated in Asia, early Europe, and modern Europe/America/Australia are *semi-brachytic 1* (*uzu1*; 3HL), *breviaristatum-e* (*ari-e*; 5HL), and *semi-dwarf 1* (*sdw1/denso*; 3HL), respectively (Xu et al., 2017). The *sdw1* locus includes the alleles *sdw1.a*, *sdw1.c* (*denso*), *sdw1.d*, and *sdw1.e* (Xu et al., 2017).

Genetic Tools and Resources in Barley

The restriction fragment length polymorphisms (RFLPs), isozyme, and morphological trait loci were used as markers in the first genetic map of barley. The first genetic map of barley covered an area of 870 cM and contained 114 RFLP markers using the Igri x Franka (IF) doubled haploid (DH) population. This population was chosen because it had different *Mla* gene alleles conferring resistance to powdery mildew (Graner et al., 1991).

Subsequent maps employed RFLPs, random amplified polymorphic DNA markers (RAPDs), isozymes, and morphological trait loci or amplified fragment length polymorphism (AFLPs) with the Steptoe x Morex (SM) DH population (Kleinhofs et al., 1993) and the L94 x Vada recombinant inbred lines (RILs) population (Qi et al., 1998). Parental lines were selected based on their distinct agronomic characteristics and leaf rust resistance and spanned 1250 and 1062 cM, respectively (Kleinhofs et al., 1993; Qi et al., 1998). A total of 253 simple sequence repeats (SSR) markers were mapped with the Lina x Canada Park DH population (Ramsay et al., 2000). Utilization of DH mapping populations continued to be prevalent in QTL mapping and development of varieties in winter barley breeding programs (Behn et al., 2005; Hearnden et al., 2007; Powell et al., 1997; Sato et al., 2011; Szűcs et al., 2009; Thomas et al., 1998; Thomas et al., 1995). Using six DH populations and one F_2 population, the first barley consensus map was generated (Langridge et al., 1995). As part of the North American Barley Genome Mapping Project which combined various mapping populations and molecular markers, four DH

populations were used to create maps anchoring SSR markers to already-existing RFLP maps (Close et al., 2009).

Following the development of two barley oligonucleotide pool assays (BOPAs) containing 1,536 SNPs each, the first genetic barley maps based on SNP genotyping were generated. Four DH mapping populations of SM, Morex x Barke, Oregon Wolfe Barley, and Haruna Nijo x OHU602 were utilized to generate a consensus map of barley using these two assays, which resulted in a genetic map consisting of 2,943 SNPs from the two BOPAs in 975 unique bins spanning 1,010 cM (Close et al., 2009). In addition, increased population genotyping has improved the consensus map and contributed to the creation of the 9K iselect SNP array and later the 50K SNP array (Bayer et al., 2017; Comadran et al., 2012). Also, custom SNP targeting has been created, enabling the use of novel SNPs or fewer SNPs using the Illumina BeadXpress platform (Moragues et al., 2010), restriction site associated digest-genotyping by sequencing (Elshire et al., 2011), polymerase chain reaction-genotyping by sequencing (Richards et al., 2016; Sharma Poudel et al., 2018), or genotyping by multiplex sequencing (Ruff et al., 2020).

The first draft genome of barley was derived from the six-row spring malting cultivar Morex in North America by integrating the BAC physical map with the genetic map and whole genome shotgun sequencing. Approximately 84% of the barley genome contains mobile elements or repeated structures. The barley genome is approximately 5.1 GB harboring ~ 26,159 high-confidence genes (IBGSC, 2012). In the second version of the Morex genome assembly, two paired-end and three mate-pair libraries, linked reads from the 10X Genomics (ChromiumTM) library, and chromosome conformation capture from Dovetail (DovetailTM Hi-C and ChicagoTM) were employed (Monat et al., 2019). New sequencing technology demonstrated the ability of modern sequencing platforms in resolving difficult-to-assemble

regions by sequencing the Morex reference genome at 20X coverage using a PacBio Sequel II for version 3 (Mascher et al., 2021). Moreover, the TRITEX pipeline of Morex version 2 was used to publish the barley pangenome, which included twenty unique barley genotypes. The barley pan-genome indicated approximately 37,000 gene annotated per line (Jayakodi et al., 2020).

Host-Parasite Interactions

Plant pathogens are divided into three distinct types according to their feeding styles on their suitable hosts, biotroph, hemi-biotroph, and necrotroph. Biotrophic pathogens obtain nutrients from living host tissues, whereas necrotrophic pathogens obtain nutrients from decomposing or dying host cells. Certain pathogens can be classified categorically as biotrophs or necrotrophs. Many others, on the other hand, exhibit both biotrophic and necrotrophic behavior, depending on their environment or growth stage. These pathogens are referred to as hemi-biotrophs. Numerous fungi that are commonly classified as necrotrophs are actually hemi-biotrophs, as they undergo a biotrophic stage early in the infection process and shortly after switch to a necrotrophic phase (Glazebrook, 2005).

Unlike mammals, plants do not have mobile defender cells or a somatic adaptive immune system. Instead, they rely on the innate immunity in each cell, as well as the systemic signals initiated from the infected cells. Upon plant pathogen invasion, two branches of immune responses are elicited in hosts (Jones and Dangl, 2006). First, the immune system is activated when recognition of conserved and exposed pathogen molecules, referred to as pathogen-associated molecular patterns (PAMPs) or microbe-associated molecular patterns (MAMPs), by host membrane-localized pattern recognition receptors (PRRs) results in the initiation of PAMP-triggered immunity (PTI) to stop pathogen colonization (Newman et al., 2013; Nürnberger and

Brunner, 2002). Bacterial flagellin (*Flg*), elongation factor (*EF-TU*), and fungal chitin are all well-known PAMPs or MAMPs from pathogens. Similarly, extracellular plasma membrane-localized receptor-like kinases (RLKs) or receptor-like proteins (RLPs) are examples of general pattern recognition receptors (PRRs) in plants that recognize PAMPs/MAMPs. The recognition of bacterial flagellin (*flg22*) by the flagellin receptor (*FLS2*), a leucine rich repeat (LRR)-RLK, initiates an early PTI response in *Arabidopsis* (Gomez-Gomez and Boller, 2002). Adaptive pathogens may be able to overcome the PTI but may not when the second line of immune response is activated (Jones and Dangl, 2006).

Successful pathogens suppress host PTI responses by secreting effectors referred to as avirulence (Avr) proteins via a specialized structure that allow pathogens to promote infection and complete their life cycle (Thomma et al., 2011). However, hosts responded by evolving cytoplasmic *R* genes encoding nucleotide binding (NB) and leucine rich repeat (LRR) proteins (NB-LRR) that detect the presence of these effectors and generate an effector triggered immunity (ETI) as the second line of immune response in the form of hypersensitive response (HR) which is localized, and dramatic programmed cell death (PCD) that restricts pathogen growth.

To overcome ETI response, pathogens evolve or diversify their effectors to establish effector triggered susceptibility (ETS). These shifts in responses illustrate the continuous arm race between plants and pathogens interactions, which was mechanically explained by the zig-zag model (Jones and Dangl, 2006; Petre and Kamoun, 2014; Selin et al., 2016).

The host interaction with biotrophic pathogens such as *Puccinia graminis*, which causes stem rust disease on barley, follows a gene-for-gene model when a pathogen-produced effector is recognized by a dominant host resistance (R) gene, resulting in an incompatible (resistant) interaction. The absence of pathogen Avr protein (or effector) results in a compatible interaction

or susceptibility. On the other hand, necrotrophic pathogens, such as *Pyrenophora teres*, which causes net blotch disease on barley, follows an inverse gene-for-gene model by which recognition of effectors by host resistance genes lead to susceptibility. Friesen et al., (2007) first proposed the inverse gene-for-gene model, in which a single necrotrophic effector (NE) (synonym = host-selective toxin) targets a corresponding susceptibility gene in the host. Thus, necrotrophic pathogens can hijack the resistance signaling pathways to biothrophs by releasing NEs to induce necrotrophic effector-triggered susceptibility (NETS) (Liu et al., 2015). NETS triggers the production of reactive oxygen species (ROS) and hypersensitive response (HR), which results in uncontrolled PCD and the release of nutrients for the necrotrophs (Liu et al., 2015).

Net Blotch Diseases

Pyrenophora species are ascomycetes within the *Dothideomycetes* class (Ellwood et al., 2012). One of the critical *Pyrenophora* pathogens is *Pyrenophora teres,* causing net blotch diseases in barley. Two forms of *P. teres* are present: *P. teres* f. *teres* (*Ptt*) and *P. teres* f. *maculata* (*Ptm*). They are indistinguishable morphologically but can be differentiated based on the symptoms observed on susceptible barley plants (McLean et al., 2009; Smedegård-Petersen, 1971). *Ptt* causes the formation of transverse and longitudinal net-like lesions surrounded by chlorotic regions, hence the disease is named net form net blotch (NFNB) (Mathre, 1997). The *Ptm* pathogen produces elliptical necrotic lesions surrounded by chlorosis, which leads to the spot form net blotch (SFNB) disease (McLean et al., 2009; Smedegård-Petersen, 1971). Net blotch pathogens favor high humidity, precipitation, and cool conditions (Mathre, 1997). Moreover, both *Ptt* and *Ptm* can infect leaves, stems, and kernels, leading to reduced kernel size and compromised malting quality (Liu et al., 2011). Both forms can cause up to 10 to 40% yield

losses in barley production when environmental conditions are favorable and a susceptible variety is present (Mathre, 1997). It was estimated that every 1% increase in SFNB severity results in a 0.77% yield loss in barley production in ND (Duellman, 2015). Since SFNB was first reported in North Dakota in 2006, it has become a significant issue for the state's barley production (Liu and Friesen, 2010).

Net Blotch Disease Cycle and Infection Process

The life cycles of *Ptt* and *Ptm* pathogens are polycyclic and almost identical. They start with primary inoculum which comes from overwinter-structure pseudothecia (sexual fruiting bodies) as ascospores on infected barley residues. Ascospores are produced within asci, and each ascus contains 8 ascospores that are disseminated by the wind. Conidia and mycelia from infected seeds or plant stubbles can also act as a primary source of inoculum (Mathre, 1997). After primary infections occur, conidia are produced and dispersed by rain splash as the secondary inoculum to cause additional infections throughout the season (Mathre, 1997).

The infection process of the disease starts with spores landing, adhesion, germination, penetration, and infection. After *Ptm* spores land on the leaf surface, they germinate and form a germ tube within a few hours if moisture and temperature conditions are favorable (Kenneth, 1962; Shipton et al., 1973; Van den Berg and Rossnagel, 1990). The germ tubes are germinated from almost every cell within a spore (Van Caeseele and Grumbles, 1979). Each tube forms an appressorium, a swollen club-shaped structure that puts pressure on the leaf surface and aids penetration. Multiple factors, such as enzymatic hydrolysis of the cuticle and appressoria induced leaf pressure, contribute to direct penetration of the leaf surface (Keon and Hargreaves, 1983; Van Caeseele and Grumbles, 1979) Following penetration, the hypha grows into a large intracellular vesicle (primary vesicle) which forms secondary vesicles within the epidermal cells.

Eventually, the intracellular hypha expands within the mesophyll cells and transforms into intercellular hypha. Unlike *Ptt, Ptm* grows near the epidermal cells and forms haustoria-like intracellular vesicles to absorb nutrients as a biotroph, followed by a transition to the necrotrophic phase. *Ptt* growth is mostly intercellular and able to infect and feed on other cells further from the penetration site. Compared to *Ptt*, *Ptm* has slower germination and growth. (Keon and Hargreaves, 1983; Lightfoot and Able, 2010).

Net Blotch Diseases Management

Management of net blotch diseases is essential to reduce disease pressure and avoid economic losses. Chemical treatments using fungicide application on seeds or upper leaves could reduce the primary inoculum during seed filling. Cultural practices such as tillage, crop rotation, and lower crop density may help to control the disease at lower levels. However, most varieties cultivated in the US, especially in ND, are susceptible to the disease, which reduces the efficacy of cultural practices. Therefore, the deployment of resistant varieties is the most effective and environmentally friendly method for disease management (Liu et al., 2011; Mclean et al., 2009). Nevertheless, the virulence profiles of both pathogen populations are very variable, and this may cause challenges for resistance breeding against these diseases (Liu et al., 2011). Compared to NFNB, resources and knowledge of deploying resistance against SNFB are limited for the upper Midwestern barley breeding programs.

Screening for SFNB Resistance

In comparison to NFNB, fewer studies have been conducted to explore SFNB resistance or susceptibility. In Williams et al., (1999), 96 barley lines were screened with five different isolates of *Ptm*, and only four lines showed broad-spectrum resistance to SFNB (Galleon (Australia), WI2976 (Australia), OK82850 (USA), and Dairokkaku (Japan). Also, McLean et al.,

(2012) tested 95 barley lines at the seedling stage against two diverse *Ptm* isolates, and only two lines, Esperance Orge 289 and TR3189, were resistant to all isolates. In the further screening, 15 lines expressed resistant responses at the adult stage when challenged with 19 diverse isolates (McLean et al., 2012). Neupane et al., (2015) evaluated a core collection of 2,062 barley lines with 4 *Ptm* isolates collected from different regions including the United States (FGO), Australia (SG1), New Zealand (NZKF2), and Denmark (DEN 2.6), and only 15 lines were resistant to all the isolates used at the seedling stage. Regional differences in virulence of the isolates were also identified, with the FGO isolate being more virulent than the others. Furthermore, Clare et al., (2022) evaluated 177 *Ptm* isolates collected from ND, MT, and ID. Results showed that the virulence profiles of ID isolates were distinct from the others when tested on 30 differential barley lines. In summary, the *Ptm*-barley pathosystem is complex due to the variation in both *Ptm* virulence profiles and host responses.

Genetic Resistance to SFNB

It was initially thought that the genetics of barley reactions to *Ptm* was simple in comparison to *Ptt*, given only three major genes designated *Rpt4*, *Rpt6*, and *Rpt8* (all reviewed in Clare et al., 2020). However, the persistence of *Ptm* as a significant agricultural problem suggests that *Ptm* resistance/susceptibility is more quantitative than it was first perceived. Since then, many significant and minor quantitative trait loci (QTL) correlated with resistance/susceptibility to *Ptm* have been identified on all seven barley chromosomes (Clare et al., 2020). In addition, some of the *Ptt*-resistant QTL were identified to be effective against *Ptm* as well, even though further investigations are needed to determine if the associated genes are the same (Clare et al., 2020). Different genetic mapping studies have identified these QTL using

biparental mapping populations derived from RILs, DH populations, and genome-wide association studies (GWAS) (Clare et al., 2020).

The first major resistance QTL, named *Rpt4*, was identified on chromosome 7H by using a DH population derived from Galleon x Haruna Nijo population in Australia (Williams et al., 1999). The *Rpt4* resistance was used in breeding lines for adult plant resistance (APR), but these lines had lower levels of resistance compared to seedlings stage, suggesting that additional genes were required (Williams et al., 2003). This locus was confirmed by other independent studies via GWAS (Tamang et al., 2015; Wang et al., 2015) and using different resistant lines, such as CI9214, Keel, Tilga, and Chebec (Williams et al., 2003), PI67381, and PI84314 (Tamang et al., 2019), TR251 (Grewal et al., 2008), and Baudin (Cakir et al., 2011), CI9214 and Tifang (Alhashel et al., 2021). *Rpt6* was identified as the second major locus on chromosome 5H, contributing 65-84% of the disease variation in the line CI9819 against isolates P1332 and P1333 collected from Finland (Manninen et al., 2006; Tamang et al., 2015). Friesen et al., (2006) identified the third locus, *Rpt8*, against New Zealand *Ptm* isolate NZKF2 on chromosome 4H. *Rpt8* explained 64% of the phenotypic variation contributed by barley line Q21861 (Franckowiak and Platz, 2013), and subsequent GWAS confirmed this locus (Daba et al., 2019; Tamang et al., 2015). Some QTL conferring NFNB resistance/susceptibility have been found to be involved in reactions to SFNB as well, such as *Rpt1* (Burlakoti et al., 2017; Tamang et al., 2015)*, Rpt5/Spt1* (Daba et al., 2019; Grewal et al., 2008; Tamang et al., 2015; Wang et al., 2015) and *Rpt7* (Grewal et al., 2008; Tamang et al., 2015). Tamang et al., (2015) discovered *Rpt1* on 3H chromosome as a possible locus against the isolate *Ptm* NZKF2 and the North Dakota isolate FGOB10*Ptm*-1, and Burlakoti et al., (2017) identified that *Rpt1* was also effective against the Montana isolate SNFB-MT09. The *Rpt5/Spt1* locus on 6H chromosome was discovered in the

Ptm-barley interaction via two bi-parental mapping studies (Grewal et al., 2008 and Tamang et al., 2019) and GWAS (Daba et al., 2019; Tamang et al., 2019; Wang et al., 2015). Tamang et al., (2019) identified *Rpt5/Spt1* against four isolates: isolate FGOB10*Ptm*-1, Montana isolate PA14, Danish isolate DEN2.6, and NZKF2, confirming prior GWAS results with the same isolates except the Montana isolate (Tamang et al., 2015). Grewal et al., (2008) found *Rpt7* against the Canadian isolate WRS857, and Tamang et al., (2015) identified *Rpt7* against the strains DEN2.6, NZKF2, and Australian isolate SG1. In addition, four GWAS studies on *Ptm* resistance in barley have identified additional QTL that are not mapped to the previously described major loci. Wang et al., (2015) used elite breeding lines from the Northern region of Australia and identified a few resistance QTL. Of those, 2, 5, and 22 QTL are linked to the resistance at seedling stage, adult stage, and both stages, respectively. Tamang et al., (2015) tested disease reactions of 1480 worldwide barley lines to globally collected *Ptm* isolates. A total of 27 QTL were identified, and 21 of those were novel. Using *Ptm* MT09 isolate and 76 advanced barley lines, 10 QTL were identified on chromosomes 2H, 3H, 5H, 6H, and 7H (Burlakoti et al., 2017). Recently, Daba et al., (2019) conducted GWAS study using Ethiopian, ICARDA, and NDSU-barley panels and found one unique locus against *Ptm* ND111 isolate. Additional research is required to determine if these loci could effectively improve resistance to *Ptm* in barley breeding programs.

Net Blotch Effectors

Effectors are used by plant pathogens to inhibit the host's immune system and cause disease. Effectors are described as small-secreted proteins or metabolites that are essential for pathogenicity and virulence (Friesen et al., 2008). These effectors function in the apoplast or cytoplasm of the plant. Candidate effectors are commonly characterized by being small in size (less than 300 amino acids), having a predicted N-terminal signal peptide (SP) sequence, and

being expressed during host colonization (lo Presti et al., 2015). To facilitate subcellular localization to the mitochondria, chloroplast, or nucleus, many effectors contain an N-terminal post-SP translocation domain (Petre and Kamoun, 2014). Effectors also have a high cysteine content that aids in the tertiary structural stability via disulfide bonds (lo Presti et al., 2015). Effectors are typically secreted into the plant either through the general secretory pathway of hyphae or through specific feeding and infection structures such as appressoria or haustoria (Petre and Kamoun, 2014; Toruño et al., 2016). Effectors are essential for several tasks, including host entrance, defense suppression, and nutrition uptake (Toruño et al., 2016). Necrotrophic pathogens can produce these effectors, and they interact with corresponding host sensitivity genes, which result in a susceptible response following an inverse-gene-for-gene model (Friesen et al., 2008). As a result, PCD, oxidative burst, accumulation of ROS, and DNA laddering are triggered in sensitive hosts, allowing necrotrophs to obtain their nutrients from dead cells and continue their life cycle. (Liu et al., 2015). Biotrophic and necrotrophic interactions show distinct effector expression patterns. Biotrophic effectors suppress disease resistance throughout all the infection stages, unlike necrotrophic effectors which typically initiate fast and uncontrolled PCD at the beginning of the infection (Toruño et al., 2016).

Both *Ptt* and *Ptm* produce necrotic lesions encompassed by chlorosis on the susceptible leaves of barley. These chlorotic regions are typically free of filamentous growth of the pathogen, but they contain diffusible toxins or effectors (Smedegard-Peterson, 1977 ; Liu et al., 2011). Smedegård-Petersen (1977) isolated two effectors/toxins A and B from a culture filtrate of both *Ptt* and *Ptm* isolates, and infiltration assay showed that both toxins caused a sensitive response on susceptible barley. It was indicated that toxin A had a greater effect than toxin B. However, the symptoms induced by these two toxins were not consistent with those caused by

the pathogen. Thus, it was concluded that additional factors were involved during infection, and that toxins A and B contributed to virulence rather than determine pathogenicity. Then, Bach et al., (1979) used the same isolates in Smedegård-Petersen (1977) and identified an additional toxin named toxin C.

Toxin A was characterized as *N*-(2-amino-2-carboxyethyl) aspartic acid, toxin B as anhydroaspergillomarasmine A and toxin C as aspergillomarasmine A (Weiergang et al., 2002). Toxin B was found to be the least active toxin, producing light symptoms, whereas toxin A produced dark yellowish chlorotic symptoms with minimal necrosis. Toxin C was the most active and caused distinct necrotic symptoms with light-yellow chlorosis (Weiergang et al., 2002). Additionally, the structural characteristics and biosynthetic pathways of these toxins were investigated. Under low pH level in culture, toxin A was converted directly to toxin C which is a precursor of toxin C (Friis et al., 1991).

Furthermore, culture filtrates contained a mixture of proteinaceous metabolites and low molecular weight compounds (LMWCs) present in *Ptt* and *Ptm* were reported to induce necrosis and chlorosis on sensitive barley (cv. Sloop) similar to net blotch symptoms, respectively. However, they were less virulent on resistant cultivars (CI9214) and did not cause symptoms on non-host plants, such as wheat, triticale, rye, or non-relative faba bean (Sarpeleh et al., 2007). These LMWCs were thermally stable while the proteinaceous toxins were light- and temperature-sensitive, similar to SnTox1 and PtrToxA produced by *Parastagonospora nodorum* and *Pyrenophora tritici-repentis*, respectively (Manning et al., 2009, Liu et al., 2012). Toxins or effectors that are identified in both forms, could be used to rapidly determine the susceptibility or resistance of barley lines early in the breeding process (Liu et al., 2011).

Given the high number of loci identified within the *Ptm*-barley pathosystem, it was indicated taht a complex interaction involving a variety of diverse effectors produced by *Ptm*. Only two studies for mapping of the *Ptm* virulence were reported (Carlsen et al., 2017 and Skiba et al., 2022). A bi-parental population comprising 105 progenies derived from the cross FGOB10Ptm-1 (US isolate) x SG1 (Australian isolate) were evaluated on barley differential lines Skiff, TR326, 81-82/033 and PI392501. Genotyping was conducted using a restriction-site associated – genotype by sequencing (RAD-GBS) approach. Genetics mapping only identified six loci from 5 linkages groups out of 12 associated with virulence, with one QTL contributed by SG1 and five by FGOB10Ptm-1. vQTL4, located on linkage group 1.1 (chromosome 2) accounted for 30-37% of the phenotypic variation by SG1 on barley lines 81-82/033 and PI392501. Virulence conferred by vQTL5 on linkage group 5.1 (chromosome 3) of FGOB10Ptm-1 accounted for 26 % to 34 % disease variation (Carlsen et al., 2017).

Another bi-parental population was generated by crossing the virulent isolate P-A14 with the avirulent isolate CAWB05-Pt-4, and two major virulent loci were localized on chromosomes Chr1 and Chr2 that explained 25% and 51% of disease phenotype variation, respectively. In addition, single-virulence progenies were evaluated with the RIL population derived from Hockett (S) x PI 67381 (R) to identify the susceptibility targets on the host. The results demonstrated that virulence loci on Chr2 and Chr1 targeted the *Rpt4* locus on chromosome 7H and a locus on chromosome 2H short arm, respectively. Segregation ratios of F_2 plants inoculated with single-virulence genotypes fit 3:1 (S:R), suggesting that *Rpt4* and the locus on 2H both confer susceptibility to *Ptm* (Skiba et al., 2022).

Fusarium Head Blight (FHB) and Host Resistance

Fusarium graminearum Schwabe is the most common causal pathogen of Fusarium head blight (FHB, also known as scab) globally. This disease affects barley production in quality and quantity (Huang et al., 2018). Between 1993 and 2001, an estimated $485 million in economic losses were resulted in three states, North Dakota, Minnesota, and South Dakota (Nganje et al., 2004). Prolonged high humidity and warm temperatures at flowering time, coupled with a lack of effective resistant varieties, contribute to FHB epidemics. Worse than the yield loss, the FHB pathogen produces mycotoxins, known as DON, which can contaminate harvested grain and pose health risks to humans and animals. The mycotoxin is chemically and thermally stable and remain in grains from harvesting throughout end use (Miedaner et al., 2017). Advisory limits on consumption of DON and its derivatives established by the FDA have resulted in huge price discounts and increasing management costs, motivating farmers to shift to less risky crops (Dahl and Wilson 2018).

FHB disease symptoms on infected barley include shrunken kernels and spikelet discoloration ranging from tan to dark brown. When prolonged wet periods occur, pinkish to salmon-colored masses of fungal mycelium and conidia can be observed on the infected spikelets and glumes (Huang et al., 2018). *F. graminearum* survives as mycelium, perithecium initials, or chlamydospores in host crop residues from small grains such as corn, wheat, and barley. In spring, both sexual (ascospores) and asexual (conidia) spores from infected crop residues are windblown or splashed into barley spikes during wet weather (Wegulo et al., 2015). Barley spikes are most vulnerable to infection during flowering, when the heads break through the leaf sheath. In North Dakota, prolonged high humidity (48 to 72 hours) and warm temperatures ranging from 23 to 30°C are favorable for infection (NDSU-extension, 2018). Disease

occurrence and severity varies among growing seasons because FHB development is dependent on environmental conditions. Therefore, a mixture of factors, such as abundance of inoculum, prolonged or repeated periods of wetness and high humidity during flowering and kernel development, and the use of susceptible cultivars, can result in significant yield and quality losses (NDSU-extension, 2018). The infection process in barley begins with spores landing on florets, followed by hyphal growth across the surface before entry. The fungus then enters the floret through natural cervices between the palea and the lemma, causing yellow and brown lesions, and once inside, uses cervices at the base of the caryopsis to spread to the rachis (Lewandowski et al., 2006).

In order to control FHB disease under the acceptable levels, an integrated approach based on multiple methods is recommended. Planting barley varieties with type II resistance is preferable, so that the spread of the infection throughout the spike is limited. Seed treatment with the appropriate fungicide helps to avoid seedling blight caused by the pathogen. Common methods for reducing inoculum sources include burying infected crop residues through tillage and rotation of non-host crops (Wegulo et al., 2015). Staggered sowing could help avoid all the crop flowering at the same time during favorable conditions for infection. When barley heads are fully emerged, fungicide application using a board-spectrum triazole fungicide can reduce the FHB severity (NDSU-extension, 2018).

To identify FHB resistance, numerous research teams from all over the world have conducted extensive screenings of tens of thousands of gene bank accessions. Screening efforts were conducted in the United States in the late 1920s, and several moderately resistant accessions were discovered. The six-rowed Swiss landrace variety Chevron (CIho 1111) was identified with moderate resistance to FHB (Shands, 1939). Another line called MNBrite, which

is a Chevron-derived accession, demonstrated a moderate resistance to FHB as well. This line was developed inadvertently by selecting plants with bright kernals. MNBrite was crossed with the two-row accession Zhedar 2 to breed Quest, a six-row variety with superior malting qualities and moderate resistance to FHB (Rasmusson et al., 1999). Similar to MNBrite, the American two-rowed cultivar Conlon, released by North Dakota State University, was not bred for FHB resistance in mind but demonstrated moderate resistance nonetheless (Fernando et al., 2021).

After FHB epidemics in the mid-1990s, North American screening efforts to identify resistance sources were increased, and some Asian lines were also adopted in barley breeding programs. However, those lines showed poor malting qualities due to being poorly adapted to the different photoperiod conditions in North America, which posed some difficulties in terms of breeding utility (Fernando et al., 2021; Urrea et al., 2005). In addition, somaclonal lines resistant to FHB were generated via in vitro selection (IVS) and the presence of DON in the media. The use of a DH system that fixes alleles in a single generation by eliminating heterozygosity appears to be effective when combined with IVS. Norman, a DH two-row barley variety developed by adding DON to the anther culture medium, exhibited a 25-30% decreased DON accumulation compared to its parent cultivar CDC Kendall (Legge et al., 2011).

The identification of FHB resistance has been involved the screening of numerous gene bank accessions using diverse methodologies by multiple research groups. Resistance to FHB and DON buildup in barley is conferred through multiple loci on all seven chromosomes. Most revealed QTL are linked to resistance to both FHB and DON accumulation, but not always. Furthermore, some QTL were accompanied with poor agronomic features, making them unsuitable for the breeding program. For example, two important QTL, *Qrgz-2 H-8* and *Qrgz-2 H-10* confer FHB resistance, but they are linked to the late heading date, plant height, and the

row-type controlling gene *Vrs1* (Fernando et al., 2021). The QTL on chromosomes 1H and 7H contributed by Chevron are also linked with late heading and tall stature (Fernando et al., 2021). The *QDON-4 H-2* locus on chromosome 4H (bin 2) derived from a Chinese accession CI4196 explained 9–14% of the variation in DON accumulation (Horsley et al., 2006). However, this locus is correlated with plant height but not heading date (Zhu et al., 1999). Only a few of the many QTL reported for FHB resistance (78) and DON accumulation (42) are independent from other agronomic characters. Therefore, incorporating these QTL into breeding lines is difficult due to their minor effects, association with undesirable traits, and vulnerability to genotype and environmental interaction (Steffenson et al., 2016).

RNA Interference

RNA-silencing (RNAi) is a post-transcriptional gene silencing that utilizes small RNA molecules to degrade sequence-specific mRNA. This process has been observed in eukaryote kingdoms, including plants, animal, and fungi (Chang et al., 2012). RNA interference (RNAi) offers a new tool to control FHB in cereals, given that current management strategies only partially reduced the impact of FHB. The reduced pathogenicity was demonstrated in RNAi-based host-induced gene silencing (HIGS) by targeting key fungal genes upon host infection (Chen et al., 2016; Cheng et al., 2015).

RNAi is usually initiated by the introduction of long double-stranded RNAs (dsRNA) into the cell. dsRNAs can be synthesized in a variety of ways: replicating RNA from an RNA template (RNA viruses), hybridizing complementary RNA transcripts, and synthesizing hair-pinned RNAs (hpRNAs) (Chang et al., 2012). These dsRNAs are cleaved by the RNase-III-like Dicer protein into 21–24 bp RNA duplexes with two-nucleotide 3′-overhangs, which are referred to as small interfering RNAs (siRNAs). The guide strand of siRNA is loaded into an RNA-

induced silencing complex (RISC), whereas the passenger strand is degraded. The RISC's catalytic center is formed by the RNase protein ARGONAUTE. RISC degrades target mRNAs with nearly identical sequences to the siRNAs (Chang et al., 2012).

The RNAi system in *F. graminearum* consists of five RNA-dependent RNA-polymerases *RdRps* (*FgRdRp1–5*), two Argonaute proteins (*FgAgo1* and *FgAgo2*), and two Dicer proteins (*FgDicer1* and *FgDicer2*) (Machado et al., 2018). The Dicer-dependent RNAi machinery controls the growth of the sexual perithecia, but it does not participate in fungal growth, asexual conidiation, abiotic stress, or disease development. However, it appears that *FgAgo1* and *FgDicer2* are crucial in the suppression of endogenous *F. graminearum* genes triggered by the introduced hpRNA. This method made use of an RNAi vector with an intron sequence sandwiched between two inversely oriented and self-complementary target sequences, which, when expressed, result in the formation of a hairpin-shaped dsRNA molecule (Machado et al., 2018).

siRNA Movement

Locally initiated gene silencing in plants can spread to other parts of the organism via systemic or cell-to-cell transport of the silencing signal. In plants, the silencing signal is transmitted in long distances by the phloem, following the source-to-sink dynamics. Signals for short- and long-distance silencing can also be transmitted symplastically via plasmodesmata (Machado et al., 2018). The RNAi signals can also travel between organisms of the same or different species, and even across kingdoms, providing an additional level of communication, interaction, and pathogen–host warfare. In 2010, HIGS was first demonstrated in filamentous fungi through the silencing of a β-glucuronidase (*GUS*) reporter gene in a transgenic strain of *F. verticillioides* during infection of transgenic tobacco plants expressing a hairpin *GUS*-RNAi

(Tinoco et al., 2010). Consequently, transgenic barley and wheat plants were engineered to express dsRNA targeting transcripts of the virulence factor to combat other pathogens. It is hypothesized that the transport of siRNAs from the plant to the invading organism, such as a fungal pathogen, is mediated by exosomes (secreted vesicles) formed by the fusion of early secretion pathway-derived vesicles with the plasma membrane (Rutter and Innes, 2017). However, other mechanisms, such as passive diffusion, membrane-associated transporters, and receptors, can be involved in siRNA trafficking (Machado et al., 2018). Moreover, the RNAi signals can travel in the opposite direction, from the pathogen to the host, and suppress target genes of the host. As with the necrotrophic pathogen *Botrytis cinerea*, which has been shown to transfer siRNA into Arabidopsis and tomato cells. The fungal siRNAs are capable of utilizing the plant RNAi machinery, including the *Argonaute* proteins, to silence transcripts involved in innate immunity, thereby facilitating plant infection (Weiberg et al., 2013).

RNAi for FHB Control

Researchers have investigated the effect of RNAi silencing to attain higher resistance against pathogenic *Fusarium* species using HIGS or spray-induced gene silencing (SIGS). SIGS is an alternative way of non-transgenic applications of RNAi, uses either long dsRNA or siRNA that can be taken up by host or pathogen target cells to achieve higher resistance as well. The sterol 14-demethylase (*CYP51*) genes are required for ergosterol biosynthesis to maintain membrane integrity and fungal virulence. HIGS targeting CYP51 genes resulted in a decrease in *F. graminearum* growth in transgenic *Arabidopsis* and barley plants (Koch et al., 2013). Chitin is the primary structural component of fungal cell walls. Two independent transgenic wheat lines expressing three RNAi constructs targeting the chitin synthase (*Chs3b*) gene, which catalyzes the biosynthesis of chitin, exhibited enhanced FHB and seedling blight resistance (Cheng et al.,

2015). Transgenic wheat plants with an RNAi hairpin construct targeting the most abundant fungal cell wall polysaccharide, β-1, 3-glucan synthase gene *FcGls1* in *F.culmorum*, showed increased resistance when infected with the pathogen in leaves and spikes (Chen et al., 2016). Furthermore, Koch et al., (2016) demonstrated in barley spraying with long dsRNAs targeting *CYP51* genes inhibited the fungal growth of *F. graminearum*. This study also revealed that the fungal growth suppression occurred at the site of spray application as well as the distal tissues, indicating the movement of CYP3-dsRNA through the plant's vascular system and the processing of CYP3-dsRNA into siRNAs by fungal DICER-LIKE 1 (*FgDCL-1*) after the pathogen's uptake. The function of *FgDCL-1* was demonstrated by a *dcl-1* mutant strain that did not exhibit decreased expression of *CYP51* genes compared to the wild type (Koch et al., 2016).

HIGS and SIGS may be effective for FHB and other diseases; however, both have advantages and disadvantages. The implementation of SIGS would solve the problem posed by HIGS regarding public acceptance of genetically modified organisms (GMOs) (Machado et al., 2018). However, there are still a number of technological obstacles that could prevent the implementation of SIGS as a conventional control method. First, because the effect of a single SIGS application in the field may only last a few days, timing is crucial for success. A recent study investigated the use of nanosheets of double-layered hydroxide clay loaded with dsRNA, which can remain on sprayed leaves for up to 30 days (Mitter et al.,2017). Second, the cost of producing and applying SIGS is significantly higher than that of conventional fungicides. However, new technologies are being developed to enable the cost-effective mass production of RNA for topical RNAi applications in agriculture, with the ultimate goal of producing RNAs for less than $2/g (Le Page, 2017).

Controlling multiple pathogens with a single strategy across is highly desirable. This can be achieved by carefully designing the HIGS construct using the gene sequences highly conserved in different fungal species (Panwar et al., 2016). Off-target of gene silencing may occur in host plants as well as in beneficial plant-associated organisms, such as mycorrhizas, rhizobia, and biocontrol species. For instance, a HIGS study in maize to reduce the production of aflatoxin in *Aspergillus flavus* resulted in stunting and reduced kernel placement in transgenic plants, possibly because of off-target silencing of other genes. Alternatively, transgenic maize with a different RNAi construct targeting a different pathogen gene produced less aflatoxin and displayed no morphological changes (Masanga et al., 2015; Thakare et al., 2017). Nonetheless, the off-target effect could be reduced by investigating the vast data sets of genomic and transcriptomic information during the initial construct design phase of any project. In addition, multiple silencing constructs that target multiple genes could be created and used in a concatenated/stacked HIGS cassette to confer control against multiple pathogens from a single genetic locus that is simply inherited within a breeding program (Machado et al., 2018). Lastly, pathogens could develop a suppression system and circumvent HIGS, which would be one potential defense mechanism. It was observed that *Phytophthora* species secreted effector/suppressor proteins through unidentified mechanisms, to prevent the accumulation of plant siRNAs (Qiao et al., 2013).

Literature Cited

Alhashel, A. F., Sharma Poudel, R., Fiedler, J., Carlson, C. H., Rasmussen, J., Baldwin, T., Friesen, T. L., Brueggeman, R. S., and Yang, S. (2021). Genetic mapping of host resistance to the Pyrenophora teres f. maculata isolate 13IM8.3. *G3 Genes|Genomes|Genetics*, *11*(12).

Arranz-Otaegui, A., Gonzalez Carretero, L., Ramsey, M. N., Fuller, D. Q., and Richter, T. (2018). Archaeobotanical evidence reveals the origins of bread 14,400 years ago in northeastern Jordan. *Proceedings of the National Academy of Sciences*, *115*(31), 7925-7930.

Bach, E., Christensen, S., Dalgaard, L., Larsen, P., Olsen, C., and Smedegård-Petersen, V. (1979). Structures, properties and relationship to the aspergillomarasmines of toxins produced by Pyrenophora teres. *Physiological Plant Pathology*, *14*(1), 41–46.

Bailey, A. (2022, August 4). Pet food processors have a growing appetite for barley - Agweek | #1 source for agriculture news, farming, markets. Agweek. Retrieved September 19, 2022, from https://www.agweek.com/business/pet-food-processors-have-a-growing-appetite-for-barley

Bayer, M. M., Rapazote-Flores, P., Ganal, M., Hedley, P. E., Macaulay, M., Plieske, J., Ramsay, L., Russell, J., Shaw, P. D., Thomas, W., and Waugh, R. (2017). Development and Evaluation of a Barley 50k iSelect SNP Array. *Frontiers in Plant Science*, *8*.

Behn, A., Hartl, L., Schweizer, G., and Baumer, M. (2005). Molecular mapping of QTLs for non-parasitic leaf spot resistance and comparison of half-sib DH populations in spring barley. Euphytica 141: 291– 299.

Brassac, J., and Blattner, F. R. (2015). Species-Level Phylogeny and Polyploid Relationships in Hordeum (Poaceae) Inferred by Next-Generation Sequencing and In Silico Cloning of Multiple Nuclear Loci. *Systematic biology*, *64*(5), 792–808.

Bull, H., Casao, M. C., Zwirek, M., Flavell, A. J., Thomas, W. T., Guo, W., ... and Waugh, R. (2017). Barley SIX-ROWED SPIKE3 encodes a putative Jumonji C-type H3K9me2/me3 demethylase that represses lateral spikelet fertility. *Nature Communications*, *8*(1), 1-9.

Burlakoti, R. R., Gyawali, S., Chao, S., Smith, K. P., Horsley, R. D., Cooper, B., Muehlbauer, G. J., and Neate, S. M. (2017). Genome-Wide Association Study of Spot Form of Net Blotch Resistance in the Upper Midwest Barley Breeding Programs. *Phytopathology®*, *107*(1), 100–108.

Caeseele, L. V., and Grumbles, J. (1979). Ultrastructure of the interaction between Pyrenophora teres and a susceptible barley host. *Canadian Journal of Botany*, *57*(1), 40-47.

Cantalapiedra, C.P., Boudiar, R., Casas, A.M., Igartua, E., Contreras-Moreira, B. (2015). BARLEYMAP:physical and genetic mapping of nucleotide sequences and annotation of surrounding loci in barley. Mol. Breed. 35, 13.

Carlsen, S. A., Neupane, A., Wyatt, N. A., Richards, J. K., Faris, J. D., Xu, S. S., Brueggeman, R. S., and Friesen, T. L. (2017). Characterizing the *Pyrenophora teres* f. *maculata*–Barley Interaction Using Pathogen Genetics. *G3 Genes|Genomes|Genetics*, *7*(8), 2615–2626.

Chang, S. S., Zhang, Z., and Liu, Y. (2012). RNA Interference Pathways in Fungi: Mechanisms and Functions. *Annual Review of Microbiology*, *66*(1), 305–323.

Chen, W., Kastner, C., Nowara, D., Oliveira-Garcia, E., Rutten, T., Zhao, Y., Deising, H. B., Kumlehn, J., and Schweizer, P. (2016). Host-induced silencing of Fusarium culmorumgenes protects wheat from infection. *Journal of Experimental Botany*, *67*(17), 4979–4991.

Cheng, W., Song, X. S., Li, H. P., Cao, L. H., Sun, K., Qiu, X. L., Xu, Y. B., Yang, P., Huang, T., Zhang, J. B., Qu, B., and Liao, Y. C. (2015). Host-induced gene silencing of an essential chitin synthase gene confers durable resistance to Fusarium head blight and seedling blight in wheat. *Plant Biotechnology Journal*, *13*(9), 1335–1345.

Civáň, P., and Brown, T. A. (2017). A novel mutation conferring the nonbrittle phenotype of cultivated barley. *New Phytologist*, *214*(1), 468-472.

Clare, S. J., Duellman, K. M., Richards, J. K., Poudel, R. S., Merrick, L. F., Friesen, T. L., and Brueggeman, R. S. (2022). Association mapping reveals a reciprocal virulence/avirulence locus within diverse US Pyrenophora teres f. maculata isolates. *BMC genomics*, *23*(1), 1-17.

Clare, S. J., Wyatt, N. A., Brueggeman, R. S., and Friesen, T. L. (2020). Research advances in the*Pyrenophora teres*–barley interaction. *Molecular Plant Pathology*, *21*(2), 272–288.

Clark, H.H. (1967). The origin and early history of the cultivated barleys. Agric. Hist. Rev. 15: 1–18.

Close, T.J. et al. (2009). Development and implementation of high-throughput SNP genotyping in barley. BMC Genomics 10: 582.

Close, T.J., Wanamaker, S.I., Caldo, R.A., Turner, S.M., Ashlock, D.A., Dickerson, J.A., Wing, R.A., Muehlbauer, G.J., Kleinhofs, A., and Wise, R.P. (2004). A new resource for cereal genomics: 22K barley GeneChip comes of age. Plant Physiol. 134: 960–968.

Comadran, J. et al. (2012). Natural variation in a homolog of Antirrhinum CENTRORADIALIS contributed to spring growth habit and environmental adaptation in cultivated barley. Nat. Genet. 44: 1388.

Daba, S. D., Horsley, R., Brueggeman, R., Chao, S., and Mohammadi, M. (2019). Genome-wide Association Studies and Candidate Gene Identification for Leaf Scald and Net Blotch in Barley (*Hordeum vulgare* L.). *Plant Disease*, *103*(5), 880–889.

Dahl, B., and Wilson, W. W. (2018). Risk premiums due to Fusarium Head Blight (FHB) in wheat and barley. *Agricultural Systems*, *162*, 145–153.

Dai, F. et al. (2012). Tibet is one of the centers of domestication of cultivated barley. *Proceedings of the National Academy of Sciences*, *109*(42), 16969-16973.

de Souza Moraes, T., van Es, S. W., Hernández-Pinzón, I., Kirschner, G. K., van der Wal, F., da Silveira, S. R., ... and van Esse, G. W. (2021). The TCP transcription factor HvTB2 heterodimerizes with VRS5 (HvTB1) and controls spike architecture in barley. *bioRxiv*.

Duellman, K., 2015 Characterizing *P. teres* f. *maculata* in the northern United States and impact of spot form net blotch on yield of barley. 10.13140/RG.2.1.3045.9925.

Dixon, L. E., Greenwood, J. R., Bencivenga, S., Zhang, P., Cockram, J., Mellers, G., ... and Boden, S. A. (2018). TEOSINTE BRANCHED1 regulates inflorescence architecture and development in bread wheat (Triticum aestivum). *The Plant Cell*, *30*(3), 563-581.

Ellwood, S. R., Syme, R. A., Moffat, C. S., and Oliver, R. P. (2012). Evolution of three Pyrenophora cereal pathogens: Recent divergence, speciation and evolution of non-coding DNA. *Fungal Genetics and Biology*, *49*(10), 825–829.

Elshire, R.J., Glaubitz, J.C., Sun, Q., Poland, J.A., Kawamoto, K., Buckler, E.S., and Mitchell, S.E. (2011). A Robust, Simple Genotyping-by-Sequencing (GBS) Approach for High Diversity Species. PLoS One 6: e19379.

Fastnaught, C.E., (2001). Barley fiber. In: Cho, S., Dreher, M. (Eds.), Handbook of Dietary Fiber. MarcelDekker, New York, pp: 519-542

Fernando, W. D., Oghenekaro, A. O., Tucker, J. R., and Badea, A. (2021). Building on a foundation: advances in epidemiology, resistance breeding, and forecasting research for reducing the impact of fusarium head blight in wheat and barley. *Canadian Journal of Plant Pathology*, *43*(4), 495–526.

Franckowiak, J.D. and Platz, G.J. (2013). International database for barley genes and barley genetic stocks. Barley Genet. Newsl. 43, 48–223.

Friesen, T. L., Faris, J. D., Lai, Z., and Steffenson, B. J. (2006). Identification and chromosomal location of major genes for resistance to*Pyrenophorateres*in a doubled-haploid barley population. *Genome*, *49*(7), 855–859.

Friesen, T. L., Faris, J. D., Solomon, P. S., and Oliver, R. P. (2008). Host-specific toxins: effectors of necrotrophic pathogenicity. *Cellular Microbiology*, *10*(7), 1421–1428.

Friesen, T. L., Meinhardt, S. W., and Faris, J. D. (2007). The Stagonospora nodorum-wheat pathosystem involves multiple proteinaceous host-selective toxins and corresponding host sensitivity genes that interact in an inverse gene-for-gene manner. *The Plant Journal*, *51*(4), 681–692.

Friis, P., Olsen, C., and Møller, B. (1991). Toxin production in Pyrenophora teres, the ascomycete causing the net-spot blotch disease of barley (Hordeum vulgare L.). *Journal of Biological Chemistry*, *266*(20), 13329–13335.

Gómez-Gómez, L., and Boller, T. (2002). Flagellin perception: a paradigm for innate immunity. *Trends in Plant Science*, *7*(6), 251–256.

Graner, A., Jaboor, A., Schondelmaier, J., Siedler, H., Pillen, K., Fischbeck, G., Wenzel, G., and Hermann,R.G. (1991). Construction of an RFLP map of barley. Theor. Appl. Genet. 83: 250–256.

Grewal, T. S., Rossnagel, B. G., Pozniak, C. J., and Scoles, G. J. (2008). Mapping quantitative trait loci associated with barley net blotch resistance. Theoretical and Applied Genetics, 116(4), 529-539.

Gupta, M., Abu-Ghannam, N., and Gallaghar, E. (2010). Barley for brewing: Characteristic changes during malting, brewing and applications of its by-products. *Comprehensive reviews in food science and food safety*, *9*(3), 318-328.

Harlan, J. R. (1978). The origins of cereal agriculture in the old world. In Origins of Agriculture (ed Reed, C. A.), The Hague: Mouton Publishers. pp. 357-383

Hearnden, P.R., Eckermann, P.J., McMichael, G.L., Hayden, M.J., Eglinton, J.K., and Chalmers, K.J. (2007). A genetic map of 1,000 SSR and DArT markers in a wide barley cross. Theor. Appl. Genet. 115: 383

Horsley, R. D., Schmierer, D., Maier, C., Kudrna, D., Urrea, C. A., Steffenson, B. J., Schwarz, P. B., Franckowiak, J. D., Green, M. J., Zhang, B., and Kleinhofs, A. (2006). Identification of QTLs Associated with Fusarium Head Blight Resistance in Barley Accession CIho 4196. *Crop Science*, *46*(1), 145–156.

Hsiao, C., Chatterton, N. J., Asay, K. H., and Jensen, K. B. (1995). Phylogenetic relationships of the monogenomic species of the wheat tribe, Triticeae (Poaceae), inferred from nuclear rDNA (internal transcribed spacer) sequences. Genome. 38: 211–223

Huang, Y., Haas, M., Heinen, S., Steffenson, B. J., Smith, K. P., and Muehlbauer, G. J. (2018). QTL Mapping of Fusarium Head Blight and Correlated Agromorphological Traits in an Elite Barley Cultivar Rasmusson. *Frontiers in Plant Science*, *9*.

IBGSC. (2012). A physical, genetic and functional sequence assembly of the barley genome. Nature 491:711–717.

Jayakodi, M. et al. (2020). The barley pan-genome reveals the hidden legacy of mutation breeding. Nature.

Jia, Q., Wang, J., Zhu, J., Hua, W., Shang, Y., Yang, J., and Liang, Z. (2017). Toward identification of black lemma and pericarp gene Blp1 in barley combining bulked segregant analysis and specific-locus amplified fragment sequencing. *Frontiers in Plant Science*, *8*, 1414.

Jones, J. D. G., and Dangl, J. L. (2006). The plant immune system. *Nature*, *444*(7117), 323–329.

Jouve, N., Al, C., de Bustos, A., and Cuadrado, Á. (2018). The Phylogenetic relationships of species and cytotypes in the genus Hordeum based on molecular karyotyping. *Curr Res Phylogenetics Evol Biol: CRPEB-102. DOI*, *10*.

Kenneth, R. (1962). On the taxonomy, morphology and geographical origins of Pyrenophora teres Drechsler and allied species. Bull. Res. Council Israel, 11D, 55–82.

Keon, J., and Hargreaves, J. (1983). A cytological study of the net blotch disease of barley caused by Pyrenophora teres. *Physiological Plant Pathology*, *22*(3), 321-IN14.

Kirby, E. J. M., and Riggs, T. J. (1978). Developmental consequences of two-row and six-row ear type in spring barley: 2. Shoot apex, leaf and tiller development. *The Journal of Agricultural Science*, *91*(1), 207-216.

Kleinhofs, A. et al. (1993). A molecular, isozyme, and morphological map of the barley (*Hordeum vulgare* genome). Theor. Appl. Genet. 86: 705–712.

Knutson, J. (2020, February 13). Area barley industry switching to two-row - Agweek | #1 source for agriculture news, farming, markets. Agweek. Retrieved September 19, 2022, from https://www.agweek.com/business/area-barley-industry-switching-to-two-row

Koch, A., Biedenkopf, D., Furch, A., Weber, L., Rossbach, O., Abdellatef, E., Linicus, L., Johannsmeier, J., Jelonek, L., Goesmann, A., Cardoza, V., McMillan, J., Mentzel, T., and Kogel, K. H. (2016). An RNAi-Based Control of Fusarium graminearum Infections Through Spraying of Long dsRNAs Involves a Plant Passage and Is Controlled by the Fungal Silencing Machinery. *PLOS Pathogens*, *12*(10), e1005901.

Koch, A., Kumar, N., Weber, L., Keller, H., Imani, J., and Kogel, K. H. (2013). Host-induced gene silencing of cytochrome P450 lanosterol C14α-demethylase–encoding genes confers strong resistance to *Fusarium* species. *Proceedings of the National Academy of Sciences*, *110*(48), 19324–19329.

Komatsuda, T., Pourkheirandish, M., He, C., Azhaguvel, P., Kanamori, H., Perovic, D., ... and Yano, M. (2007). Six-rowed barley originated from a mutation in a homeodomain-leucine zipper I-class homeobox gene. *Proceedings of the National Academy of Sciences*, *104*(4), 1424-1429.

Komatsuda, T., Tanno, K., Salomon, B., Bryngelsson, T., and Roland, v. B. (1999). Phylogeny in the genus hordeum based in nucleotide sequences closely linked to the vrs 1 locus (row number of spikelets). Genome, 42(5), 973-81.

König, P., Beier, S., Basterrechea, M., Schüler, D., Arend, D., Mascher, M., Stein, N., Scholz, U., and Lange, M. (2020). BRIDGE – A Visual Analytics Web Tool for Barley Genebank Genomics. Front. Plant Sci. 11: 701.

Lang, L., Rakszegi, M., and Bedo, Z. (2013). Cereal production and its characteristics. Engineering aspects of cereal and cereal-based products.

Langridge, P., Karakousis, A., Collins, N., Kretschmer, J., and Manning, S. (1995). A consensus linkage map of barley. Mol. Breed. 1: 389–395.

Le Page, M. (2017). Gene-silencing spray lets us modify plants without changing DNA. *New scientist*.

Legge, W. G., et al. (2011). Norman barley. Canadian Journal of Plant Science, 91(6), 1105-1113.

Lewandowski, S. M., Bushnell, W. R., and Evans, C. K. (2006). Distribution of Mycelial Colonies and Lesions in Field-Grown Barley Inoculated with Fusarium graminearum. *Phytopathology®*, *96*(6), 567–581.

Li, C., Ni, P., Francki, M., Hunter, A., Zhang, Y., Schibeci, D., Li, H., Tarr, A., Wang, J., Cakir, M., Yu, J., Bellgard, M., and Lance, R. (2004). Genes controlling seed dormancy and pre-harvest sprouting in a rice-wheat-barley comparison. Appels RFunct Integr Genomics.4 (2):84-93.

Lightfoot, D. J., and Able, A. J. (2010). Growth of *Pyrenophora teres in planta* during barley net blotch disease. *Australasian Plant Pathology*, *39*(6), 499.

Liller, C. B., Walla, A., Boer, M. P., Hedley, P., Macaulay, M., Effgen, S., ... and Koornneef, M. (2017). Fine mapping of a major QTL for awn length in barley using a multiparent mapping population. *Theoretical and Applied Genetics*, *130*(2), 269-281.

Linder, H. P. (1987). The evolutionary history of the Poales/Restionales: a hypothesis. Kew Bulletin. 42: 297–318.

Liu, L., Wang, J., Rosenberg, D., Zhao, H., Lengyel, G., and Nadel, D. (2018). Fermented beverage and food storage in 13,000 y-old stone mortars at Raqefet Cave, Israel: Investigating Natufian ritual feasting. *Journal of Archaeological Science: Reports*, *21*, 783-793.

Liu, Z. H., and Friesen, T. L. (2010). Identification of *Pyrenophora teres* f. *maculata*, Causal Agent of Spot Type Net Blotch of Barley in North Dakota. *Plant Disease*, *94*(4), 480.

Liu, Z. H., Zhong, S., Stasko, A. K., Edwards, M. C., and Friesen, T. L. (2012). Virulence Profile and Genetic Structure of a North Dakota Population of *Pyrenophora teres* f. *teres*, the Causal Agent of Net Form Net Blotch of Barley. Phytopathol. 102:539-546

Liu, z., Ellwood, s. R., Oliver, r. P., and Friesen, T. L. (2011). Pyrenophora teres: profile of an increasingly damaging barley pathogen. *Molecular Plant Pathology*, *12*(1), 1–19.

Liu, Z., Holmes, D. J., Faris, J. D., Chao, S., Brueggeman, R. S., Edwards, M. C., and Friesen, T. L. (2015). Necrotrophic effector-triggered susceptibility (NETS) underlies the barley-*Pyrenophora teres*f.*teres* interaction specific to chromosome 6H. *Molecular Plant Pathology*, *16*(2), 188–200.

lo Presti, L., Lanver, D., Schweizer, G., Tanaka, S., Liang, L., Tollot, M., Zuccaro, A., Reissmann, S., and Kahmann, R. (2015). Fungal Effectors and Plant Susceptibility. *Annual Review of Plant Biology*, *66*(1), 513–545.

Lundqvist, U., Franckowiak, J. D., and Konishi, T. (1997). New and revised descriptions of barley genes. *Barley genetics newsletter*.

Machado, A. K., Brown, N. A., Urban, M., Kanyuka, K., and Hammond-Kosack, K. E. (2018). RNAi as an emerging approach to control Fusarium head blight disease and mycotoxin contamination in cereals. *Pest management science*, *74*(4), 790-799.

Manninen, O., Jalli, M., Kalendar, R., Schulman, A., Afanasenko, O., and Robinson, J. (2006). Mapping of major spot-type and net-type net-blotch resistance genes in the Ethiopian barley line CI 9819. *Genome*, *49*(12), 1564–1571.

Manning, V.A., Chu, A.L., Steeves, J.E., Wolpert, T.J., Ciuffetti, L.M., (2009). A Host-Selective Toxin of *Pyrenophora tritici-repentis*, Ptr ToxA, Induces Photosystem Changes and Reactive Oxygen Species Accumulation in Sensitive Wheat. Molecular Plant-Microbe Interactions 22, 665–676. doi:10.1094/MPMI-22-6-0665.

Masanga, J. O., Matheka, J. M., Omer, R. A., Ommeh, S. C., Monda, E. O., and Alakonya, A. E. (2015). Downregulation of transcription factor aflR in Aspergillus flavus confers reduction to aflatoxin accumulation in transgenic maize with alteration of host plant architecture. *Plant cell reports*, *34*(8), 1379-1387.

Mascher, M., Wicker, T., Jenkins, J., et al. (2021). Long-read sequence assembly: a technical evaluation in barley. *Plant Cell* 33, 1888–1906.

Mathre, D. E. (1997). Net blotch, p.28-31, *In* D.E. Mathre, ed. Compendium of Barley Diseases. 2nd edition. American Phytopathological Society, St. Paul, MN.

McLean, M. S., Howlett, B. J., and Hollaway, G. J. (2009). Epidemiology and control of spot form of net blotch (Pyrenophora teres f. maculata) of barley: a review. *Crop and Pasture Science*, *60*(4), 303.

McLean, M. S., Howlett, B. J., Turkington, T. K., Platz, G. J., and Hollaway, G. J. (2012). Spot Form of Net Blotch Resistance in a Diverse Set of Barley Lines in Australia and Canada. *Plant Disease*, *96*(4), 569–576.

Middleton, C. P., Senerchia, N., Stein, N., Akhunov, E. D., Keller, B., Wicker, T., and Kilian, B. (2014). Sequencing of chloroplast genomes from wheat, barley, rye and their relatives provides a detailed insight into the evolution of the Triticeae tribe. *PloS one*, *9*(3), e85761.

Miedaner, T., Gwiazdowska, D., and Waśkiewicz, A. (2017). Editorial: Management of Fusarium Species and their Mycotoxins in Cereal Food and Feed. *Frontiers in Microbiology*, *8*.

Milne, L., Bayer, M., Rapazote-Flores, P., Mayer, C.-D., Waugh, R., and Simpson, C.G. (2021). EORNA, a barley gene and transcript abundance database. Sci. Data 8: 90.

Mitter, N., Worrall, E. A., Robinson, K. E., Li, P., Jain, R. G., Taochy, C., ... and Xu, Z. P. (2017). Clay nanosheets for topical delivery of RNAi for sustained protection against plant viruses. *Nature plants*, *3*(2), 1-10.

Monat, C. et al. (2019). TRITEX: chromosome-scale sequence assembly of Triticeae genomes with opensourcetools. Genome Biol. 20: 284.

Moore, G., Devos, K. M., Wang, Z., and Gale, M. D. (1995). Cereal genome evolution. Grasses, line up and form a circle. *Current biology : CB*, *5*(7), 737–739.

Moragues, M., Comadran, J., Waugh, R., Milne, I., Flavell, A.J., and Russell, J.R. (2010). Effects of ascertainment bias and marker number on estimations of barley diversity from high-throughput SNP genotype data. Theor. Appl. Genet. 120: 1525–1534.

Nadel, D., Weiss, E., Simchoni, O., Tsatskin, A., Danin, A., and Kislev, M. (2004). From the Cover: Stone Age Hut in Israel Yields World's Oldest Evidence of Bedding. The National Academy of Sciences.101, 6821

National Agricultural Statistics Service (NASS). (2022). Crop Production 20221 Summary. ISSN: ISSN: 1949-162X 1057-7823.

Neupane, A., Tamang, P., Brueggeman, R. S., and Friesen, T. L. (2015). Evaluation of a Barley Core Collection for Spot Form Net Blotch Reaction Reveals Distinct Genotype-Specific Pathogen Virulence and Host Susceptibility. *Phytopathology®*, *105*(4), 509–517.

Newman, C.W. and Newman, R.K. (2006). A Brief History of Barley Foods. Cereal Foods World 51: 4–7.

Newman, M. A., Sundelin, T., Nielsen, J. T., and Erbs, G. (2013). MAMP (microbe-associated molecular pattern) triggered immunity in plants. *Frontiers in Plant Science*, *4*.

Nganje, W. E., Bangsund, D. A., Leistritz, F. L., Wilson, W. W., and Tiapo, N. M. (2004). Regional Economic Impacts of Fusarium Head Blight in Wheat and Barley. *Review of Agricultural Economics*, *26*(3), 332–347.

North Dakota State University Extension (NDSU-Extension). (2018). Fusarium Head Blight (Scab) of Small Grains. https://www.ag.ndsu.edu/publications/crops/fusarium-head-blight-scab-of-small-grains

Nürnberger, T., and Brunner, F. (2002). Innate immunity in plants and animals: emerging parallels between the recognition of general elicitors and pathogen-associated molecular patterns. *Current Opinion in Plant Biology*, *5*(4), 318–324.

Panwar, V., McCallum, B., Jordan, M., Loewen, M., Fobert, P., McCartney, C., and Bakkeren, G. (2016). RNA silencing approaches for identifying pathogenicity and virulence elements towards engineering crop resistance to plant pathogenic fungi. *CAB Rev*, *11*, 1-13.

Paterson, A. H., Bowers, J. E., Peterson, D. G., Estill, J. C., and Chapman, B. A. (2003). Structure and evolution of cereal genomes. *Current opinion in genetics and development*, *13*(6), 644-650.

Petre, B., and Kamoun, S. (2014). How Do Filamentous Pathogens Deliver Effector Proteins into Plant Cells? *PLoS Biology*, *12*(2), e1001801.

Poehlman, J.M. (1994). Breeding barley and oats, p. 378-420, *In* J.M. Poehlman, ed. Breeding Field Crops (3rd ed), Iowa State University Press, Ames, Iowa.

Pourkheirandish, M., and Komatsuda, T. (2007). The importance of barley genetics and domestication in a global perspective. *Annals of Botany*, *100*(5), 999-1008.

Pourkheirandish, M., Hensel, G., Kilian, B., Senthil, N., Chen, G., Sameri, M., Azhaguvel, P., Sakuma, S., Dhanagond, S., Sharma, R., Mascher, M., Himmelbach, A., Gottwald, S., Nair, S. K., Tagiri, A., Yukuhiro, F., Nagamura, Y., Kanamori, H., Matsumoto, T., Willcox, G., … Komatsuda, T. (2015). Evolution of the Grain Dispersal System in Barley. *Cell*, *162*(3), 527–539.

Powell, W., Thomas, W.T.B., Baird, E., Lawrence, P., Booth, A., Harrower, B., McNicol, J.W., and Waugh, R. (1997). Analysis of quantitative traits in barley by the use of Amplified Fragment Length Polymorphisms. Heredity (Edinb). 79: 48–59.

Qi, X., Stam, P., and Lindhout, P. (1998). Use of locus-specific AFLP markers to construct a high-density molecular map of barley. Theor. Appl. Genet. 96: 376–384.

Qiao, Y., Liu, L., Xiong, Q., Flores, C., Wong, J., Shi, J., ... and Ma, W. (2013). Oomycete pathogens encode RNA silencing suppressors. *Nature genetics*, *45*(3), 330-333.

Quinde, Z., Ullrich, S. E., and Baik, B. K. (2004). Genotypic Variation in Color and Discoloration Potential of Barley-Based Food Products. *Cereal Chemistry Journal*, *81*(6), 752–758.

Ramsay, L. et al. (2000). A simple sequence repeat-based linkage map of barley. Genetics 156: 1997–2005.

Ramsay, L., Comadran, J., Druka, A., Marshall, D. F., Thomas, W. T., Macaulay, M., ... and Waugh, R. (2011). INTERMEDIUM-C, a modifier of lateral spikelet fertility in barley, is an ortholog of the maize domestication gene TEOSINTE BRANCHED 1. *Nature genetics*, *43*(2), 169-172.

Rasmusson, D. C., Wilcoxson, R. D., Dill-Macky, R., Schiefelbein, E. L., and Wiersma, J. V. (1999). Registration of 'MNBrite' Barley. *Crop Science*, *39*(1), 290.

Richards, J., Chao, S., Friesen, T., and Brueggeman, R. (2016). Fine mapping of the barley chromosome 6H net form net blotch susceptibility locus. G3 Genes|Genomes|Genetics 6: 1809–1818.

Ruff, T.M., Marston, E.J., Eagle, J.D., Sthapit, S.R., Hooker, M.A., Skinner, D.Z., and See, D.R. (2020). Genotyping by multiplexed sequencing (GMS): A customizable platform for genomic selection. PLoS One 15: e0229207.

Rutter, B. D., and Innes, R. W. (2017). Extracellular vesicles isolated from the leaf apoplast carry stress-response proteins. *Plant physiology*, *173*(1), 728-741.

Salamini, F., Özkan, H., Brandolini, A., Schäfer-Pregl, R., and Martin, W. (2002). Genetics and geography of wild cereal domestication in the near east. *Nature Reviews Genetics*, *3*(6), 429-441.

Sang, T. (2009). Genes and mutations underlying domestication transitions in grasses. *Plant Physiology*, *149*(1), 63-70.

Sarpeleh, A., Wallwork, H., Catcheside, D. E. A., Tate, M. E., and Able, A. J. (2007). Proteinaceous Metabolites from *Pyrenophora teres* Contribute to Symptom Development of Barley Net Blotch. *Phytopathology®*, *97*(8), 907–915.

Sato, K., Close, T.J., Bhat, P., Muñoz-Amatriaín, M., and Muehlbauer, G.J. (2011). Single Nucleotide Polymorphism Mapping and Alignment of Recombinant Chromosome Substitution Lines in Barley. Plant Cell Physiol. 52: 728–737.

Schwarz, P., Horsley, R., and Heisel, S. (2011). History of barley production in the USA. Proc. MBAA Conf.

Selin, C., de Kievit, T. R., Belmonte, M. F., and Fernando, W. G. D. (2016). Elucidating the Role of Effectors in Plant-Fungal Interactions: Progress and Challenges. *Frontiers in Microbiology*, *7*.

Shands, R. G. (1939). Chevron a barley variety resistant to stem rust and other diseases. Phytopathology. 29:209–211.

Sharma Poudel, R., Al-Hashel, A.F., Gross, T., Gross, P., and Brueggeman, R. (2018). Pyramiding *rpg4*- and *Rpg1*-mediated stem rust resistance in barley requires the *Rrr1* gene for both to function. Front. Plant Sci. 9: 1789.

Shipton, W.A., Khan, T.N., Boyd, W.J.R., (1973). Net blotch of barley. Rev. Plant Pathol. 52, 269–290.

Skiba, R. M., Wyatt, N. A., Kariyawasam, G. K., Fiedler, J. D., Yang, S., Brueggeman, R. S., and Friesen, T. L. (2022). Host and pathogen genetics reveal an inverse gene-for-gene association in the P. teres f. maculata–barley pathosystem. *Theoretical and Applied Genetics*, *135*(10), 3597-3609.

Slafer, G.A., Molina-Cano, J.-L., Savin, R., Araus, J.L., and Romagosa, I. (2002). Physiological changes associated with genetic improvement of grain yield in barley. In Barley: Recent Advances from Molecular Biology to Agronomy of Yield and Quality, pp. 361–386.

Smedegård-Petersen, V. (1971). *Pyrenophora teres* f. *maculata* and *Pyrenophora teres* f. *teres* on barley in Denmark. Kgl. Vet. Landbohojsk. Arsskr. 124–144.

Smedegård-Petersen, V. (1977). Isolation of two toxins produced by Pyrenophora teres and their significance in disease development of net-spot blotch of barley. *Physiological Plant Pathology*, *10*(3), 203–211.

Steffenson, B. J., Haas, M., and Sallam, A. (2016, December). A meta-analysis of the genetics of Fusarium head blight resistance in barley. In 2016 National Fusarium Head Blight Forum (p. 94).

Sun, Q., and Zhou, D. X. (2008). Rice jmjC domain-containing gene JMJ706 encodes H3K9 demethylase required for floral organ development. *Proceedings of the National Academy of Sciences*, *105*(36), 13679-13684.

Szűcs, P., Blake, V.C., Bhat, P.R., Chao, S., Close, T.J., Cuesta-Marcos, A., Muehlbauer, G.J., Ramsay, L., Waugh, R., and Hayes, P.M. (2009). An Integrated Resource for Barley Linkage Map and Malting 70 Quality QTL Alignment. Plant Genome 2: 134–140.

Taketa, S., Amano, S., Tsujino, Y., Sato, T., Saisho, D., Kakeda, K., Nomura, M., Suzuki, T., Matsumoto, T., Sato, K., Kanamori, H., Kawasaki, S., and Takeda, K. (2008). Barley grain with adhering hulls is controlled by an ERF family transcription factor gene regulating a lipid biosynthesis pathway. *Proceedings of the National Academy of Sciences of the United States of America*, *105*(10), 4062–4067.

Tamang, P., Neupane, A., Mamidi, S., Friesen, T., and Brueggeman, R. (2015). Association Mapping of Seedling Resistance to Spot Form Net Blotch in a Worldwide Collection of Barley. *Phytopathology®*, *105*(4), 500–508.

Tamang, P., Richards, J. K., Alhashal, A., Sharma Poudel, R., Horsley, R. D., Friesen, T. L., and Brueggeman, R. S. (2019). Mapping of barley susceptibility/resistance QTL against spot form net blotch caused by Pyrenophora teres f. maculata using RIL populations. *Theoretical and Applied Genetics*, *132*(7), 1953–1963.

Tan, C., Chapman, B., Wang, P., Zhang, Q., Zhou, G., Zhang, X., Barrero, R.A., Bellgard, M.I., and Li, C. (2020). BarleyVarDB: a database of barley genomic variation. Database 2020.

Thakare, D., Zhang, J., Wing, R. A., Cotty, P. J., and Schmidt, M. A. (2017). Aflatoxin-free transgenic maize using host-induced gene silencing. *Science Advances*, *3*(3), e1602382.

Thomas, W.T.B., Baird, E., Fuller, J.D., Lawrence, P., Young, G.R., Russell, J., Ramsay, L., Waugh, R., and Powell, W. (1998). Identification of a QTL decreasing yield in barley linked to *Mlo* powdery mildew resistance. Mol. Breed. 4: 381–393.

Thomas, W.T.B., Powell, W., Waugh, R., Chalmers, K.J., Barua, U.M., Jack, P., Lea, V., Forster, B.P., Swanston, J.S., Ellis, R.P., Hanson, P.R., and Lance, R.C.M. (1995). Detection of quantitative trait loci for agronomic, yield, grain and disease characters in spring barley (*Hordeum vulgare* L.). Theor. Appl. Genet. 91: 1037–1047.

Thomma, B. P., Nürnberger, T., and Joosten, M. H. (2011). Of PAMPs and Effectors: The Blurred PTI-ETI Dichotomy. *The Plant Cell*, *23*(1), 4–15.

Toruño, T. Y., Stergiopoulos, I., and Coaker, G. (2016). Plant-Pathogen Effectors: Cellular Probes Interfering with Plant Defenses in Spatial and Temporal Manners. *Annual Review of Phytopathology*, *54*(1), 419–441.

United States Department of Agriculture, Foreign Agricultural Service (USDA-FAS). (2022). World Agricultural Production. Available online at https://apps.fas.usda.gov/psdonline/circulars/production.pdf

Urrea, C. A., Horsley, R. D., Steffenson, B. J., and Schwarz, P. B. (2005). Agronomic Characteristics, Malt Quality, and Disease Resistance of Barley Germplasm Lines with Partial Fusarium Head Blight Resistance. *Crop Science*, *45*(4), 1235–1240.

Van den Berg, C., and Rossnagel, B. (1990). Effects of temperature and leaf wetness period on conidium germination and infection of barley by*Pyrenophora teres*. *Canadian Journal of Plant Pathology*, *12*(3), 263–266.

van Esse, G. W., Walla, A., Finke, A., Koornneef, M., Pecinka, A., and Von Korff, M. (2017). Six-Rowed Spike3 (VRS3) is a histone demethylase that controls lateral spikelet development in barley. *Plant physiology*, *174*(4), 2397-2408.

Wang, X., Mace, E. S., Platz, G. J., Hunt, C. H., Hickey, L. T., Franckowiak, J. D., and Jordan, D. R. (2015). Spot form of net blotch resistance in barley is under complex genetic control. *Theoretical and Applied Genetics*, *128*(3), 489–499.

Wang, Y. L., Ye, H., Liu, L., Wu, J. H., Ru, W. M., and Sun, G. L. (2019). Molecular insights on the domestication of barley (Hordeum vulgare L.). *Critical reviews in plant sciences*, *38*(4), 280-294.

Weaver, J. C. (1950). American Barley Production. Burgess Publishing, Minneapolis, MN.

Wegulo, S. N., Baenziger, P. S., Hernandez Nopsa, J., Bockus, W. W., and Hallen-Adams, H. (2015). Management of Fusarium head blight of wheat and barley. *Crop Protection*, *73*, 100–107.

Weiberg, A., Wang, M., Lin, F. M., Zhao, H., Zhang, Z., Kaloshian, I., ... and Jin, H. (2013). Fungal small RNAs suppress plant immunity by hijacking host RNA interference pathways. *Science*, *342*(6154), 118-123.

Weiergang, I., Lyngs JØrgensen, H., MØller, I., Friis, P., and Smedegaard-petersen, V. (2002). Correlation between sensitivity of barley to Pyrenophora teres toxins and susceptibility to the fungus. *Physiological and Molecular Plant Pathology*, *60*(3), 121–129.

Whipple, C. J., Kebrom, T. H., Weber, A. L., Yang, F., Hall, D., Meeley, R., ... and Jackson, D. P. (2011). grassy tillers1 promotes apical dominance in maize and responds to shade signals in the grasses. *Proceedings of the National Academy of Sciences*, *108*(33), E506-E512.

Williams, K. J., Lichon, A., Gianquitto, P., Kretschmer, J. M., Karakousis, A., Manning, S., Langridge, P., and Wallwork, H. (1999). Identification and mapping of a gene conferring resistance to the spot form of net blotch (Pyrenophora teres f maculata) in barley. *Theoretical and Applied Genetics*, *99*(1–2), 323–327.

Williams, K. J., Platz, G. J., Barr, A. R., Cheong, J., Willsmore, K., Cakir, M., and Wallwork, H. (2003). A comparison of the genetics of seedling and adult plant resistance to the spot form of net blotch (Pyrenophora teres f. maculata). *Australian Journal of Agricultural Research*, *54*(12), 1387.

Xu, Y., Jia, Q., Zhou, G., Zhang, X. Q., Angessa, T., Broughton, S., ... and Li, C. (2017). Characterization of the sdw1 semi-dwarf gene in barley. *BMC plant biology*, *17*(1), 1-10.

Youssef, H. M., Eggert, K., Koppolu, R., Alqudah, A. M., Poursarebani, N., Fazeli, A., ... and Schnurbusch, T. (2017). VRS2 regulates hormone-mediated inflorescence patterning in barley. *Nature Genetics*, *49*(1), 157-161.

Zhu, H., Gilchrist, L., Hayes, P., Kleinhofs, A., Kudrna, D., Liu, Z., Prom, L., Steffenson, B., Toojinda, T., and Vivar, H. (1999). Does function follow form? Principal QTLs for Fusarium head blight (FHB) resistance are coincident with QTLs for inflorescence traits and plant height in a doubled-haploid population of barley. *Theoretical and Applied Genetics*, *99*(7–8), 1221–1232.

Zwirek, M., Waugh, R., and McKim, S. M. (2019). Interaction between row-type genes in barley controls meristem determinacy and reveals novel routes to improved grain. *New phytologist*, *221*(4), 1950-1965.

CHAPTER 2: GENETIC MAPPING OF HOST RESISTANCE TO THE PYRENOPHORA TERES F. MACULATA ISOLATE 13IM8.3[2]

Abdullah Fahad Alhashel[1, 2], Roshan Sharma Poudel[1], Jason Fiedler[3, 4], Craig H. Carlson[4], Jack Rasmussen[1], Thomas Baldwin[1], Timothy L. Friesen[1, 4], Robert S. Brueggeman[5], Shengming Yang[1, 3, 4,*]

[1] Department of Plant Pathology, North Dakota State University, Fargo, ND 58102, USA
[2] Department of Plant Protection, College of Food and Agriculture Sciences, King Saud University, Riyadh 11451, Saudi Arabia
[3] Department of Plant Sciences, North Dakota State University, Fargo, ND 58102, USA
[4] Cereals Crops Research Unit, Edward T. Schafer Agriculture Research Center, USDA-ARS, Fargo, ND 58102, USA
[5] Department of Crop and Soil Sciences, Washington State University, Pullman, WA 99164
*Author to whom correspondence should be addressed; E-Mail: Shengming.Yang@usda.gov Tel.: +1-701-412-1309; Fax: +1-701-412-1369.

Abstract

Spot form net blotch (SFNB), caused by the necrotrophic fungal pathogen *Pyrenophora teres* f. *maculata* (*Ptm*), is a foliar disease of barley that results in significant yield losses in major growing regions worldwide. Understanding the host-parasite interactions between pathogen virulence/avirulence genes and the corresponding host susceptibility/resistance genes is important for the deployment of genetic resistance against SFNB. Two recombinant inbred mapping populations were developed to characterize genetic resistance/susceptibility to the *Ptm* isolate 13IM8.3, which was collected from Idaho (ID). An Illumina Infinium array was used to produce a genome wide marker set. Quantitative trait loci (QTL) analysis identified ten significant resistance/susceptibility loci, with two of the QTL being common to both populations. One of the QTL on 5H appears to be novel, while the remaining loci have been reported

[2] SY conceived and designed the project. AFA performed most of the experiments in collaboration with all other authors. RSP, JDF, and CHC contributed new reagents/analytic tools. AFA and SY wrote the first draft of the manuscript. All authors including JR, TB, and RSB commented on previous versions and approved the final version of the manuscript.

previously. Single nucleotide polymorphisms (SNPs) closely linked to or delimiting the significant QTL have been converted to user-friendly markers. Loci and associated molecular markers identified in this study will be useful in genetic mapping and deployment of the genetic resistance to SFNB in barley.

KEYWORDS

Barley Spot form net blotch Genetic mapping SNP array Disease resistance

Introduction

Barley (*Hordeum vulgare* L.) is one of the most important and first-cultivated cereal crops globally. It belongs to the monocotyledonous grass family Poaceae. It is mostly utilized for malting, but also as animal fodder and human food (Poehlman 1994). However, barley production is severely compromised by many diseases. Of those, net blotch, caused by the necrotrophic fungal pathogen *P. teres,* has emerged as one of the most prevalent foliar diseases resulting in significant yield losses (Liu *et al.,* 2011).

Net blotch occurs in two forms, spot-form net blotch (SFNB) and net-form net blotch (NFNB) caused by *P. teres* f. *maculata* (*Ptm*) and *P. teres* f. *teres* (*Ptt*), respectively. Although morphologically identical, *Ptm* and *Ptt* are genetically distinct and induce different symptoms on susceptible host genotypes. Recently, SFNB has become more prevalent in barley growing regions worldwide (Liu *et al.,* 2011). The *Ptm* pathogen favors high humidity, precipitation, and cool temperatures, resulting in elliptical necrotic lesions surrounded by chlorosis on susceptible barley plants. Management strategies to reduce disease pressure and avoid economic losses include fungicide application and cultural practices such as tillage, crop rotation, and low crop density. It is well known that the deployment of host resistance is the most effective and environment-friendly strategy for SFNB control (McLean *et al.,* 2009*,* Liu *et al.,* 2011). However, compared to NFNB, our understanding on the SFNB resistance is limited.

Ptm populations can be sexually and asexually reproduced and thus their virulence profiles have the potential to change rapidly (Arabi *et al.,* 2003*,* McLean *et al.,* 2014). Due to the diversity of *Ptm* virulence effectors, host resistance to SFNB is usually quantitative and under complex genetic control (Wang *et al.,* 2015). Many QTL across all seven barley chromosomes conferring SFNB resistance at seeding or adult stages have been identified by several mapping

studies using various pathotypes (Clare *et al.,* 2020). A few major QTL conferring seedling resistance/susceptibility to SFNB were consistently identified in most of these studies, such as *Rpt4* (or *QRpt7*) on 7H (Grewal *et al.,* 2008*,* Manninen *et al.,* 2006*,* Richards *et al.,* 2016), *Rpt6* on 5H (Manninen *et al.,* 2006), *Rpt8* on 4H (Franckowiak and Platz 2013*,* Friesen *et al.,* 2006*,* Daba *et al.,* 2019), *Rpt7* (*QRpts4*, *Rpt-4H-5-7*, or *QPt.4H-3*) on 4H (Franckowiak and Platz 2013*,* Raman *et al.,* 2003*,* Yun *et al.,* 2005*,* Vatter *et al.,* 2017), and *QRpt6* (or *Rpt5/Spt1*) on 6H (Manninen *et al.,* 2006*,* Richards *et al.,* 2016*,* Grewal *et al.,* 2008*,* Grewal *et al.,* 2012). In a recent effort to determine if susceptible or resistant elite lines contained common susceptibility/resistance loci to diverse *Ptm* isolates, a major QTL on 7H, named *QRptm-7H-119-137*, was found to be a dominant susceptibility gene in susceptible barley lines (Tamang *et al.,* 2019). Very likely, this locus is the same as those previously reported, because it resides in the same region as *Rpt4* and *QRpt7* (Tamang *et al.,* 2019).

Moreover, due to the diversity of *Ptm* virulence effectors (Duellman 2015), a specific resistance locus may be effective against a certain pathotype, but it may be susceptible to other pathotypes from other regions. Regional differences in virulence and variation in pathotypes of *Ptm* populations have been identified in several independent studies. Khan and Tekauz (1982) compared 16 barley genotypes challenged with two groups of *Ptm* isolates, each from Western Australia and Canada. Fourteen responded similarly but two cultivars showed differential reactions to the two groups of isolates (Khan and Tekauz 1982). Differential reactions were also observed when 20 barley genotypes were challenged with 15 and 5 *Ptm* isolates from Montana and Mediterranean regions, respectively. The Montana isolates tended to cause more necrosis and chlorosis than the Mediterranean isolates (Karki and Sharp 1986). Neupane *et al.,* (2015) also found that an isolate from the United States appeared to be more virulent than isolates from

Australia, New Zealand, and Denmark. Virulence of 177 *Ptm* isolates collected from six regions in North Dakota, Montana and Idaho was assessed with thirty barley genotypes (Duellman 2015). It was shown that the Idaho isolates, including 13IM8.3, were differentiated from others based on the population structure analysis and virulence profile. The Idaho isolates possessed a significantly different virulence profile in comparison with isolates collected from other regions, suggesting a distinct set of virulence/avirulence effectors. However, host genes conferring resistance/susceptibility to these unique Idaho isolates have not been identified.

Since the migration of pathogen populations among barley growing regions commonly occurs, there was a need to identify resistance to the Idaho *Ptm* isolates before they migrated to other barley growing regions. In the meanwhile, novel loci or alleles for SFNB resistance may be discovered and can be exploited for breeding purposes. Therefore, in the present study, we conducted genetic analysis with two bi-parental populations to identify QTL conferring resistance/susceptibility to the unique Idaho *Ptm* isolate 13IM8.3.

Materials and Methods

Plant Materials

Genetic mapping was carried out using two recombinant inbred line (RIL) populations developed by single-seed descent. One RIL population (CI97_CI92) consisted of a total of 143 $F_{2:6}$ progenies derived from a cross between the six-rowed South Korean landrace CIho 9214 (CI9214) and the two-rowed Morroccan line CI9776. Previously used by Koladia *et al.,* (2017), the second population (CT) contained 117 $F_{2:6}$ progenies derived from a cross between an Ethiopian breeding line CI5791 and a Manchurian line Tifang. Both CI5791 and CI9776 are susceptible, whereas CI9214 and Tifang are resistant to the *Ptm* isolate used in this study (Duellman 2015).

Disease Phenotyping

The *Ptm* isolate 13IM8.3, collected from Idaho, USA, was used to phenotype the CI97_CI92 and CT RIL populations. Inoculum preparation, inoculation, phenotyping, and rating scale were conducted as described previously by Neupane *et al.,* (2015) with some modifications. In brief, the inoculum was cultured on V8-PDA media (150 ml V8 juice, 10 g Difco PDA, 3 g $CaCO_3$,10 g agar, and 850 ml H_2O) under a 12h/12h - light/dark condition for good sporulation. The conidial concentration was adjusted to 2,000 conidia/ml for inoculation after conidia were harvested using sterile distilled water. Two drops of Tween 20 were applied to every 100 ml inoculum. Each RIL was planted in a single cone (3.8 cm diameter x 20 cm long) with three seeds per cone, and all cones were placed on racks bordered with the susceptible check (Pinnacle) to reduce any edge effect. Each rack also contained the two parental lines, resistant check (PI67381) and susceptible check (Pinnacle). A complete randomized design was used for each rack, and plants were placed inside a growth chamber with a 16 h light, 21°C/8 h dark, 21°C regime. Inoculation was performed at the seedling stage when the second leaf was fully expanded (~ two weeks) using an air sprayer at 15 to 20 psi. Before the inoculated plants were moved back into the growth chamber, they were kept at 100% relative humidity for 24 hours under continuous light. Phenotyping was conducted 7 days post inoculation (DPI) using a 1–5 rating scale with 1 being highly resistant (small pinpoint lesions with no surrounding necrosis) and 5 being highly susceptible (necrotic lesions coalescing and covering greater than 70% of the leaf area) (Neupane *et al.,* 2015). Plants displaying approximately equal amounts of two reaction types were rated as intermediate. For example, equal amounts of reaction type 2 and 3 were given a 2.5 rating. The three plants in each cone were scored collectively as a single

replicate, and three independent replicates for each RIL population were sequentially assessed. The average value of the three replicates was used as the phenotypic score.

SNP Genotyping

DNA was extracted according to the CTAB protocol (Murray and Thompson 1980). Around 100 mg leaf samples were collected from plants at the three-leaf stage and quantified using a NanoDrop 8000 spectrophotometer (NanoDrop, Thermo Fisher Scientific) according to the manufacturer's instructions. The final concentration was adjusted to 100 ng/µL for further analysis. The CI97_CI92 RIL population was genotyped with the barley 50k iSelect SNP Array (Bayer *et al.,* 2017). Genotype calling was performed with the *de novo* calling algorithm in GenomeStudio V3.0 (Illumina). Clusters of polymorphic SNPs were inspected and manually adjusted if necessary. Genotyping data for the CT population was obtained from the previous study (Koladia *et al.,* 2017), which was conducted by using the 9k iSelect SNP Array including 7824 markers (Comadran *et al.,* 2012).

Linkage Mapping

Called SNPs derived from the CI97_CI92 population were filtered to maintain a minor allele frequency (MAF) > 0.05 and missing data < 10%, and used to generate a genetic map with Mapdisto version 2.1.7 (Lorieux 2012). Linkage groups were identified using the default minimum LOD of 3.0, r_{max} of 0.3, and the Kosambi mapping function (Kosambi 1943) was used to estimate genetic distance. Redundant co-segregating markers were thinned to a single marker, and linkage groups were then refined and validated using the 'ripple order', 'check inversions', and 'drop locus' commands. Linkage analysis for the CT population was adopted from Koladia *et al.,* (2017).

Assessment of Map Order and Quality

Marker sequences were aligned to the *H. vulgare* cv. 'Morex' v3 reference genome assembly (Mascher *et al.,* 2021) via standalone BLAST version 2.12.0 using 'makeblastdb' and 'blastn' with default parameters and an e-value of 1×10^{-5}. The highest bitscore was used to determine approximate physical position. In instances where sequences were best aligned (highest bitscore) to unassembled scaffolds (chrUn), the next best pseudomolecule hit was returned. For both mapping populations, pairwise recombination fractions and LOD linkage between markers were visualized using heatMap (lmax =12, rmin = 0) in ASMap (Taylor and Butler, 2017) in R (R Core Team, 2021).

QTL Analysis

Average disease score from four independent replicates and the MapDisto marker positions were used for QTL analysis with QGene version 4.4.0 (Joehanes and Nelson 2008). The single-trait multiple interval mapping-generalized liner model (MIM-GLZ) method was applied to locate significant QTL conferring resistance/susceptibility to 13MI8.3. A permutation test was conducted with 1000 iterations to identify LOD thresholds at significance levels of α = 0.05 and α = 0.01. The consistency of genetic and physical locations for markers linked to QTL were checked manually.

Marker Development

The linked SNPs to resistance/susceptibility in either populations were used to develop semi-thermal asymmetric reverse PCR (STARP) markers to genotype the selected RILs from both populations (Long *et al.,* 2017). PCR was conducted in a 10 µl reaction volume consisting of 100 ng genomic DNA, 0.9x $NH4^+$ buffer, 1.5 mM $MgCl_2$, 50 uM dNTPs, 0.8 M betaine, 0.04% (w/v) bovine serum albumin (BSA), 200 nM common reverse primer, 200 nM of each

priming element-adjustable primer (PEA-primer 1 and PEA-primer 2), 40 nM of each asymmetrically modified allele-specific primer (AMAS forward primer1 and AMAS forward primer 2), and 1 U of Taq DNA polymerase (without 3' -> 5' exonuclease activity). Sequences of PEA-primer 1 and 2 are 5′-AGCTGGTT-SP9-GCAACAGGAACCAGCTATGAC-3' and 5'-ACTGCTCAAGAG-SP9-GACGCAAGTGAGCAGTATGAC-3', respectively. PCR conditions were 94°C for 5 min followed by 6 cycles of 94°C for 30 s, 56°C for 2 min, and the annealing temperature decreased 1°C each cycle. This touchdown cycle was followed by 40 cycles of 94°C for 20 s, 62°C for 30 s, 72°C for 1 min, and a final extension at 72°C for 10 min. Amplicons were electrophoresed on 6% polyacrylamide gels, stained with GelRed™ nucleic acid stain (MilliporeSigma), and imaged using a Typhoon™ FLA 9500 variable mode laser scanner (GE Healthcare Life Sciences, Marlborough, MA).

Results

Trait Evaluations

Based on the rating scale of 1-5 described by Neupane *et al.,* (2015), resistant parental lines CI9214 and Tifang exhibited average disease reactions of 1.25 and 1.08, while CI9776 and CI5791 were intermediately susceptible with average disease reactions of 3 and 2.8, respectively (Table 2.1). The CI97_CI92 population appeared to be more susceptible based on the higher susceptibility of the parents and progenies in comparison to those of CT (Table 2.1*,* Tables A1 and A2). The CT population expressed average disease reactions that ranged from 1 to 3.1 in response to the pathogen (Table 2.1*,* Tables A1 and A2). It is noteworthy that, although we did not observe RILs that were more resistant than Tifang or CI9214 in the respective populations, some lines displayed higher reaction types than their susceptible parents. Therefore, transgressive segregation for susceptibility might be present in both evaluated populations.

Table 2.1. Summary of phenotype evaluations for both RIL populations.

Population	Resistant parent (RP)	Susceptible parent (SP)	Range	Average
CI97_CI92	1.25 ± 0.25	3.0 ± 0	1.3 ± 0.38 — 3.9 ± 0.25	2.47 ± 0.5
CT	1.08 ± 0.14	2.8 ± 0.14	1 ± 0 — 3.1 ± 0.42	1.92 ± 0.54

Mean value and standard deviation were given for disease severity. Value represents rating scale, with a higher value indicating more susceptibility and a lower value indicating more resistance.

QTL Mapping with the CI97_CI92 Population

A total of 11756 SNPs was called with the CI97_CI92 population, selected with MAF > 0.05 and missing data < 10%. Of those, 1750 non-redundant markers were identified by Mapdisto for linkage mapping (Table S3). Seven linkage groups (LGs) were constructed with a total map length of 920.53 cM and an average marker density of 0.53 cM/locus (Table A3). The genetic map quality was evaluated by generating a heat map using pair-wise recombination values for the mapped SNPs (Figure 2.1A). The LGs are distinctly clustered, and strong linkage between nearby markers was indicated by the consistent heat across the markers within LGs (Figure 2.1A). The genetic positions of the SNPs were plotted against their physical positions to highlight the potential ordering errors (Figure 2.1B). Although one outlier each in LG2 and LG7, in general, marker order was extensively conserved on each chromosome (Figure 2.1B). Significant QTL were detected with LOD thresholds of 3.807 and 5.654 calculated with 1000 permutation at significant levels of 0.05 and 0.01, respectively.

A QTL associated with the SNP SCRI_RS_165434, designated *QRptm-1H-108-122* (based on the LG and genetic location), was mapped on chromosome 1H with a LOD value of 5.556 and R^2 = 16.4% (Figure 2.1C, Table A5). Flanked by SNPs JHI-Hv50k-2016-55796 (516.6 Mb) and SCRI_RS_175218 (520.65 Mb), QTL *QRptm-3H-45-52* with a LOD value of 6.97 and R^2 = 20.1% was detected on 3H. Two significant QTL were mapped on chromosome 4H. QTL

QRptm-4H-93-109 contributes the largest effect to the disease phenotype with R^2 = 36.8% and the highest LOD score of 14.24, delimited by SNPs JHI-Hv50k-2016-268933 (609.39 Mb) and JHI-Hv50k-2016-272270 (616.55 Mb) (Figure 2.1C*,* Table A5). The other locus on 4H, designated as *QRptm-4H-43-57* between SNPs SCRI_RS_188822 (876.2 Mb) and SCRI_RS_10607 (457.88 Mb), was identified as the second largest major QTL (LOD = 12.65, and R^2 = 33.5%) (Figure 2.1C*,* Table A5). A significant QTL on 5H (*QRptm-5H-12-21*), flanked by SNPs JHI-Hv50k-2016-278862 (4.663 Mb) and JHI-Hv50k-2016-281470 (9.353 Mb), only contributed a minor effect on disease phenotype. Positioned between SNPs JHI-Hv50k-2016-500801 (597.29 Mb) and SCRI_RS_130990 (602.19 Mb), one QTL was mapped on 7H, named *QRptm-7H-96-107,* accounting for only 20.6% phenotypic variation and exhibiting a LOD score of 7.174 (Figure 2.1C*,* Table A5).

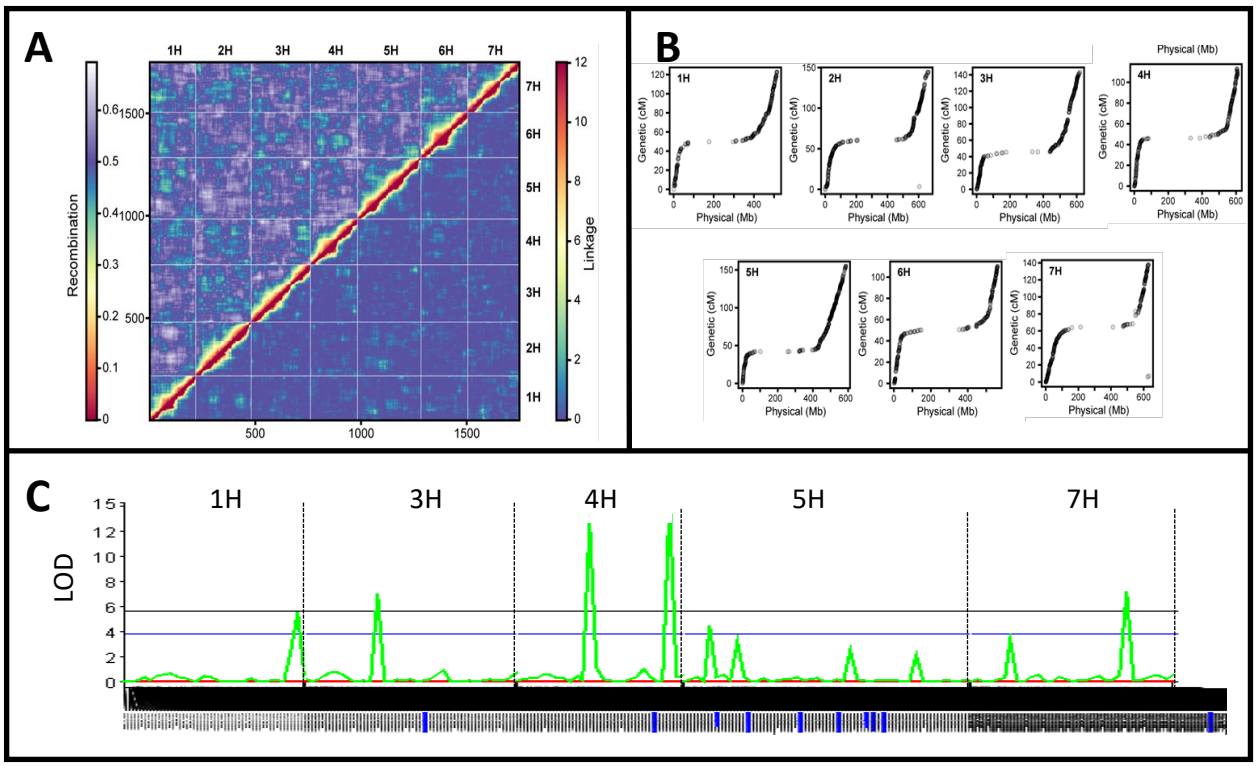

Figure 2.1. QTL mapping of SFNB resistance/susceptibility with the CI97_CI92 population. **A** Heat map showing a matrix of pair-wise recombination values for markers along LGs. The X-axis and Y-axis represent markers. The markers of each row and column were ordered according to the genetic map. The colors represent the strength of linkage in recombination values between all pairs of markers. The blue color indicates the highest recombination scores, which suggest no linkage between markers. The red color indicates the lowest recombination scores, which suggest a strong linkage between markers. **B** Scatter plots showing **c**omparison between genetic and physical positions for the markers on LG1 - LG7. Physical distance is on the X-axis, and genetic distance is on the Y-axis. The physical positions with low recombination rates represent the centromere regions, and telomeres have higher recombination rates. **C** QTL mapping. Position of markers is shown on the X-axis and LOD values on the Y-axis. The LOD threshold lines were represented by the blue and black lines at 0.05 and 0.01 significance levels, respectively. A total of 6 significant QTL ($\alpha = 0.05$) were identified in this population.

QTL Mapping with the CT Population

Genetic maps for the CT population were obtained from Koladia *et al.,* (2017). In brief, 827 non-redundant SNP markers (Table S5) were used to create 7 linkage groups with a total length of 1012.2 cM and marker density of 1.2 cM/locus (Table A4). Tight linkage between adjacent markers on each LG was indicated by the heat map, and it changed to weak gradually

when genetic distance increased (Figure 2.2A). A one-to-one correspondence was observed when we compared genetic and physical positions for the mapped markers (Figure 2.2B). It was showed that the SNPs were well ordered. Therefore, the genetic map was generated with high quality and reliability for QTL analysis. Significant QTL were identified with LOD thresholds of 4.774 and 6.307 calculated by 1000 permutation at significant levels of 0.05 and 0.01, respectively. Overall, four significant QTL were detected in this population ($\alpha = 0.05$) and three were highly significant ($\alpha = 0.01$).

A major QTL was mapped on 4H, *QRptm-4H-4-8*, accounting for 71.64% phenotypic variation with the highest LOD value and additive effect of 31.95 and 0.4, respectively (Figure 2.2C, Table A6). This QTL (chr4: 612295812-624215195) resides at the similar physical position with *QRptm-4H-93-109* (chr4: 606875364-621950894) which was identified in CI97_CI92 (Tables A5 and A6), suggesting they may be allelic. The QTL on 5H, *QRptm-5H-81-88* was identified with a LOD value of 5.38 and $R^2 = 19.1\%$ (Figure 2.2C, Table A6). This QTL was positioned between SNPs SCRI_RS_231239 (519.31 Mb) and SCRI_RS_88710 (514.85 Mb) (Figure 2.1C). One minor QTL each was detected on 6H and 7H with similar R^2 values, named *QRptm-6H-60-64* ($R^2 = 25.1\%$) and *QRptm-7H-34-38* ($R^2 = 28.8\%$), respectively (Figure 2.2C, Table A6). Indicated by positions of closely linked SNPs, *QRptm-7H-34-38* on 7H may be at the same locus with *QRptm-7H-96-107* which was identified in CI97_CI92.

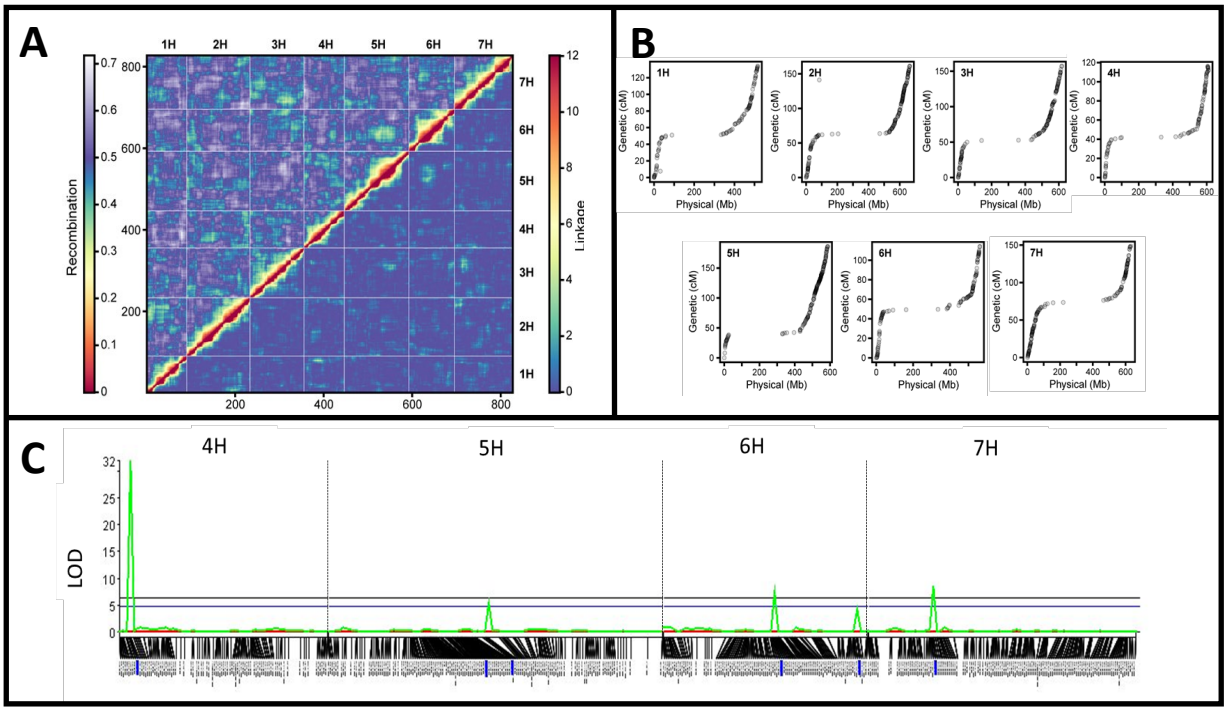

Figure 2.2. QTL mapping of SFNB resistance/susceptibility with the CT population. Heat map indicated strong linkage between nearby markers (A). Scatter plots showed genetic position is consistent with physical positions for the mapping SNPs on LG1 -LG7 (C). QTL mapping idented a total of 4 significant QTL ($\alpha = 0.05$) (C). The LOD threshold lines were represented by the blue and black lines at 0.05 and 0.01 significance levels, respectively.

Development of User-Friendly Markers

QTL with major effect have great potential in breeding applications. Therefore, user-friendly markers are required for effective breeding selection. Based on the high-resolution genetic maps generated in the present study, we converted the peak SNPs to PCR-based STARP markers for the significant QTL (Table A7). Different alleles for each locus can be distinguished unambiguously with these markers (Figures A1-2). These markers also can be used to develop segregating sub-populations to finely localize the major QTL for the purpose of gene cloning. Moreover, marker analysis also indicated susceptible alleles were contributed by the resistant parent at several loci, such as *QRptm-3H-45-52* and *QRptm-5H-12-21* in CI97_CI92, and

QRptm-5H-81-88 and *QRptm-6H-60-64* in CT (Figures A1-2, Tables A5 and A6). We tested an SFNB differential set of 31 barley lines for reaction response to 13IM8.3 (Table 2.2). Genotyping survey showed that the QTL peak markers were not diagnostic across these 31 lines (Fig. A3). It was indicated novel resistance/susceptibility QTL might be carried by the differential lines.

Table 2.2. Reaction response of 31 differential lines to 13IM8.3.

Genotype	Disease severity	Category[a]
Pinnacle	4.83 ± 0.14	
81-82/033	4 ± 0.43	
Arimont	3.83 ± 0.76	
Chebec	4.33 ± 0.14	
Skiff	5 ± 0	
CI3576	3.5 ± 0.25	
CIho3694	3.92 ± 0.63	
Ciho4050	4.92 ± 0.14	
MXB468	4.5 ± 0.25	
PI269151	4.83 ± 0.14	
PI369731	2.75 ± 0.66	Susceptible
PI392501	3.58 ± 0.58	
PI467375	4.25 ± 0.25	
PI467729	5 ± 0	
PI485524	3 ± 0	
PI498434	4.42 ± 0.38	
PI573662	5 ± 0	
TR250	2.58 ± 0.38	
TR326	3.08 ± 0.14	
Golden Promise	4.83 ± 0.29	
Tradition	4 ± 0.25	
Keel	2.17 ± 0.58	
Kombar	1.75 ± 0.43	
CI9819	1.83 ± 0.14	
CI7584	1.5 ± 0	
CI14219	2.25 ± 0.25	Resistant
CI2353	2.17 ± 0.63	
PI513205	1.42 ± 0.14	
PI565826	1.5 ± 0.25	
PI67381	1.67 ± 0.14	
PI84314	1.42 ± 0.29	

[a] Disease score ≥ 2.5 was considered as susceptible in this study.

Discussion

Localization of QTL is important for the development of genetic markers, determination of novel loci, and for the ultimate cloning of responsible genes to understand genetic mechanisms underlying disease resistance/susceptibility. This *Ptm* isolate 13IM8.3, collected from Idaho, exhibited a virulence profile distinct from isolates collected from other nearby regions in the US (Duellman 2015). The regional differentiation might be caused by the susceptibility of locally predominant varieties. To cope with the potential prevalence and invasion of this unique isolate in new barley growing areas, effective resources for advanced and higher resistance is needed.

Using two biparental populations, we conducted QTL mapping to identify loci resistant/susceptible to 13IM8.3 in this study. High quality and reliability of genetic maps was demonstrated by heat maps and the scatter plots of marker genetic position against physical position. Six and four significant QTL ($\alpha = 0.05$) were detected in the CI97_CI92 and CT population, respectively. Although the additive effect exerted by the QTL on the phenotype value ranges 0.12 - 0.23 or 0.12 - 0.4, total additive effect is 1.06 or 0.83 in the populations (Tables A5 and A6). Considering the phenotype difference between parental lines is 1.8 in both populations (Table 2.1), pyramiding the homozygous resistant QTL alleles will significantly improve barley resistance to 13IM8.3. However, due to the complex nature of resistance to SFNB, the putative QTL need to be validated in different populations or under different environments.

Several *Ptm* resistance QTL have been identified on 1H using double haploid populations and association mapping panels (Wang *et al.,* 2015*,* Tamang *et al.,* 2015). Most of them are distant from *QRptm-1H-108-122*, the QTL we identified in the CI97_CI92 population. However,

the *QRptms1* locus, which provides resistance against the Canadian isolate WRS857 at the seedling stage is contiguous to this location (Grewal *et al.,* 2012). Furthermore, the *Qns-1H* QTL conferring resistance to net blotch under field conditions is also physically close to this position (Daba *et al.,* 2019). The QTL identified on 1H, *QRptm-1H-108-122*, may reside at the same locus with *QRptms1* and *Qns-1H* (Table A5).

Closely linked to the SNP SCRI_RS_152172, *QRptm-3H-45-52* was flanked by SNPs of BOPA1_10126_999 (446.7Mb) and SCRI_RS_222102(476.6 Mb) (Table A5). Various studies have identified QTL for resistance/susceptibility to both forms of net blotch, and several of them are close to or overlapped with *QRptm-3H-45-52*, such as *QTL_Tamang_3H_65.16*, *QRptms3-2* and *SFNB-3H-58.64* (Wang *et al.,* 2015*,* Burlakoti *et al.,* 2017*,* Tamang *et al.,* 2015). These QTL only provide minor effects to their corresponding isolates with R^2 values of < 10%. However, two other QTL identified in the same location with *QRptm-3H-45-52*, *Qns-3H.3* and *QRptm-3H-56-65*, explained >20% disease variation against isolates ND111 and SG1, respectively (Daba *et al.,* 2019*,* Tamang *et al.,* 2019). Thus, the QTL on 3H reported here might be the same as those previously detected to interact with different *Ptm* isolates at this location.

Strikingly, the loci on 4H identified in both populations contributed major effects to the 13IM8.3 susceptibility/resistance. Flanked by SCRI_RS_188822 (876.2 kb) and SCRI_RS_10607 (457.88 Mb), *QRptm-4H-43-57* was detected in the CI97_CI92 population only (Table A5*,* Figure 2.1C). Based on the physical location, it may be same with *QTL_Tamang_4H_47.17* (against the *Ptm* isolate *SG1)*, and *QTL_Tamang_4H_53.67-59.22* (against *Ptm* isolates of *DEN2.6* and *NZKF2*), (Tamang *et al.,* 2015*,* Tamang *et al.,* 2019). This locus was also identified as *QRpts4*, *AL_QRptt4-1*, and *Rpt7* showing significant effectiveness to various *Ptt* isolates (Franckowiak and Platz 2013*,* Raman *et al.,* 2003*,* Grewal *et al.,* 2008). As

for the second QTL (*QRptmB-4H-42-49.2* or *QRptm-4H-4.4-8.9*), it functions in both populations as a major locus. Particularly in CT, it accounts for 72% of disease phenotype, acting as a major susceptibility gene. This locus may have been detected and designated as *Rpt8* (Table A6) (Franckowiak and Platz 2013). It was previously identified as *QRpts4* or *Qns-4H.2* for seedling resistance to net blotch (Daba *et al.,* 2019*,* Grewal *et al.,* 2008), an unnamed major locus on 4H for seedling resistance to SFNB (Friesen *et al.,* 2006), and *QNFNBAPR.Al/S-4Hb* for adult resistance to NFNB (Lehmensiek *et al.,* 2007). Therefore, this QTL provides broad-spectrum resistance to net blotch and has a significant potential for barley genetic improvement.

The QTL *QRptm-5H-12-21* on 5H was identified with the CI97_CI92 population, and is flanked by JHI-Hv50k-2016-278862 (466.37 kb) and JHI-Hv50k-2016-281470 (935.35 kb) (Figure 2.1C*,* Table A5). Although it is a minor gene in the present study, this locus may be the same as *Rpt6*, a major isolate-specific resistance gene explaining up to 84% of the phenotypic variation in infection response to *Ptm* in the Ethiopian line CI9819 (Manninen *et al.,* 2006). Another QTL on 5H identified with CT, *QRptm-5H-81-88*, spans a 5.5 Mb region (Table A6). This locus has not been reported for resistance to any forms of net blotch. Therefore, it appears to be a novel locus for the resistance to *Ptm*.

The QTL on 6H, *QRptm-6H-60-64*, was identified in the CT population only. Its physical position indicated it might be *QRpt6* or the *Rpt5*/*Spt1* locus (Table A6) (Franckowiak and Platz 2013*,* Manninen *et al.,* 2006*,* Shjerve *et al.,* 2014*,* Friesen *et al.,* 2006*,* Martin *et al.,* 2018*,* Liu *et al.,* 2015*,* Liu *et al.,* 2010*,* Richards *et al.,* 2016). The *Rpt5* region is highly complex and has been extensively studied for resistance to NFNB (Richards *et al.,* 2016*,* Abu Qamar *et al.,* 2008*,* Liu *et al.,* 2010). The *Rpt5* allele in CI5791 provides dominant resistance to certain *Ptm* isolates, but it also confers dominant susceptibility in other barley genotypes. Differential disease

phenotype may depend on the allele-effector combinations underlying the barley-*Ptt* interaction (Richards *et al.,* 2016*,* Clare *et al.,* 2020). Genetic mapping delimited this locus within a ~9.5 Mb region, and six putative immunity receptor-like genes were selected as candidates (Richards *et al.,* 2016). However, it has been inconclusive if this locus contains a single gene, two tightly linked genes, or a "susceptibility island" comprising multiple genes in recognition of various necrotrophic effectors (Richards *et al.,* 2016). The further confirmation and validation of these candidate genes will help understand the molecular basis of the Rpt5/Spt1 function.

The QTL on 7H identified in CI97_CI92 and CT locate to a similar position, which is overlapped with *Rpt4, QRpt7* or *QRptm7-6* providing resistance/susceptibility to *Ptm* at both seedling and adult stage (Tables A5 and A6) (Williams *et al.,* 2003*,* Wang *et al.,* 2015*,* Grewal *et al.,* 2008*,* Clare *et al.,* 2020). A major locus at the same location was once identified in Tradition and Pinnacle conferring broad susceptibility to *Ptm* isolates collected from different countries (Tamang *et al.,* 2019). In the present study, this locus only explained 20-28% of phenotype variation.

Although six and four QTL were identified respectively by the 50k and 9k SNP array, it does not mean that the 9k array has a lower power for QTL detection. A simulation study for interval mapping showed that a marker density of 10–20 cM is sufficient for precise QTL detection, and higher marker densities had no advantages in precision of QTL localization and estimation of genetic effects (Darvasi *et al.,* 1994). Similar findings were also reported by Piepho (2000) that marker densities below 10 cM have insignificant effects on QTL analysis. Another simulation based on linkage maps with marker densities of 1, 2, and 5 cM confirmed that high-density maps neither improved the QTL detection power nor the valuation of QTL effect (Stange et al., 2013). In our study, while the 'CI97_CI92' map more completely saturated the barley

genome, genetic to physical distances were not appreciably dissimilar from the 'CT' population (Figures 1B and 2B). Nevertheless, Hori et al., (2003) demonstrated that high-density mapping presented tightly QTL-linked markers that are beneficial and can be used directly for marker-assisted breeding. Given the marker densities of 0.53 cM and 1.2 cM we used, both 50k and 9k SNP arrays provide sufficient precision for QTL analysis, as well as genetic markers for breeding selection.

The distinct virulence profile of isolates collected from Idaho suggests this isolate possibly contains unique effectors. Although *Ptm* and *Ptt* both produce necrotrophic effectors to trigger disease susceptibility, a brief biotrophic growth is established in *Ptm* before it switches to necrotrophic stage (Liu *et al.,* 2011). Therefore, besides the susceptibility protein-necrotrophic effector interaction for compatible infection, the *Ptm*-barley pathosystem may involve R-Avirulence (Avr) recognition as well for dominant resistance (Clare *et al.,* 2020). Numerous QTL have been identified for the *Ptm* susceptibility/resistance in barley, but the nature of quantitative resistance and high diversity of virulent effectors impedes the development of SFNB-resistant varieties (Duellman 2015). QTL mapping conducted in this study indicated that the previously reported susceptibility/resistance loci, such as *Rpt4*, *Rpt5*, *Rpt6*, and *Rpt8*, may also function in response to Idaho isolates. Particularly, the *Rpt8* allele in CI5791 acts as a major susceptibility gene within CT. Fine mapping and cloning of this gene will help unravel the complicated molecular basis for the *Ptm* susceptibility. In the meantime, the user-friendly markers associated with the major QTL and the recessive *rpt8* allele will be utilized to enhance the immunity for unarmed barley varieties to the specialized Idaho isolates.

Supplementary Information

Data availability

All data are included in the paper, tables, figures, or the associated supplemental materials. Tables S1 and S2 showed the average disease scores for the segregating populations. Tables S3 and S5 provided genotype scores used for generation of linkage maps. Tables S4 and S6 showed the summary of seven genetic linkage groups generated with different RIL populations. Tables S7 and S8 provided detailed summary for the identified QTL. Table S9 included primer sequences for the STARP markers used in the present study. Figures S1 and S2 presented the STARP markers designed to assist breeding selection. Sequences for barley 50k and 9k SNP arrays are available at https://ics.hutton.ac.uk/50k and https://wheat.pw.usda.gov/GG3/node/483, respectively. All other reagents are commercially available or can be sent upon request. Supplemental material available at figshare: https://doi.org/10.6084/m9.figshare.14414588.

Acknowledgments

The authors thank Xiaohong (Sherry) Jiang, Madison Skadberg, and Patrick Gross for their technical assistance.

Funding

This research was supported by the US Department of Agriculture–Agriculture Research Service (USDA-ARS) Current Research Information System (CRIS) Project 3060-21000-038-00D (to S.Y.), and the North Dakota Barley Council (to S.Y.).

Conflict of Interest

The authors declare that they have no conflict of interest.

Literature Cited

Abu Qamar, M., Z.H. Liu, J.D. Faris, S. Chao, M.C. Edwards *et al.*, 2008 A region of barley chromosome 6H harbors multiple major genes associated with net type net blotch resistance. Theor. Appl. Genet. 117:1261-1270.

Arabi, M.I.E., B. Al-Safadi, and T. Charbaji, 2003 Pathogenic variation among isolates of *Pyrenophora teres*, the causal agent of barley net blotch. J. Phytopathol. 151:376-382.

Bayer, M.M., P. Rapazote-Flores, M. Ganal, P.E. Hedley, M. Macaulay *et al.*, 2017 Development and evaluation of a barley 50k iSelect SNP array. Front. Plant Sci. 8:1792.

Burlakoti, R.R., S. Gyawali, S. Chao, K.P. Smith, R.D. Horsley *et al.*, 2017 Genome-wide association study of spot form of net blotch resistance in the upper midwest barley breeding programs. Phytopathology 107:100-108.

Clare, S.J., N.A. Wyatt, R.S. Brueggeman, and T.L. Friesen, 2020 Research advances in the *Pyrenophora teres*-barley interaction. Mol. Plant Pathol. 21:272-288.

Comadran, J., B. Kilian, J. Russell, L. Ramsay, N. Stein *et al.*, 2012 Natural variation in a homolog of Antirrhinum CENTRORADIALIS contributed to spring growth habit and environmental adaptation in cultivated barley. Nat. Genet. 44:1388-1392.

Daba, S.D., R. Horsley, R. Brueggeman, S.A.M. Chao, and M. Mohammadi, 2019 Genome-wide association studies and candidate gene identification for leaf scald and net blotch in barley (*Hordeum vulgare* L.). Plant Dis. 103:880-889.

Darvasi, A., A. Weinreb, V. Minke, J.I. Weller, and M. Soller, 1993 Detecting marker-QTL linkage and estimating QTL gene effect and map location using a saturated genetic map. Genetics 134:943-951

Duellman, K., 2015 Characterizing *P. teres* f. *maculata* in the northern United States and impact of spot form net blotch on yield of barley. 10.13140/RG.2.1.3045.9925.

Franckowiak, J.D., and G.J. Platz, 2013 International database for barley genes and barley genetic stocks. Barley Genet. Newsl. 43:48–223.

Friesen, T.L., J.D. Faris, Z. Lai, and B.J. Steffenson, 2006 Identification and chromosomal location of major genes for resistance to *Pyrenophora teres* in a doubled-haploid barley population. Genome 49:855-859.

Grewal, T.S., B.G. Rossnagel, C.J. Pozniak, and G.J. Scoles, 2008 Mapping quantitative trait loci associated with barley net blotch resistance. Theor. Appl. Genet. 116:529-539.

Grewal, T.S., B.G. Rossnagel, and G.J. Scoles, 2012 Mapping quantitative trait loci associated with spot blotch and net blotch resistance in a doubled-haploid barley population. Mol. Breed. 30:267-279.

Hori, K., T. Kobayashi, A. Shimizu, K. Sato, and K. Takeda *et al*., 2003 Efficient construction of high-density linkage map and its application to QTL analysis in barley. Theor. Appl. Genet. 107:806-813.

Joehanes, R., and J.C. Nelson, 2008 QGene 4.0, an extensible Java QTL-analysis platform. Bioinformatics 24:2788-2789.

Julian T, and B. David, 2017. R package ASMap: Efficient genetic linkage map construction and diagnosis. J. Stat. Softw. 79: 1–29.

Karki, C.B., and E.L. Sharp, 1986 Pathogenic variation in some isolates of *Pyrenophora teres* f. *sp. maculata* on Barley. Plant Dis. 70:684-687.

Khan, T.N., and A. Tekauz, 1982 Occurrence and pathogenicity of *Drechslera teres* isolates causing spot-type symptoms on barley in Western Australia. Plant Dis. 66:423-425

Koladia, V.M., J.D. Faris, J.K. Richards, R.S. Brueggeman, S. Chao *et al.*, 2017 Genetic analysis of net form net blotch resistance in barley lines CIho 5791 and Tifang against a global collection of *P. teres* f. *teres* isolates. Theor. Appl. Genet. 130 (1):163-173.

Lehmensiek, A., G.J. Platz, E. Mace, D. Poulsen, and M.W. Sutherland, 2007 Mapping of adult plant resistance to net form of net blotch in three Australian barley populations. Aust. J. Agric. Res. 58:1191-1197.

Liu, Z., S.R. Ellwood, R.P. Oliver, and T.L. Friesen, 2011 *Pyrenophora teres*: profile of an increasingly damaging barley pathogen. Mol. Plant Pathol. 12:1-19.

Liu, Z., D.J. Holmes, J.D. Faris, S. Chao, R.S. Brueggeman *et al.*, 2015 Necrotrophic effector-triggered susceptibility (NETS) underlies the barley-*Pyrenophora teres* f. *teres* interaction specific to chromosome 6H. Mol. Plant Pathol. 16:188-200.

Liu, Z.H., J.D. Faris, M.C. Edwards, and T.L. Friesen, 2010 Development of Expressed Sequence Tag (EST)-based markers for genomic analysis of a barley 6H region harboring multiple net form net blotch resistance genes. Plant Genome 3:41-52.

Long, Y.M., W.S. Chao, G.J. Ma, S.S. Xu, and L.L. Qi, 2017 An innovative SNP genotyping method adapting to multiple platforms and throughputs. Theor. Appl. Genet. 130:597-607.

Lorieux, M., 2012 MapDisto: fast and efficient computation of genetic linkage maps. Mol. Breed. 30:1231-1235.

Manninen, O.M., M. Jalli, R. Kalendar, A. Schulman, O. Afanasenko *et al.*, 2006 Mapping of major spot-type and net-type net-blotch resistance genes in the Ethiopian barley line CI 9819. Genome 49:1564-1571.

Martin, A., G.J. Platz, D. de Klerk, R.A. Fowler, F. Smit *et al.*, 2018 Identification and mapping of net form of net blotch resistance in South African barley. Mol. Breed. 38:53.

Mascher, M., T. Wich, W. Thomas, J. Jenkins, C. Plot *et al*., 2021 Long-read sequence assembly: a technical evaluation in barley. Plant Cell 6:1888-1906

Mascher, M., H. Gundlach, A. Himmelbach, S. Beier, S.O. Twardziok *et al.*, 2017 A chromosome conformation capture ordered sequence of the barley genome. Nature 544:427-433.

McLean, M.S., B.J. Howlett, and G.J. Hollaway, 2009 The epidemiology and control of spot form of net blotch (*Pyrenophora teres* f. *maculata*) of barley: a review. Crop Pasture Sci. 60:303–315.

McLean, M.S., A. Martin, S. Gupta, M.W. Sutherland, G.J. Hollaway *et al.*, 2014 Validation of a new spot form of net blotch differential set and evidence for hybridisation between the spot and net forms of net blotch in Australia. Australas. Plant Pathol. 43:223-233.

Murray, M.G., and W.F. Thompson, 1980 Rapid isolation of high molecular weight plant DNA. Nucleic Acids Res. 8:4321-4325.

Neupane, A., P. Tamang, R.S. Brueggeman, and T.L. Friesen, 2015 Evaluation of a barley core collection for spot form net blotch reaction reveals distinct genotype-specific pathogen virulence and host susceptibility. Phytopathology 105:509-517.

Piepho, H.P., 2000 Optimal marker density for interval mapping in a backcross population. Heredity 84:437-440.

Poehlman, J.M., 1994 Breeding barley and oats. *In J.M. Poehlman, ed.* Breeding Field Crops (3rd ed), Iowa State University Press, Ames, Iowa.p. 378-420.

Raman, H., G.J. Platz, K.J. Chalmers, R. Raman, B.J. Read *et al.*, 2003 Mapping of genomic regions associated with net form of net blotch resistance in barley. Aust. J. Agric. Res. 54:1359–1367.

R Core Team, 2021 R: A language and environment for statistical computing. R Foundation for Statistical Computing, Vienna, Austria. Richards, J., S. Chao, T. Friesen, and R. Brueggeman, 2016 Fine mapping of the barley chromosome 6H net form net blotch susceptibility locus. G3 (Bethesda) 6:1809-1818.

Shjerve, R.A., J.D. Faris, R.S. Brueggeman, C. Yan, Y. Zhu *et al.*, 2014 Evaluation of a *Pyrenophora teres* f. *teres* mapping population reveals multiple independent interactions with a region of barley chromosome 6H. Fungal. Genet. Biol. 70:104-112.

Stange, M., H.F. Utz, T.A. Schrag, A.E. Melchinger, and T. Wurschum, 2013 High-density genotyping: an overkill for QTL mapping? Lessons learned from a case study in maize and simulations. Theor. Appl. Genet. 126:2563-2574.

Tamang, P., A. Neupane, S. Mamidi, T. Friesen, and R. Brueggeman, 2015 Association mapping of seedling resistance to spot form net blotch in a worldwide collection of barley. Phytopathology 105:500-508.

Tamang, P., J.K. Richards, A. Alhashal, R. Sharma Poudel, R.D. Horsley *et al.*, 2019 Mapping of barley susceptibility/resistance QTL against spot form net blotch caused by *Pyrenophora teres* f. *maculata* using RIL populations. Theor. Appl. Genet. 132:1953-1963.

Vatter, T., A. Maurer, D. Kopahnke, D. Perovic, F. Ordon *et al.*, 2017 A nested association mapping population identifies multiple small effect QTL conferring resistance against net blotch (*Pyrenophora teres* f. *teres*) in wild barley. PLoS One 12:e0186803.

Wang, X., E.S. Mace, G.J. Platz, C.H. Hunt, L.T. Hickey *et al.*, 2015 Spot form of net blotch resistance in barley is under complex genetic control. *Theor. Appl. Genet.* 128:489-499.

Williams, K.J., G.J. Platz, A.R. Barr, J. Cheong, K. Willsmore *et al.*, 2003 A comparison of the genetics of seedling and adult plant resistance to the spot form of net blotch (*Pyrenophora teres* f. *maculata*). Aust. J. Agric. Res. 54:1387-1394.

Yun, S.J., L. Gyenis, P.M. Hayes, I. Matus, K.P. Smith *et al.*, 2005 Quantitative trait loci for multiple disease resistance in wild barley. *Crop Sci.* 45:2563–2572.

CHAPTER 3: GENETIC AND PHYSICAL LOCALIZATION OF A MAJOR SUSCEPTIBILITY GENE TO *PYRENOPHORA TERES* F. *MACULATA* IN BARLEY[3]

Abdullah F. Alhashel[1, 2], Jason D Fiedler[3, 4], Raja Nandety[4], Ryan M Skiba[4], Robert S Bruggeman[5], Thomas Baldwin[1], Timothy L. Friesen[1, 4], Shengming Yang[1, 3, 4, *]
[1] Department of Plant Pathology, North Dakota State University, Fargo, ND 58102, USA
[2] Department of Plant Protection, College of Food and Agriculture Sciences, King Saud University, Riyadh 11451, Saudi Arabia
[3] Department of Plant Sciences, North Dakota State University, Fargo, ND 58102, USA
[4] Cereals Crops Research Unit, Edward T. Schafer Agriculture Research Center, USDA-ARS, Fargo, ND 58102, USA
[5] Department of Crop and Soil Sciences, Washington State University, Pullman, WA 99164
*Author to whom correspondence should be addressed; E-Mail: Shengming.Yang@usda.gov Tel.: +1-701-412-1309; Fax: +1-701-412-1369.

Abstract

Spot form net blotch (SFNB), caused by the necrotrophic fungal pathogen *Pyrenophora teres* f. *maculata* (*Ptm*), is an economically important foliar diseases in barley. Although various resistance loci have been identified, breeding for SFNB-resistant varieties has been hampered due to the complex virulence profile of *Ptm* populations. One resistance locus in the host may be effective against one specific isolate, but it may confer susceptibility to other isolates. A major susceptibility QTL on chromosome 7H, named *Sptm1*, was consistently identified in many studies. In the present study, we conduct fine mapping to localize *Sptm1* with high resolution. A segregating population was developed from selected F_2 progenies of the cross Tradition (S) × PI 67381 (R), in which the disease phenotype was determined by the *Sptm1* locus alone. Disease phenotypes of critical recombinants were confirmed in the following two consecutive generations. Genetic mapping anchored the *Sptm1* gene to an ~400 kb region on chromosome

[3] SY conceived and designed the project. AFA performed most of the experiments in collaboration with all other authors. JDF and RN contributed new reagents/analytic tools. All authors analyzed the experimental data. AFA and SY wrote the first draft of the manuscript. All authors commented on previous versions and approved the final version of the manuscript.

7H. Gene prediction and annotation identified six protein-coding genes in the delimited *Sptm1* region, and the gene encoding a putative cold responsive protein kinase was selected as a strong candidate. Therefore, providing fine localization and candidate of *Sptm1* for functional validation, our study will facilitate the understanding of susceptibility mechanism underlying the barley-*Ptm* interaction and offers a potential target for gene editing to develop valuable materials with broad-spectrum resistance to SFNB.

Key message

Genetic characterization of a major susceptibility locus to spot form net blotch using linkage mapping to identify the candidate gene and user-friendly markers in barley.

Introduction

Barley (*Hordeum vulgare* L.) is an important cereal crop in the grass family Poaceae. It is the fourth largest cereal crop in both yield and cultivation area globally, after wheat, rice, and corn (Poehlman 1987). Barley is primarily grown for animal feed and malt which is important in the brewing and distilling industries. In some developing countries, it is also a staple food for human consumption. However, barley production is seriously threatened by various diseases. One of the important foliar diseases in barley is net blotch (NB) caused by the fungal pathogen *Pyrenophora teres*, resulting in up to 10-40% yield losses when susceptible varieties are grown (Mouchacca 1999).

Net blotch occurs in two forms, spot form (SFNB) and net form (NFNB) caused by *P. teres* f. *maculata* (*Ptm*) and *P. teres* f. *teres* (*Ptt*), respectively. Although hybrids can be obtained in the lab, *Ptm* and *Ptt* are genetically distinct, and they induce different symptoms on susceptible hosts (Liu et al. 2011). Diagnostic markers have been developed to differentiate the two forms of *P. teres* (Leisova et al. 2006). Moreover, *Ptt* infects as a necrotroph and grows mostly in the apoplast. In contrast, *Ptm* intially forms intracellular vesicles near the penetration site before switching to intercellular growth resulting in necrosis (Lightfoot and Able 2010). The early laten phase indicated that *Ptm* may secrete additional effectors to suppress host defense responses at the intial infection stage (Whisson et al. 2007). Both forms of *P. teres* secreted phytotoxins or necrotrophic effector responsible for the necrosis and chlorosis, while *Ptt* produces significantly more toxins in the culture medium (Lightfoot and Able 2010; Sarpeleh et al. 2007; Sarpeleh et al. 2008). Many of these host specific toxins or necrotrophic effectors are proeinatious (Sarpeleh et al. 2007). Hijacking the host defense in an inverse gene-for-gene manner, necrotrophic effectors manipulate host susceptibility proteins or targets to induces

programmed cell death (PCD) for necrotrophs to acquire nutrients from destroyed cells (Friesen and Faris 2021).

SFNB has been increasingly damaging in barley growing regions (Liu et al. 2011). Harnessing genetic resistance is an effective and sustainable means for disease control. Nevertheless, due to the sexual recombination in *Ptm* populations, the rapid evolution of effectors diversifies the virulence profiles. As a result, host reactions to *Ptm* are complex and controlled by various quantitative trait loci (QTL). Additionally, a QTL effective against certain isolates may be susceptible to others. Genome-wide association and linkage mapping studies have identified only a few major QTL which have been consistently detected using various *Ptm* isolates, including *Rpt4* (on chromosome 7H), *Rpt5* (6H), *Rpt6* (5H), *Rpt7* (4H), and *Rpt8* (4H) (Alhashel et al. 2021; Daba et al. 2019; Franckowiak and Platz 2013; Friesen et al. 2006; Grewal et al. 2008; Manninen et al. 2006; Raman et al. 2003; Richards et al. 2016; Tamang et al. 2019; Vatter et al. 2017; Yun et al. 2005). These QTL provide valuable resources for breeding broad-spectrum resistance to SFNB. However, the identity and functional mechanisms of the genes underlying these QTL have been elusive.

The *Rpt4* locus is strikingly important among the major QTL. This locus confers broad spectrum resistance/susceptibility to *Ptm* including some isolates with unique virulence profiles, and it is effective against multiple *Ptt* isolates as well (Alhashel et al. 2021; Daba et al. 2019; Duellman 2015; Grewal et al. 2008; Wonneberger et al. 2017). Furthermore, although *Rpt4* was identified as a dominant seedling resistance, it also contributed to adult plant resistance (APR) (Williams et al. 1999). The broad specificity of *Rpt4* was confirmed by Tamang et al. (2019) using six geographically distinct isolates, but segregation ratios in the biparental population suggested that *Rpt4* conditioned dominant susceptibility to SFNB (Tamang et al. 2019). Recent

research in barley-*Ptm* interactions identified two major virulence loci located on *Ptm* Chr1 and Chr2, respectively, with the *Ptm* virulence on Chr2 targeting a dominant susceptibility gene at the *Rpt4* locus on barley 7H (Skiba et al. 2022). An inverse gene-for-gene association was demonstrated by the host and pathogen genetics in the barley-*Ptm* pathosystem (Skiba et al. 2022).

In the present study, we conducted genetic and physical mapping to identify the gene underlying the *Rpt4* locus. To avoid misperception, the gene is designated *Susceptibility to Ptm 1* (*Sptm1*) hereafter. Genetic mapping delimited the *Sptm1* gene within a ~400 kb region on 7H. A total of six protein-coding genes were identified in the *Sptm1* region. Of those, one gene encoding a putative protein kinase was selected as a promising candidate for functional validation. Therefore, our research lays a foundation to isolate this agronomically and genetically important *Sptm1* gene, which will facilitate our understanding of the molecular mechanisms regulating the barley-*Ptm* interactions and provide a target for gene manipulation to develop SFNB-resistant resources.

Materials and Methods

Ptm Isolate and Plant Materials

Ptm isolate Cel-A17 (CA17) collected in Montana State was used to map *Sptm1* in this study. Using a recombinant inbred line (RIL) population derived from the cross between Tradition (six-rowed, susceptible) and PI 67381 (two-rowed, resistant). Tamang et al. (2019) identified a total of three QTL against CA17 including the susceptibility gene *Sptm1* on 7H. The other two QTL were located on 2H (*QRptm-2H-1-31*) and 3H (*QRptm-3H-81-88*) (Tamang et al. 2019). Using SNP markers flanking these three loci, we identified six plants from 200 Tradition × PI 67381 F_2 population that were heterozygous for *Sptm1* and homozygous recessive for

QRptm-2H-1-31 and *QRptm-3H-81-88*. Segregating populations used to map *Sptm1* were developed by selfing the selected six F_2 plants. A total of 702 $F_{2:3}$ plants were used for genetic mapping. Critical recombinants were assessed in the next generation with at least 40 $F_{3:4}$ plants, and the derived homozygous $F_{3:4}$ recombinant representing immortal critical recombinant (ICR) were used to increase seeds for further phenotyping. At least 30 ICRs ($F_{4:5}$) were used to confirm the phenotype for each original $F_{2:3}$ recombinant.

Inoculum Preparation and Phenotyping

The CA17 inoculum preparation, inoculation, and phenotyping was conducted as described by Neupane et al. (2015). Briefly, spores were collected with sterilized distilled water from V8-PDA culture plates (150 ml V8 juice, 10 g Difco PDA, 3 g $CaCO_3$,10 g agar, and 850 ml H_2O). The spore concentration was adjusted to 2000 spores/ml with two drops of Tween-20 per 100 ml added. Barley segregants together with Tradition and PI 67381 were individually grown in super-cell cones placed in RL98 trays. Inoculation was performed when the second leaf was fully expanded (~2 weeks) using an air sprayer at 15 to 20 psi. The inoculated plants were kept in a mist chamber at 100% relative humidity for 24 h under continuous light, and then moved to a growth chamber under a 12 h/12h—light/dark cycle at 21 ℃. Disease reactions were assessed 7 days post inoculation (DPI) using a 1–5 rating scale with 1 being highly resistant and 5 being highly susceptible (Neupane et al. 2015).

Barley genotypes used for pangenome sequencing were also tested for disease responses with at least eight plants for each line planted in racks (Jayakodi et al. 2020). A complete randomized design was used for each rack, and plants were placed inside a growth chamber with the same conditions mentioned above. All racks were bordered with the susceptible check (Pinnacle) to reduce any edge effect. Two plants in each cone were scored collectively as a

single replicate, and at least four independent replicates for each genotype were conducted. The average value of all replicates was used as the phenotypic score.

Genotyping, Marker Development, and Linkage Mapping

The CTAB protocol was used to extract DNA (Murray and Thompson 1980). Around 100 mg of leaf tissue were collected from plants at the three-leaf stage. DNA concentration was quantified using a NanoDrop spectrophotometer (NanoDrop 8000, Thermo Fisher Scientific) according to the manufacturer's instructions. The parental lines Tradition and PI 67381 were genotyped using the barley 50k iSelect SNP Array to identify markers (Bayer et al. 2017). GenomeStudio V2.0 (Illumina) was used for genotype calling with the *de novo* calling algorithm. The called SNPs, together with those flanking *Sptm1*, *QRPtm-2H-1-31* (2H), and *QRPtm-3H-81-88* (3H) reported by Tamang et al. (2019), were converted to semi-thermal asymmetric reverse PCR (STARP) markers (Table B1) (Long et al. 2017). PCR protocol and conditions were followed as previously described (Long et al. 2017). Amplicons were assayed on a 6% polyacrylamide gel stained with GelRed™ (MilliporeSigma), which was imaged using a Typhoon™ FLA 9500 variable mode laser scanner (GE Healthcare Life Sciences, Marlborough, MA). Simple sequence repeats (SSRs) markers were also developed using the barley cv. Morex v3 reference assembly (Mascher et al. 2017).

More SNPs were obtained to saturate the *Sptm1* genetic region by genome re-sequencing of Tradition and PI 67381. Paired-end sequencing of the genomic libraries was performed on an Illumina Novaseq 6000 system with 150 bp paired ends. All the Illumina paired end reads were cleaned with bbduk using the following parameters, ktrim=r; K=23; mink=11 and hdist=1 (Bushnell 2021). The cleaned reads are aligned to the Morex v3 reference genome, and alignment files were then sorted and indexed using SAMtools (Danecek et al. 2021; Langmead et

al. 2009). Filtered with a minimum mapping quality score of 30 and a minimum reads depth coverage of 4, raw single nucleotide variants and indels were called using SAMtools and bcftools v1.14, (Li 2011). SNP and indel variants were annotated with BEDtools (Quinlan and Hall 2010). A Genetic map was constructed using JoinMap 3.0 (Stam 1993). All markers used for genetic mapping of *Sptm1* are listed in Table B2.

Physical Mapping and Sequence Analysis of Candidate Genes in The *Sptm1* Region

The programs FGENESH and Pfam 32.0 were used to perform gene prediction and annotation. The predicted gene structure was verified using BaRTv1.0, a high-quality, non-redundant barley reference transcripts database (Barley Reference Transcripts – BaRTv1.0) (Rapazote-Flores et al. 2019). We extracted the fasta sequences of the annotated genes from the Morex v3 genome assembly corresponding to the *Sptm1* region (Chr7H:592631221-593037317). with extra 1000 bp flanking coding region for each of the annotated gene. Genome re-sequencing reads of parental lines were mapped to the Morex v3 genome, and the aligned bam files were subset to the *Sptm1* region using bcftools to generate variant call format files (VCFs). The generated variant files were visualized along with the bam files using Integrative Genomics Viewer (IGV) to identify sequence polymorphisms between alleles.

Results

Population Development and Phenotype Evaluation

Tamang et al. (2019) identified 3 QTL associated with susceptibility to *Ptm* isolate CA17 using RILs of Tradition (S) × PI 67381 (R), including *Sptm1*, *QRptm-2H-1-31* (2H) and *QRptm-3H-81-88* (3H). Using the SNP markers flanking these three QTL (Table B1) we identified six plants from 200 F_2 lines of Tradition × PI 67381 that contained homozygous PI 67381 alleles at the 2H and 3H loci but heterozygous *Sptm1* alleles at the 7H locus. Segregating populations were

developed by selfing the six selected F_2 plants. Besides the resistant and susceptible $F_{2:3}$ extremes, we identified a large number of plants showing intermediate disease types. $F_{2:3}$ plants carrying homozygous PI 67381 allele (n = 15), indicated by *Sptm1*-flanking SNP markers, exhibited an average disease reaction of 1.38 which was not significantly different from the score of PI 67381 (1.5) (Table 3.1). $F_{2:3}$ plants carrying homozygous Tradition allele (n = 15) showed typical SFNB symptoms 7 DPI with large necrotic lesions surrounded by a chlorotic halo on infected leaves, although their average disease type (3.3) was lower that of Tradition (4.5) (Fig. 3.1, Table 3.1). Therefore, based on the disease types of homozygous segregants, plants were considered to be resistant, intermediate, and susceptible if they displayed a reaction type ≤ 1.5, ≥ 2 but < 3, and ≥ 3, respectively. Phenotyping of an initial 178 $F_{2:3}$ plants identified 35 resistant, 97 intermediate, and 46 susceptible. The segregation ratio fits 1:2:1 ($\chi^2 = 2.80$, d$f = 2$, $P = 0.25$), suggesting that the disease reaction is controlled by a single gene with dosage effect.

Table 3.1. Phenotype analysis with Tradition, PI67381, and homozygous $F_{2:3}$ plants. Disease severity for each genotype was indicated by the average reaction type and standard deviation.

Genotype	Average Reaction Type
PI 67381	$1.5^{a} \pm 0$
Tradition	$4.53^{c} \pm 0.41$
$F_{2:3}$ with homozygous PI 67381 allele of *Sptm1*	$1.38^{a} \pm 0.44$
$F_{2:3}$ with homozygous Tradition allele of *Sptm1*	$3.30^{b} \pm 0.51$

Note: the average values with different letters were significantly different based on Tukey test at the 0.05 level of probability.

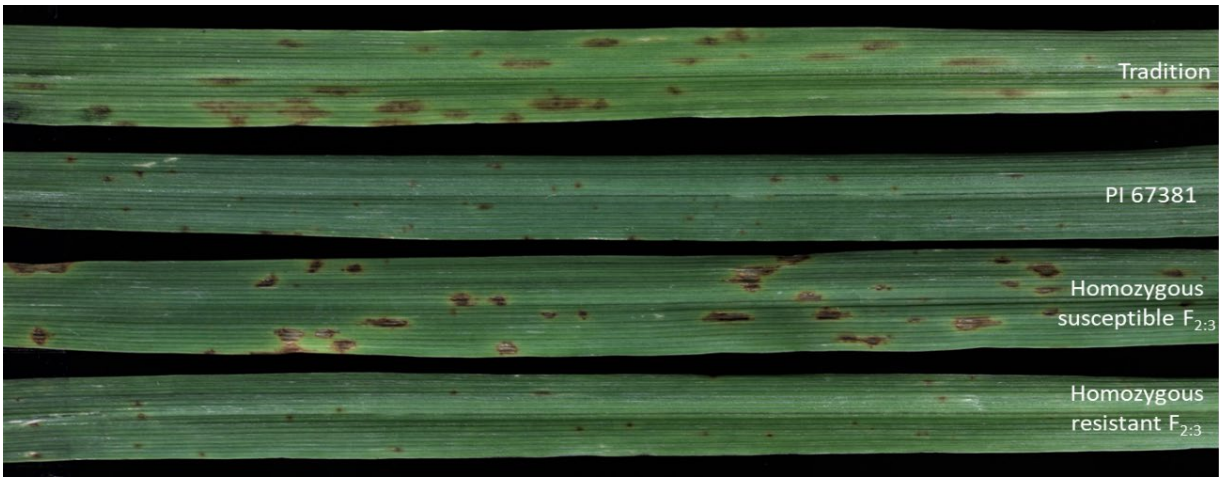

Figure 3.1. Phenotypic responses of parental lines Tradition and PI 67381 and homozygous $F_{2:3}$ plants to *Ptm* isolate CA17. Typical SFNB symptom with large necrotic lesions was shown in Tradition homozygous susceptible $F_{2:3}$ plant, while PI 67381 and homozygous resistant $F_{2:3}$ plant were incompatible with the pathogen.

Genetic and Physical Mapping

SNP markers on 7H were identified through genotyping of parental lines using the barley 50k SNP array (Table B2). Genetic mapping of *Sptm1* was first conducted with the 178 $F_{2:3}$ plants. Using 81 resistant and susceptible $F_{2:3}$ extremes, we initially delimited the *Sptm1* gene to a 6 Mb region flanked by SNP markers M24 and M33 (Fig. 3.2A). Plants including intermediate individuals genotyped as recombinants by M24 and M33 were saved for seed increase. All recombinants went through phenotype confirmation using both $F_{3:4}$ plants and the derived homozygous ICRs. Relying on the critical recombinants TP1-15 (the 15th plant in batch 1 tested), TP1-169, and TP1-25, the *Sptm1* region was narrowed down to 1.2 Mb flanked by M28 and M29 (Fig. 3.2A). To increase the mapping resolution, we enlarged the population to 702 $F_{2:3}$ individuals (Fig. 3.2B). More SNPs were called using short-read sequencing of Tradition and PI 67381 to saturate the *Sptm1* region (Table B2). A total of 20 recombinants were identified between M28 and M29. Taking advantage of the same phenotyping strategy involving $F_{3:4}$ plants and ICRs, the *Sptm1* gene was finally delimited to an ~400 kb region (Chr7H: 592631221-

593037317) flanked by M69 and M87 based on three critical recombinants TP2-64, TP3-32, and TP5-78 (Fig. 3.2B).

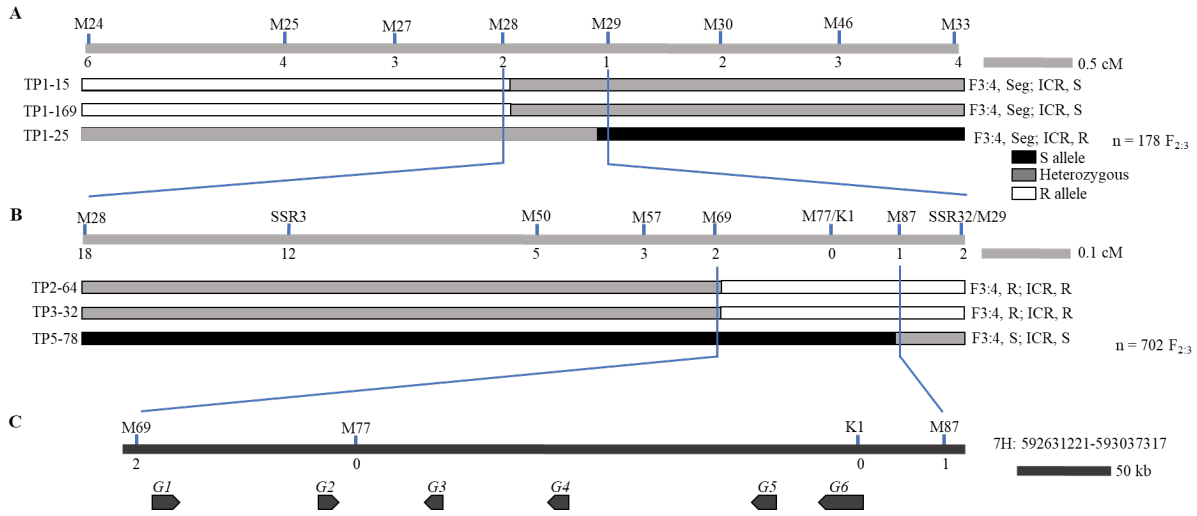

Figure 3.2. Fine mapping of *Sptm1*. Genetic mapping was conducted sequentially with 178 (A) and 524 (B) $F_{2:3}$ individuals representing 356 and 1048 gametes, respectively. Phenotypes of critical recombinants were first confirmed with $F_{3:4}$ plants from which ICRs were selected. At least 30 ICRs for each recombinant were also tested to verify the disease response. Each recombinant is shown by a combination of differential boxes. Black box represents homozygous susceptible genotype, empty for homozygous resistant, and gray for heterozygous. Numbers below the linkage group indicate the number of recombination breakpoints separating the marker from *Sptm1*. A total of six protein-coding genes were identified in the *Sptm1* region spanning ~ 400 kb (C). The maps are drawn to scale. M, marker; ICR, immortal critical recombinant; Seg, segregating; R, resistant; S, susceptible; G, gene.

Gene annotation and prediction identified a total of six putative protein-coding genes according to the Morex v3 genome assembly (Fig 3.2C, Table 3.2). Of those, four genes (*G1-G4*) encode either hypothetical or uncharacterized proteins (Table 3.2). The coding product of *G5* (*HORVU.MOREX.r3.7HG0735550*) is homologous to human protein Werner Syndrome Exonuclease (WEX) with an exonuclease domain. *G6* (*HORVU.MOREX.r3.7HG0735560*) encodes a protein with homology to Cold-responsive Protein Kinase 1 (CRPK1, At1G16670) in *Arabidopsis thaliana* (Table 3.2) (Liu et al. 2017). Because protein kinases play crucial roles in

various signal transduction cascades, particularly in plant-microbe interactions, we focused on *G6* for further analysis.

Table 3.2. Predicted genes in the *Sptm1* region. G, gene

Gene	Gene id	Homology
G1	*HORVU.MOREX.r3.7HG0735510*	Hypothetic protein with unknown function
G2	*HORVU.MOREX.r3.7HG0735520*	No homology
G3	*HORVU.MOREX.r3.7HG0735530*	No homology
G4	*HORVU.MOREX.r3.7HG0735540*	Hypothetic protein with unknown function
G5	*HORVU.MOREX.r3.7HG0735550*	Werner Syndrome-like exonuclease
G6	*HORVU.MOREX.r3.7HG0735560*	Cold-responsive protein kinase 1

Allelic Polymorphisms Between Resistant and Susceptible *G6* Alleles

The coding region of *G6* contains 6 exons and 5 introns, encoding a protein of 384 amino acids (aa) with a molecular weight of 42.8 kDa, composed of the catalytic domain of serine/threonine-specific and tyrosine-specific protein kinases (Fig. 3.3A). Allelic sequences of *G6* were obtained by mapping WGS reads to the Morex v3 genome reference. A total of five SNPs, three in exons and two in introns, were identified between Tradition and PI 67381 alleles, resulting in only one aa substitution D19N at the N-terminus (Fig. 3.3A-B). All SNPs were confirmed by Sanger sequencing as well.

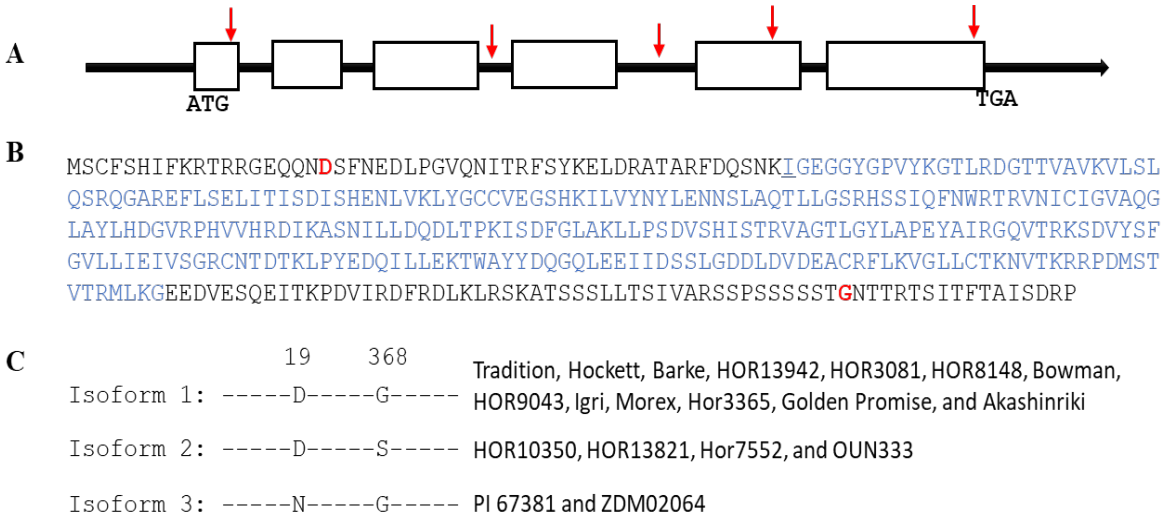

Figure 3.3. Sequence analysis of *G6*. The coding region of *G6* contains 6 exons and 5 introns (A), encoding a protein of 384 aa (B). Exons are shown as empty boxes, and black line for introns. The SNPs identified between Tradition and PI 67381 alleles are indicated by red arrows. The catalytic domain of protein kinase is highlighted in blue. The aa substitutions identified among allele products are highlighted in red (B). Three *G6* isoforms were identified using pangenome references and Bowman, and the D19N substitution is associated with disease type (C).

The pangenome derived from 20 barley accessions representing the global diversity provides an important tool to reveal the hidden allelic variations (Jayakodi et al. 2020). To investigate if the protein haplotype is associated with disease phenotype, we assessed 17 available pangenome references and a transformable variety Bowman. The result showed that 17 accessions including Morex were susceptible or intermediately susceptible, but ZDM02064 (Chiba) was the only line resistant to CA17 (Fig. 3.3C, Table 3.3). Two protein isoforms were identified among the susceptible lines, distinguished by an aa substitution at the distal C-terminus, G368S. Most susceptible lines (13 lines) carry the same protein isoform as Tradition (Fig. 3.3C). Notably, although the aa substitution D19N is outside of the conserved functional domain (Fig.3.3B), the resistant line ZDM02064 shares the same protein isoform as the resistant parental line PI 67831 (Fig. 3.3C), which therefore strengthens the candidacy for this protein kinase gene.

Table 3.3. Disease response of barley pan-genome lines to *Ptm* isolate CA17.

Genotype	Average disease score	Score category
ZDM02064	1 ± 0	Resistant
HOR 13942	2.25 ± 0.25	Intermediate
Akashinriki	2.5 ± 0	
HOR 9043	2.75 ± 0.25	
Igri	2.75 ± 0.25	
HOR 13821	3 ± 0	Susceptible
Golden Promise	3 ± 0	
HOR 3365	3 ± 0	
HOR 7552	3.25 ± 0.25	
HOR 21599	3.5 ± 0	
Bowman	4 ± 0	
HOR 8148	3.75 ± 0.25	
HOR 10350	4 ± 0	
OUN333	4± 0	
Barke	4.25 ± 0.25	
HOR 3081	4.25 ± 0.25	
Morex	4.5 ± 0	
Hockett	4.5 ± 0	

Discussion

SFNB has been increasingly damaging for barley production. Genetic resistance has been identified in barley and its wild relatives, and the introgression of resistance from various sources into barley may facilitate achievement of more effective and durable resistance. However, the complex and quantitative nature of host responses has posed a major challenge to deploying effective and durable resistances (Wang et al. 2015), which also limits the understanding of molecular mechanisms controlling barley-*Ptm* interactions. Conferring broad spectrum recognition to both *Ptm* and *Ptt*, the *Sptm1* locus provides a valuable resource for breeders and geneticists in barley improvement and genetic studies (Alhashel et al. 2021; Skiba et al. 2022; Tamang et al. 2019; Williams et al. 1999; Williams et al. 2003). In the present research, we conducted genetic and physical mapping towards cloning of the molecular determinant of *Sptm1*. Using ICRs derived from selected F_2 lines of Tradition × PI 67381, we precisely anchored the

Sptm1 gene to an ~400 kb region on 7H, and *G6* (*HORVU.MOREX.r3.7HG0735560*) homologous to *AtCRPK1* was identified as a promising candidate. In addition, the SNP identified between resistant and susceptible alleles can be used as a diagnostic marker to assist breeding selection.

In a joint genetic analysis of *Ptm* virulence and host susceptibility, Skiba et al. (2022) reported that the *Sptm1* allele of Hockett on 7H interacted with the virulence locus on *Ptm* Chr2 in an inverse gene-for-gene pattern. Of the six putative genes in the *Sptm1* region, *G6* is the only one whose coding product are known to be involved in protein-protein interactions and signal transduction. Although a transmembrane domain for signal sensing is missing in *G6*, several kinases containing only the catalytic domain have been identified to function in responses to plant pathogens, such as the tomato bacterial speck resistance gene *Pto* (Martin et al. 1993), wheat powdery mildew resistance gene *Pm21* (Cao et al. 2011), wheat stripe rust resistance gene *Yr15* (Klymiuk et al. 2018), wheat stem rust resistance gene *Sr60* (Chen et al. 2020), barley stem rust resistance gene *Rpg1* (Brueggeman et al. 2002), and wheat septoria nodorum blotch susceptibility gene *Snn3* (Zhang et al. 2021). It is noteworthy that *Pto*, lacking a transmembrane domain, interacts directly with the corresponding avirulence factor *avrPto* (Frederick et al. 1998). Therefore, under these scenarios, *G6* encoding a protein kinase was designated a strong candidate for *Sptm1*.

An intriguing question is how a protein homologous to *AtCRPK1* is involved in plant-microbe interactions. Loss-of-function mutation in *AtCRPK1* results in increased cold tolerance in *Arabidopsis thaliana* (Liu et al. 2017). Located on the plasma membrane, *AtCRPK1* phosphorylated 14-3-3 proteins, and the phosphorylated 14-3-3 proteins translocate from cytosol to the nucleus where they destabilize the key cold-responsive C-repeat-binding factor (CBF)

proteins. In line with this, overexpression of 14-3-3 reduced freezing tolerance, while mutations in 14-3-3 improved freezing tolerance. The prominent role of CBF proteins in cold acclimation have been extensively characterized, but there is no precedent for CBFs being involved in plant responses to biotic stress (Shi et al. 2018; Yamaguchi-Shinozaki and Shinozaki 2006). In contrast, 14-3-3 proteins, acting as sensors for the phosphorylation status at specific sites, play significant roles in plant-pathogen interaction as the targets of pathogen effectors or interacting with defense-related proteins (Oh and Martin 2011; Teper et al. 2014; Yang et al. 2009). Therefore, 14-3-3 proteins may be the potential link between the putative *CRPK1* encoded by *G6* and the susceptibility to *Ptm* pathogen.

The aa substitution D19N associated with disease phenotype is outside the conserved functional domain (CFD) in *G6* (Fig. 3.3), but it is not uncommon that nonsynonymous mutations beyond the CFD disrupts protein function (Li et al. 2021; Li et al. 2016). The specific localization of *AtCRPK1* on the plasma membrane indicated the presence of a signal peptide in the protein, although an obvious signal peptide is missing (Liu et al. 2017). The N-terminal sequence of *G6* harboring the D19N substitution is homologous to that in *AtCRPK1*. There may be an uncharacterized signal peptide at the N-terminus, and the aa substitution disturbs protein localization.

In summary, as one of the few genes conferring broad recognition specificity to *Ptm*, *Sptm1* is valuable for variety improvement and fundamental research in barley. The high-resolution mapping in this study provides user-friendly markers and a candidate gene for *Sptm1*. Cloning of *Sptm1* will unravel the genetic mechanism underlying barley susceptibility to this important fungal pathogen, and it will provide a target for gene editing to develop resistant materials. Moreover, it is interesting to investigate if *Sptm1* is also involved in cold tolerance.

Nevertheless, the candidate of *Sptm1* will be functionally validated with genetic transformation or CRISPR/Cas9-mediated mutagenesis in barley.

Supplementary Information

Acknowledgement

This work was supported by North Dakota Barley Council (SY) and the U.S. Department of Agriculture, Agricultural Research Service through project 3060–21000-038-00D (SY). Mention of trade names or commercial products in this publication is solely for the purpose of providing specific information and does not imply recommendation or endorsement by the U.S. Department of Agriculture. USDA is an equal opportunity provider and employer.

Data availability

The re-sequencing data in this manuscript have been deposited in NCBI Sequence Read Archive under accession number PRJNA890669.

Conflicts of interest

The authors declare no conflict of interest.

Literature Cited

Alhashel AF, Poudel RS, Fiedler J, Carlson CH, Rasmussen J, Baldwin T, Friesen TL, Brueggeman RS, Yang SM (2021) Genetic mapping of host resistance to the *Pyrenophora teres* f. *maculata* isolate 13IM8.3. G3-Genes Genom Genet 11

Bayer MM, Rapazote-Flores P, Ganal M, Hedley PE, Macaulay M, Plieske J, Ramsay L, Russell J, Shaw PD, Thomas W, Waugh R (2017) Development and evaluation of a barley 50k iSelect SNP array. Front Plant Sci 8

Brueggeman R, Rostoks N, Kudrna D, Kilian A, Han F, Chen J, Druka A, Steffenson B, Kleinhofs A (2002) The barley stem rust-resistance gene *Rpg1* is a novel disease-resistance gene with homology to receptor kinases. Proc Natl Acad Sci USA 99:9328-9333

Bushnell B (2021) BBTools. 38.79 edn. http://sourceforge.net/projects/bbmap/

Cao A, Xing L, Wang X, Yang X, Wang W, Sun Y, Qian C, Ni J, Chen Y, Liu D, Wang X, Chen P (2011) Serine/threonine kinase gene *Stpk-V*, a key member of powdery mildew

resistance gene *Pm21*, confers powdery mildew resistance in wheat. Proc Natl Acad Sci USA 108:7727-7732

Chen S, Rouse MN, Zhang W, Zhang X, Guo Y, Briggs J, Dubcovsky J (2020) Wheat gene *Sr60* encodes a protein with two putative kinase domains that confers resistance to stem rust. New Phytol 225:948-959

Daba SD, Horsley R, Brueggeman R, Chao SAM, Mohammadi M (2019) Genome-wide association studies and candidate gene identification for leaf scald and net blotch in barley (*Hordeum vulgare* L.). Plant Disease 103:880-889

Danecek P, Bonfield JK, Liddle J, Marshall J, Ohan V, Pollard MO, Whitwham A, Keane T, McCarthy SA, Davies RM, Li H (2021) Twelve years of SAMtools and BCFtools. Gigascience 10

Duellman K (2015) Characterizing *P. teres* f. *maculata* in the northern United States and impact of spot form net blotch on yield of barley. 10.13140/RG.2.1.3045.9925.

Franckowiak JD, Platz GJ (2013) International database for barley genes and barley genetic stocks. Barley Genet Newsl 43:48–223

Frederick RD, Thilmony RL, Sessa G, Martin GB (1998) Recognition specificity for the bacterial avirulence protein AvrPto is determined by Thr-204 in the activation loop of the tomato Pto kinase. Mol Cell 2:241-245

Friesen TL, Faris JD (2021) Characterization of effector-target interactions in necrotrophic pathosystems reveals trends and variation in host manipulation. Annu Rev Phytopathol 59:77-98

Friesen TL, Faris JD, Lai Z, Steffenson BJ (2006) Identification and chromosomal location of major genes for resistance to *Pyrenophora teres* in a doubled-haploid barley population. Genome 49:855-859

Grewal TS, Rossnagel BG, Pozniak CJ, Scoles GJ (2008) Mapping quantitative trait loci associated with barley net blotch resistance. Theor Appl Genet 116:529-539

Jayakodi M, Padmarasu S, Haberer G, Bonthala VS, Gundlach H, Monat C, Lux T, Kamal N, Lang DI, Himmelbach A, Ens J, Zhang XQ, Angessa TT, Zhou GF, Tan C, Hill C, Wang PH, Schreiber M, Boston LB, Plott C, Jenkins J, Guo Y, Fiebig A, Budak H, Xu DD, Zhang J, Wang CC, Grimwood J, Schmutz J, Guo GG, Zhang GP, Mochida K, Hirayama T, Sato K, Chalmers KJ, Langridge P, Waugh R, Pozniak CJ, Scholz U, Mayer KFX, Spannagl M, Li CD, Mascher M, Stein N (2020) The barley pan-genome reveals the hidden legacy of mutation breeding. Nature 588

Klymiuk V, Yaniv E, Huang L, Raats D, Fatiukha A, Chen S, Feng L, Frenkel Z, Krugman T, Lidzbarsky G, Chang W, Jaaskelainen MJ, Schudoma C, Paulin L, Laine P, Bariana H, Sela H, Saleem K, Sorensen CK, Hovmoller MS, Distelfeld A, Chalhoub B, Dubcovsky

J, Korol AB, Schulman AH, Fahima T (2018) Cloning of the wheat *Yr15* resistance gene sheds light on the plant tandem kinase-pseudokinase family. Nat Commun 9:3735

Langmead B, Trapnell C, Pop M, Salzberg SL (2009) Ultrafast and memory-efficient alignment of short DNA sequences to the human genome. Genome Biol 10

Leisova L, Minarikova V, Kucera L, Ovesna J (2006) Quantification of *Pyrenophora teres* in infected barley leaves using real-time PCR. J Microbiol Methods 67:446-455

Li H (2011) A statistical framework for SNP calling, mutation discovery, association mapping and population genetical parameter estimation from sequencing data. Bioinformatics 27:2987-2993

Li M, Hensel G, Melzer M, Junker A, Tschiersch H, Ruwe H, Arend D, Kumlehn J, Borner T, Stein N (2021) Mutation of the *ALBOSTRIANS* ohnologous gene *HvCMF3* impairs chloroplast development and thylakoid architecture in barley. Front Plant Sci 12:732608

Li PC, Yu SW, Li K, Huang JG, Wang XJ, Zheng CC (2016) The mutation of Glu at amino Acid 3838 of AtMDN1 provokes peiotropic developmental phenotypes in *Arabidopsis*. Sci Rep 6:36446

Lightfoot DJ, Able AJ (2010) Growth of *Pyrenophora teres* in planta during barley net blotch disease. Australas Plant Path 39:499-507

Liu Z, Ellwood SR, Oliver RP, Friesen TL (2011) *Pyrenophora teres*: profile of an increasingly damaging barley pathogen. Mol Plant Pathol 12:1–19.

Liu Z, Jia Y, Ding Y, Shi Y, Li Z, Guo Y, Gong Z, Yang S (2017) Plasma membrane CRPK1-mediated phosphorylation of 14-3-3 proteins induces their nuclear import to fine-tune CBF signaling during cold response. Mol Cell 66:117-128 e115

Long YM, Chao WS, Ma GJ, Xu SS, Qi LL (2017) An innovative SNP genotyping method adapting to multiple platforms and throughputs. Theoretical and Applied Genetics 130:597-607

Manninen OM, Jalli M, Kalendar R, Schulman A, Afanasenko O, Robinson J (2006) Mapping of major spot-type and net-type net-blotch resistance genes in the Ethiopian barley line CI 9819. Genome 49:1564-1571

Martin GB, Brommonschenkel SH, Chunwongse J, Frary A, Ganal MW, Spivey R, Wu T, Earle ED, Tanksley SD (1993) Map-based cloning of a protein kinase gene conferring disease resistance in tomato. Science 262:1432-1436

Mascher M, Gundlach H, Himmelbach A, Beier S, Twardziok SO, Wicker T, Radchuk V, Dockter C, Hedley PE, Russell J, Bayer M, Ramsay L, Liu H, Haberer G, Zhang XQ, Zhang QS, Barrero RA, Li L, Taudien S, Groth M, Felder M, Hastie A, Simkova H, Stankova H, Vrana J, Chan S, Munoz-Amatrian M, Ounit R, Wanamaker S, Bolser D,

Colmsee C, Schmutzer T, Aliyeva-Schnorr L, Grasso S, Tanskanen J, Chailyan A, Sampath D, Heavens D, Clissold L, Cao SJ, Chapman B, Dai F, Han Y, Li H, Li X, Lin CY, McCooke JK, Tan C, Wang PH, Wang SB, Yin SY, Zhou GF, Poland JA, Bellgard MI, Borisjuk L, Houben A, Dolezel J, Ayling S, Lonardi S, Kersey P, Lagridge P, Muehlbauer GJ, Clark MD, Caccamo M, Schulman AH, Mayer KFX, Platzer M, Close TJ, Scholz U, Hansson M, Zhang GP, Braumann I, Spannagl M, Li CD, Waugh R, Stein N (2017) A chromosome conformation capture ordered sequence of the barley genome. Nature 544:426-433

Mouchacca J (1999) Compendium of Barley Diseases, Second Edition, Mathre D.E. (Ed.). APS Press, The American Phytopathological Society, 139 Pokfulam Road, Hong Kong (1997), 90, ISBN: 0-89054-180-9.

Murray MG, Thompson WF (1980) Rapid isolation of high molecular-weight plant DNA. Nucleic Acids Res 8:4321-4325

Neupane A, Tamang P, Brueggeman RS, Friesen TL (2015) Evaluation of a barley core collection for spot form net blotch reaction reveals distinct genotype-specific pathogen virulence and host susceptibility. Phytopathology 105:509-517

Oh CS, Martin GB (2011) Tomato 14-3-3 protein TFT7 interacts with a MAP kinase kinase to regulate immunity-associated programmed cell death mediated by diverse disease resistance proteins. J Biol Chem 286:14129-14136

Poehlman JM (1987) Breeding barley and oats. Breeding field crops. Springer Netherlands, Dordrecht, pp 378-420

Quinlan AR, Hall IM (2010) BEDTools: a flexible suite of utilities for comparing genomic features. Bioinformatics 26:841-842

Raman H, Platz GJ, Chalmers KJ, Raman R, Read BJ, Barr AR, Moody DB (2003) Mapping of genomic regions associated with net form of net blotch resistance in barley. Aust J Agric Res 54:1359–1367

Rapazote-Flores P, Bayer M, Milne L, Mayer CD, Fuller J, Guo WB, Hedley PE, Morris J, Halpin C, Kam J, Mckim SM, Zwirek M, Casao MC, Barakate A, Schreiber M, Stephen G, Zhang RX, Brown JWS, Waugh R, Simpson CG (2019) BaRTv1.0: an improved barley reference transcript dataset to determine accurate changes in the barley transcriptome using RNA-seq. Bmc Genomics 20

Richards J, Chao S, Friesen T, Brueggeman R (2016) Fine mapping of the barley chromosome 6H net form net blotch susceptibility locus. G3 (Bethesda) 6:1809-1818

Sarpeleh A, Wallwork H, Catcheside DE, Tate ME, Able AJ (2007) Proteinaceous metabolites from *Pyrenophora teres* contribute to symptom development of barley net blotch. Phytopathology 97:907-915

Sarpeleh A, Wallwork H, Tate ME, Catcheside DEA, Able AJ (2008) Initial characterisation of phytotoxic proteins isolated from *Pyrenophora teres*. Physiol Mol Plant P 72:73-79

Shi Y, Ding Y, Yang S (2018) Molecular regulation of CBF signaling in cold acclimation. Trends Plant Sci 23:623-637

Skiba RM, Wyatt NA, Kariyawasam GK, Fiedler JD, Yang S, Brueggeman RS, Friesen TL (2022) Host and pathogen genetics reveal an inverse gene-for-gene association in the *P. teres* f. *maculata*-barley pathosystem. Theor Appl Genet 135:3597-3609

Stam P (1993) Construction of integrated genetic-linkage maps by means of a new computer package - JoinMap. Plant J 3:739-744

Tamang P, Richards JK, Alhashal A, Sharma Poudel R, Horsley RD, Friesen TL, Brueggeman RS (2019) Mapping of barley susceptibility/resistance QTL against spot form net blotch caused by *Pyrenophora teres* f. *maculata* using RIL populations. Theor Appl Genet 132:1953-1963

Teper D, Salomon D, Sunitha S, Kim JG, Mudgett MB, Sessa G (2014) *Xanthomonas euvesicatoria* typeIII effector XopQ interacts with tomato and pepper 14-3-3 isoforms to suppress effector-triggered immunity. Plant J 77:297-309

Vatter T, Maurer A, Kopahnke D, Perovic D, Ordon F, Pillen K (2017) A nested association mapping population identifies multiple small effect QTL conferring resistance against net blotch (*Pyrenophora teres* f. *teres*) in wild barley. PLoS One 12:e0186803

Wang X, Mace ES, Platz GJ, Hunt CH, Hickey LT, Franckowiak JD, Jordan DR (2015) Spot form of net blotch resistance in barley is under complex genetic control. Theor Appl Genet 128:489-499

Whisson SC, Boevink PC, Moleleki L, Avrova AO, Morales JG, Gilroy EM, Armstrong MR, Grouffaud S, van West P, Chapman S, Hein I, Toth IK, Pritchard L, Birch PR (2007) A translocation signal for delivery of oomycete effector proteins into host plant cells. Nature 450:115-118

Williams KJ, Lichon A, Gianquitto P, Kretschmer JM, Karakousis A, Manning S, Langridge P, Wallwork H (1999) Identification and mapping of a gene conferring resistance to the spot form of net blotch (*Pyrenophora teres* f *maculata*) in barley. Theoretical and Applied Genetics 99:323-327

Williams KJ, Platz GJ, Barr AR, Cheong J, Willsmore K, Cakir M, Wallwork H (2003) A comparison of the genetics of seedling and adult plant resistance to the spot form of net blotch (Pyrenophora teres f. maculata). Aust J Agr Res 54:1387-1394

Wonneberger R, Ficke A, Lillemo M (2017) Mapping of quantitative trait loci associated with resistance to net form net blotch (*Pyrenophora teres* f. *teres*) in a doubled haploid Norwegian barley population. PLoS One 12:e0175773

Yamaguchi-Shinozaki K, Shinozaki K (2006) Transcriptional regulatory networks in cellular responses and tolerance to dehydration and cold stresses. Annu Rev Plant Biol 57:781-803

Yang X, Wang W, Coleman M, Orgil U, Feng J, Ma X, Ferl R, Turner JG, Xiao S (2009) Arabidopsis 14-3-3 lambda is a positive regulator of RPW8-mediated disease resistance. Plant J 60:539-550

Yun SJ, Gyenis L, Hayes PM, Matus I, Smith KP, Steffenson BJ, Muehlbauer GJM (2005) Quantitative trait loci for multiple disease resistance in wild barley. Crop Sci 45:2563–2572

Zhang Z, Running KLD, Seneviratne S, Peters Haugrud AR, Szabo-Hever A, Shi G, Brueggeman R, Xu SS, Friesen TL, Faris JD (2021) A protein kinase-major sperm protein gene hijacked by a necrotrophic fungal pathogen triggers disease susceptibility in wheat. Plant J 106:720-732

CHAPTER 4: HOST-INDUCED GENE SILENCING OF THE FUNGAL GENE *FGGCN5* IN BARLEY FOR IMPROVING RESISTANCE TO FUSARIUM HEAD BLIGHT

Abstract

Fusarium head blight (FHB), caused by the mycotoxin-producing fungus *Fusarium graminearum*, is a devastating disease in barley, jeopardizing both grain yield and quality. Host-induced gene silencing (HIGS), in which hosts express double-stranded RNA (dsRNA) to silence plant pathogen genes in a sequence-specific manner, has been proposed as a potential approach for disease control. In this study, a transgenic barley line containing an RNA interference (RNAi) construct was developed to target the histone acetyltransferase-encoding gene *FgGCN5*, which is known to play significant roles in *F. graminearum* morphogenesis, DON biosynthesis, and pathogenicity. Small RNA sequencing confirmed the production of target-specific short interfering RNAs (siRNA) in the transgenic line. However, the post-infection expression level of the *FgGCN5* gene in the transgenic plant was not affected, suggesting the *FgCNG5*-siRNAs were either ineffective at silencing the target gene or were not taken up by the pathogen. The gene expression data is in line with that the comparable levels in disease severity, DON accumulation, and fungal biomass between transgenic plants and the wild type. Further investigations are needed to address why HIGS of the *FgGCN5* gene is unable to improve FHB resistance in barley.

Introduction

Acetylation of histone lysine is a post translational histone modification which plays essential roles in the dynamic changes of chromatin and epigenetic regulation of gene expression (Verdone et al., 2005). Hyperacetylation of histones is associated with the relaxed chromatin (euchromatin) and gene activation, while hypoacetylation leads to the condensed heterochromatin (heterochromatin) and transcriptional repression (Strahl and Allis, 2000). Histone acetylation is balanced by the histone acetyltransferases (HATs) and histone deacetylases (HDACs). The General Control Non-repressed 5 (*GCN5*) acetyltransferase is a prominent HAT which is one of the first identified and best characterized histone acetyltransferases (Brownell et al., 1996). Maintaining proper cellular function and development, transcription regulation through the activity of *GCN5* is tightly linked to diverse metabolic pathways in the cell (Mutlu and Puigserver, 2021). Although the importance of HATs is well known for various biological processes in eukaryotes, the relevance of HATs in plant fungal pathogens has been neglected (Jeon et al., 2014).

Crop yield is seriously affected by various plant diseases, escalating the food insecurity triggered by the increasing population globally. Fusarium head blight (FHB), caused by the fungal pathogen *Fusarium graminearum* (*Gibberella zeae*), is a devastating disease of wheat and barley. FHB not only results in enormous loss of crop yield, but also deteriorates the food quality due to the pathogen-produced mycotoxins including deoxynivalenol (DON) (McMullen et al., 1997). DON is chemically stable and not damaged during processing. Presence of toxins in the final products of wheat and barley is harmful for both human and animal (Schwarz et al., 2017). Multiple major resistance genes to FHB have been identified and extensively harnessed in wheat production, such as *Fhb1* - *Fhb7* (Cuthbert et al., 2006; Cuthbert et al., 2007; Qi L et al., 2008;

Xue et al., 2010; Xue et al., 2011; Cainong et al., 2015; and Wang et al., 2020), but effective resources has not been available to enhance the FHB resistance in barley. Besides the protection by chemical fungicides, barley, as the fourth important cereal, is vulnerable to this notorious disease.

Host-induced gene silencing (HIGS) provides an innovative strategy for efficient control of plant pathogens. Using the RNA interference (RNAi) mechanism, HIGS suppresses genes of plant pathogens in a sequence-specific manner by hosts expressing the double stranded RNA (dsRNA) (Chang et al., 2012 and Machado et al., 2017). Processing of the dsRNA by Dicer or Dicer-like proteins (DCL) gives rise to small interfering RNAs (siRNAs) with small sizes of 21-22 nucleotides. These siRNAs are mobile signals which can be transported systemically in the host and even into the cells of plant pathogen (Chang et al., 2012). SiRNAs guides RNA-induced silencing complex (RISC) to bind to the target mRNA, resulting in the enzymatic cleavage and silencing of the target (Chang et al., 2012 and Machado et al., 2017). Secondary siRNAs (secsiRNAs) are produced by cleavage of target mRNA, acting as a magnifier of RNA silencing (Chang et al., 2012). Therefore, HIGS is applied as a powerful tool to target pathogen genes critical for survival or pathogenicity through engineering the host genome. Moreover HIGS-mediated plant protection has been proven effective for disease resistance in wheat and barley (Qi et al., 2019 and Machado et al., 2017).

Targeting the sterol 14-demethylase (*CYP51*) genes regulating ergosterol biogenesis essential for membrane integrity and fungal virulence, HIGS suppressed *F. graminearum* growth in transgenic *Arabidopsis* and barley plants (Koch et al., 2013). Wheat plants expressing RNAi constructs targeting the *F. graminearum* chitin synthase *Chs3b* gene displayed increased FHB resistance (Cheng et al., 2015). In addition, wheat plants carrying an RNAi hairpin to knock

down *FcGls1* in *F.culmorum*, a gene responsible for the biosynthesis of an important fungal cell wall polysaccharide β -1, 3-glucan, showed enhanced FHB resistance in the leaf and spike (Chen et al., 2016). Therefore, the efficacy of HIGS in controlling cereal FHB has been exemplified. However, development of durable disease resistance using HIGS require the selection of new targets and highly efficient stable transformation systems.

To increase barley resistance to FHB, in the present study we used HIGS to silence *FgGCN5*, a significant histone acetyltransferase-encoding gene in *F. graminearum*. Although HAT proteins function redundantly at considerable levels, distinct roles of *GCN5* in reprogramming of the genome have been identified (Xue-Franzen et al., 2013). The importance of *FgGCN5* was also indicated in *F. graminearum* morphogenesis, DON biosynthesis, and pathogenicity (Kong et al., 2018). In the loss-of-function *Fggcn5* mutant (*ΔFgGCN5*), acetylation levels of histone H3 were significantly decreased at several specific lysins, leading to a genome-wide differential expression and impaired metabolic processes affecting pathogenicity of *F. graminearum*. The *ΔFgGCN5* mutant losses its ability to generate conidia or to form perithecia for discharge of spores. When wheat spike is inoculated with the *ΔFgGCN5* mutant, FHB symptoms were observed on the inoculated kernels only, but spread of infection to neighboring spikelets on the same head is completely blocked. The *in vitro* DON production levels of *ΔFgGCN5* are almost zero compared to wild type (Kong et al., 2018). Therefore, the critical and unique roles of *FgGCN5* in pathogenicity and genome-reprogramming make it a potential target for HIGS to control FHB in barley.

Materials and Methods

Plant Materials

Barley cv. Golden Promise (WT) was used for transformation. All transgenic plants were grown in a greenhouse under a 16 h light/8 h dark photoperiod at 25 °C.

DNA Extraction

Plant DNA was extracted according to the CTAB protocol. Around 100 mg leaf samples were collected from plants at the three-leaf stage and quantified using a NanoDrop spectrophotometer (NanoDrop 8000, Thermo Fisher Scientific) according to the manufacturer's instructions. The final concentration was adjusted to 100 ng/uL for PCR amplification.

Vector Construction and Barley Transformation

The HIGS vector was constructed using pANIC-8B through the gateway cloning method to target *FgSCN5* (XM_011317624) (Mann et al., 2012). An ~300 bp fragment in the bromodomain of *FgSCN5* was amplified with primers attached with the attB recombination sites, 5'-attB1-GTTGGGGGAATCACATATCG-3' and 5'-attB2-GTTGGGGGAATCACATATCG-3'. The destination vector was transferred into the *Agrobacterium tumefaciens* strain AGL1 using electroporation. Barley transformation followed a previously developed protocol (Bartlett et al., 2008; Harwood, 2014). Briefly, developing spikes of the spring barley cv. Golden Promise growing in the greenhouse were harvested when the immature embryos (IEs) were approximately 1–2mm in diameter. After surface sterilization, IE was isolated from the seed with the embryo axis removed under a stereomicroscope. After three days of co-cultivation, the embryos were transferred to callus induction (CI) medium containing 50 mg/L Hygromycin for selection. Timentin (250 mg/L) was used to eliminate *Agrobacterium*. The IEs were transferred to fresh CI media every two weeks for three times. Six weeks after callus induction, the calli

were placed on transition medium for two weeks. The green developing shoots were then transferred to the regeneration medium for shooting and rooting. After 2–3 roots at least 2 cm and the shoot 3-4 cm in length were developed, the plantlet was transferred to soil. The preparation for transformation media followed the recipes described by Bartlett et al. (2008).

Small RNA Sequencing

Total RNA was extracted from three biological replicates of barley spikes in WT and the homozygous transgenic line T51. Each replicate consisted of three spikes growing in a distinct pot and collected at the boot stage. NucleoSpin RNA Plant kit (Macherey-Nagel, Düren, Germany) was used for RNA extraction. M-MLV reverse transcriptase was used to generate first-strand cDNA (Invitrogen). Small RNA libraries were prepared using the TruSeq Small RNA Library Preparation Kit, and single-end sequencing was performed on the Illumina Hiseq 2500 platform to generate 50-bp reads (SE50) (Novogene, Beijing, China). Results of small RNA sequencing total reads and quality can be found in (Table C3-4). The alignment of sRNA reads to *FgGCN5* were performed in CLC Genomics Workbench using the "map reads to reference" function, and the read counts per nucleotide were exported to a comma separated values file and graphed in Microsoft Excel.

Pathogen Inoculation Assay

The *F. graminearum* isolate GZFGO5 was used for inoculation. For inoculum preparation, dried fungal mycelial plugs were used for macroconidia production by scraping the surface of mung bean agar plates (MBA) (40g of filtered mung bean broth/L, and 15g of agar) (Evans et al., 2000). Plates were placed under alternate fluorescent and near UV light cycle 12/12 at room temperature for 7 to 14 days for sporulation. Spores were collected and filtered with sterile deionized H_2O water using two lairs of cheese cloth. Spore concentration was determined

using a hemocytometer, and a final concentration of 5 x 10^5 spore/ml was used for the inoculation assay in 0.025% Tween-20. Dip-inoculation was conducted for barley infection as described in (Baldwin et al., unpublished). Spikes at boot stage were immersed in the spore suspension and immediately covered with plastic bags. Three days later, the infected spikes are either covered with a glycine bag or exposed in the air. Disease phenotype was scored at 14 day post infection (dpi). The disease severity was calculated as a percentage of diseased spikelets per spike. Conlon and WT were used as susceptible and resistant controls, respectively. Plants used for disease evaluation were sown in cones (3.8 cm diameter × 20 cm depth) placed in RL98 trays with one seed per cone. The plants were grown in growth chambers under fluorescent and incandescent lighting with a 13-h photoperiod at temperatures optimal for the rapid and healthy growth of barley: 1 h at 16 °C, 1 h at 18 °C, 10 h at 20°C, 1 h at 18 °C (light level between 54-90 µmol m2), followed by 11 hours of darkness at 16 °C. At least 5 to 9 spikes per replicate were dip-inoculated for each genotype and the average of 4 replicates were used in the final statistical analysis (Baldwin et al., unpublished). A one-way analysis of variance (ANOVA) was used to test for statistically significant differences between treatments at the 0.05 level.

DON-Measurement

DON measurement was conducted by the Malting Barley Quality Laboratory in the Department of Plant Sciences at North Dakota State University (NDSU). Bulked infected samples at 14 dpi from all genotypes WT and T51 per experiment were collected for DON measurement. All samples were freeze-dried before being grounded. Approximately 1g of pulverized infected tissue was used for DON extraction with 10 mL of acetonitrile-water (v/v 84:16) mixture, followed by filtration and dilution for sample analysis on GC-MS. Statistical significance differences among treatment were calculated using Student's t-test at 0.05 level.

Fungal Biomass Measurement

Bulked infected samples at 14 dpi from all genotypes, including WT and T51, were collected for fungal biomass analysis with three technical replications per each. All samples were freeze-dried for four days before being grounded. Total genomic DNA was isolated using Plant/Fungi DNA Isolation Kit (Norgene Bioteck Corp) following the manufacturer's protocol. Utilizing the following primers/probe gene-specific for *TRI5* gene TRI5QPF2 5'-CTCACCCAGGAAACCCTACA-3', TRI5QPr2 5'-CATCACCTGAGGGTCCTTGT-3', and TRI5QPP2 5'-GATGGTTGCTGTCTTCTCGG-3', the fungal biomass was quantified. *Actin*-specific primers/probe ActinQPF2 5'-CCAGGTATCGCTGACCGTAT-3', ActinQPP2 5'-GCTGAGTGAGGCTAGGATGG-3', ActinQPR2 5'-GAAGATCAAGGTCGTCGCTC-3' were utilized to determine the quantity of barley DNA. Taqman-probe-based multiplex qPCR assay was used for quantification of both targets within each sample. The amount of genomic DNA in each sample was standardized to 10ng/µl. PCR reaction contained qPCR reaction contained 5 ul of Bio-rad iTaq Universal Probes Supermix (2X), 0.5 ul of each forward and reverse primer (10 uM), 0.2 ul of each probe (10 uM), and 1 ul of genomic DNA per sample added with Invitrogen Nuclease-Free water to reach final volume of 10 ul per reaction. qPCR conditions were as denaturation step of 95°C for 2:45 min followed by 35 cycles of 95°C for 0:15 s, and 58°C for 30 s. Relative biomass of *F. graminearum* in the infected tissue was quantified by qPCR. The Ct value of the *F. graminearum* gene *TRI5* was calculated relative to the corresponding Ct values of the Actin gene using the $2^{-\Delta\Delta Ct}$ method (Livak and Schmittgen, 2001). Statistical significance differences among treatment were calculated using Student's t-test at 0.05 level.

Quantitative Real-Time PCR (qRT-PCR)

Infected spikes were sampled with 3 biological replicates at 4 and 14 dpi for RNA extraction from WT and T51. NucleoSpin RNA Plant kit (Macherey-Nagel, Düren, Germany) was used to extract RNA following the manufacturer's instructions. Quantitative reverse transcription PCR was performed in a two-step assay. First-strand cDNA was synthesized using iScript cDNA synthesis kit (Bio-rad, Hercules, CA, USA) following the manufacturer's instructions. Fluorescent qPCR was performed using the Bio-Rad CFX96 Touch Real-Time PCR Detection System (Bio-rad). For each reaction, 2 µL cDNA (equivalent to 100 ng of total RNA), 1.35µL (for *actin* gene) or 0.75 µL (for *FgSCN5* gene) of each gene-specific primer (10 µM), and 7.5 µL of SsoAdvanced universal SYBR Green supermix 2x (Bio-rad) and nuclease-free water were added, giving a final volume of 15 µL. The *Actin* gene was used as the internal control for real-time analysis and amplified with primers 5′- CGACAATGGAACCGGAATG -3′ and 5′- CCCTTGGCGCATCATCTC -3′. Primers 5′-GCCTTCATCTCCTACACCATC-3′ and 5′- GATTTCACCATTGCGCTCTTC -3′ were used to quantify *FgSCN5* gene expression. Amplification conditions were conducted as instructed by manufacture protocol for SsoAdvanced universal SYBR® Green supermix with some modifications as follows: initial denaturation at 95° for 30 s, followed by 40 cycles of 95° for 30 s, and annealing/extension at 60° for 45 s. Two technical replications were used per biological replicate. Statistical significant differences among treatment were calculated using ANOVA.

Results

Identification of Homozygous Transgenic Plants

The presence of the transgene was determined in transgenic plants using PCR with a gene-specific primer GCN5-1F 5′- TGTTATCGAAGAGCGCAATG-3′ and a vector-specific primer Nos-R 5′- CCCATCTCATAAATAACGTCATGC-3′. To identify homozygous transgenic plants derived from two independent transformation events, six T1 plants each were selected and at least 30 T2 plants for each T1 family were subjected to PCR analysis. As a result, T34 and T51, one for each transformation event, were genotyped as homozygous (data not shown). However, further confirmation using 18 additional plants revealed that only T51 was homozygous for the transgene (Figure 4.1).

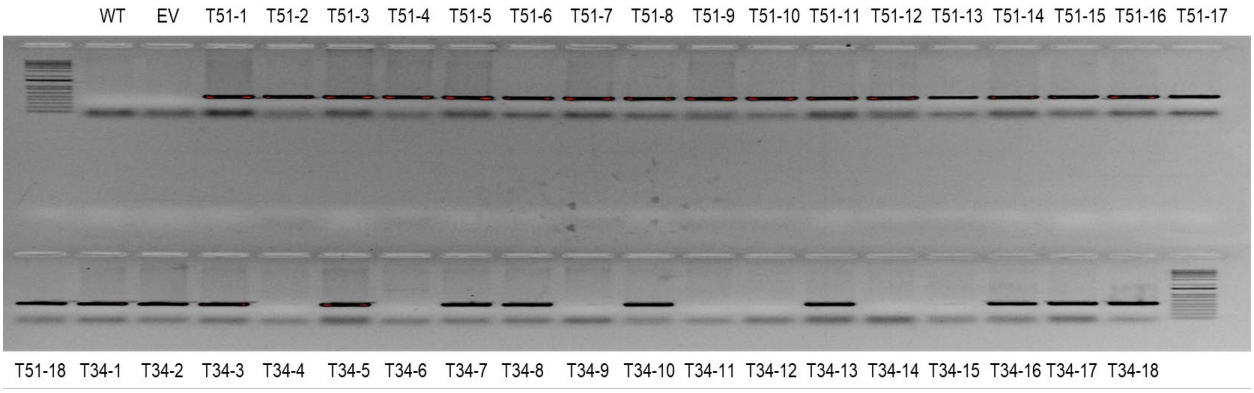

Figure 4.1. Molecular analysis of two independent T2 lines T51 and T34 to confirm the integration of *FgCNG5*-RNAi fragment. WT (wild type) and EV (empty vector) were used as negative controls.

Small RNA Sequencing

The siRNA from both WT and the transgenic line T51 were sequenced to determine if the transgenic line produced siRNA that inhibits the expression of *FgGCN5*. Three biological replicates of WT and transgenic T51 were used for total RNA extraction at the booting stage. According to sequencing results, siRNA that targets *FgGCN5* was not detected in WT but only

in T51 when all three biological replicates were examined (Table C1-2). Total mapped reads from the three T51 replications were 6889, 4330, and 11692, respectively, representing a small proportion of FgGCN5-siRNA produced, between 0.06 and 0.08 percent of the total siRNA sequenced. Most siRNAs targeting *FgGCN5* produced had an average length of 21±0.12 bp (Table C1-2) (Figure 4.2A). The siRNAs were mapped to distinct positions within the *FgGCN5* gene (Figure 4.2B).

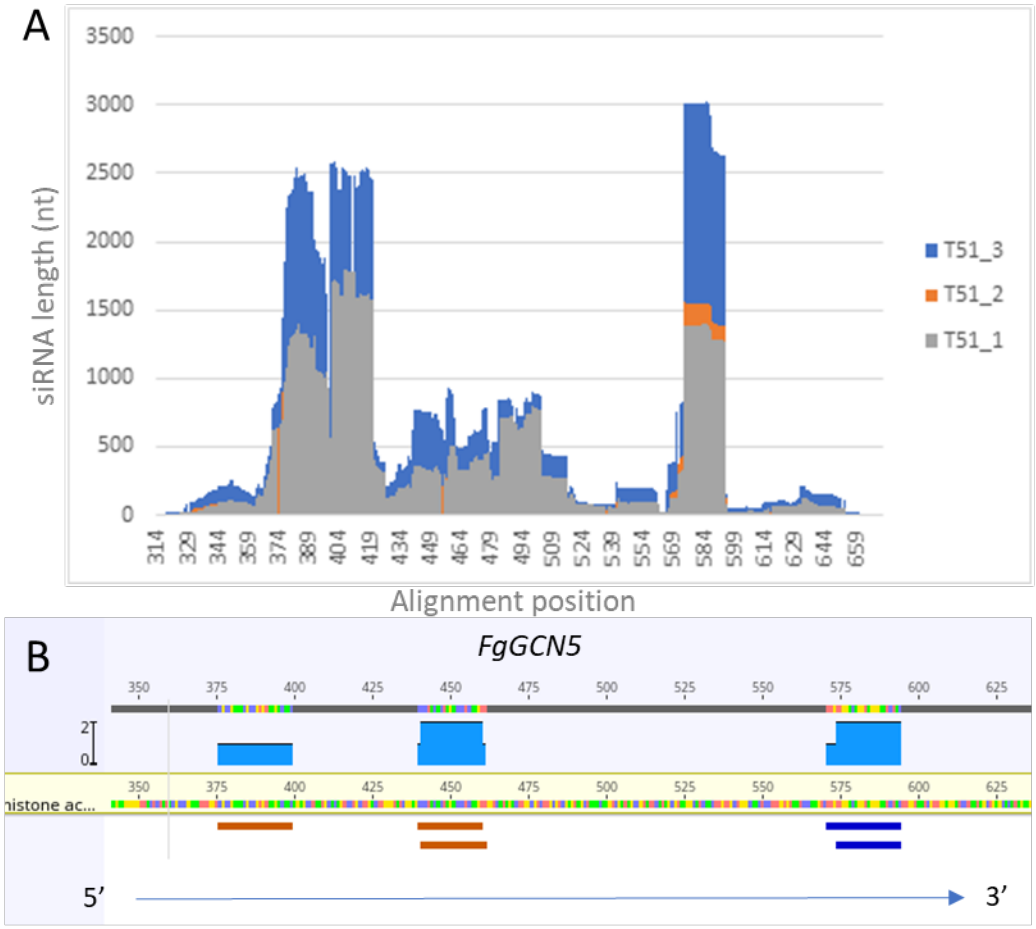

Figure 4.2. Small RNA profile of *FgCNG5*-RNAi from spikes of barley transgenic line T51. A. total count and length of the siRNA species target *FgCNG5* produced by the transgenic line T51 and B. map position of the siRNA within the target gene *FgCNG5*.

Disease Phenotype

The effect of siRNA targeting *FgGCN5* produced by transgenic line T51 on the responses to FHB was assessed. Conlon and WT, as resistant and susceptible controls, were used to compare the responses of the transgenic line T51. At the boot stage, dip-inoculation was used to inoculate the spikes of the tested lines with 5 x 10^5 spores/ml of the isolate GZFGO5. At 14 dpi, the disease severity to FHB infection was calculated by counting the number of infected and uninfected spikelets across the entire spike. For final analysis, all phenotypic scores across 3 independent experiments per genotype were averaged. The data shows that the disease severity of T51 was not significantly different from that of the WT plant. Nonetheless, the only statistically significant difference was observed when comparing the resistant check Conlon with the transgenic line T51 and the WT. Notably, transgenic line T51 had a higher disease percentage equal to 63.6% when compared to the WT which had a lower disease percentage equal to 53.2%. Conlon as resistant check showed the lowest disease percentage equal to 38.2% (Table 4.1) (Figure 4.3).

Table 4.1. Descriptive statistics for disease severity of 14 dpi with *F. graminearum* isolate GZFGO5 from three treatments Conlon, WT, and T51.

Treatments	Mean[a] (%)	Median (%)	Minimum (%)	Maximum (%)	Standard deviation
Conlon	38.25 *	32.5	0	73	22.7
WT	53.25	50	12	79	16.55
T51	63.6	68	19	96	18.1

* Indicates significant differences attested by ANOVA Pr > F = 0.0019

Figure 4.3. Visualization representing disease severity of 14 dpi spikes of Conlon, WT, and T51 genotypes inoculated with *F. graminearum* isolate GZFGO5.

Fungal Biomass Measurement

For measuring fungal biomass, 14 dpi-samples per genotype were pooled from all independent experiments and measured as a whole. Three technical replicates of qPCR were performed for each combined sample. *TRI5* and *Actin* genes were utilized to quantify and normalize fungal biomass, respectively. Results showed no significant differences between the two treatments WT and T51 (T-test= 0.69; $P > 0.05$). However, the fungal mass in T51 was 35% less than that in WT plants (Figure 4.4).

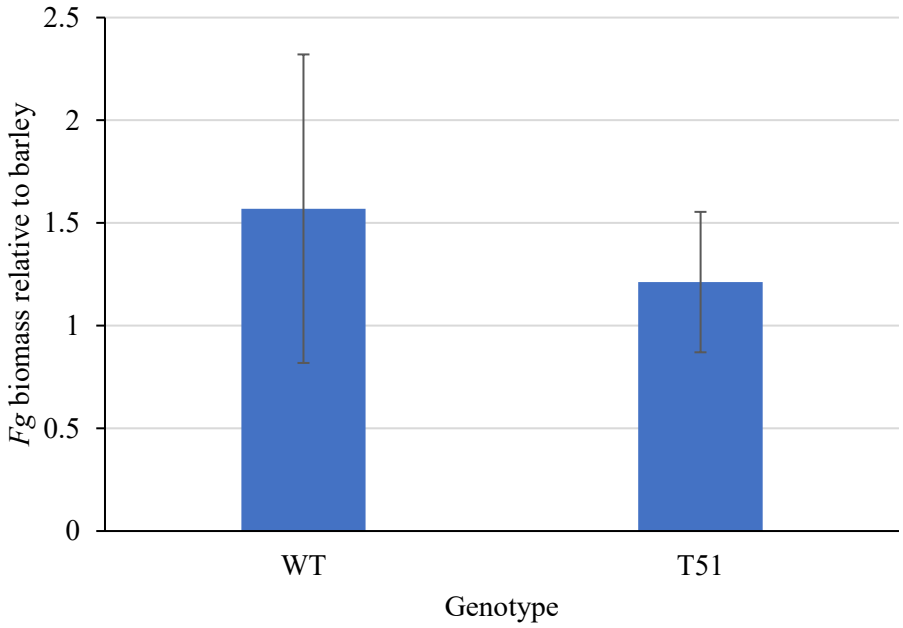

Figure 4.4. Fungal biomass analysis. Relative gene copy of *Tri5* was used to quantify the fungal mass in barley lines sampled at 14 dpi. The fold change of *Tri5* was normalized by using barley specific *β-Actin*, and relative gene copy number was calculated using equation $2^{-\Delta\Delta CT}$. Data represents the mean ± SE of three biological replicates. Statistical significance differences among treatment were calculated using Student's t-test at 0.05 level.

DON Measurement of T_3 Transgenic Line

DON was measured in the same samples used for fungal biomass analysis. GC-MS analysis was utilized for DON measurement. Results showed no significant difference between the two treatments (T-test= 0.43; $P > 0.05$). Nonetheless, transgenic line T51 accumulated a greater DON content (34.6 µg g^{-1} DON) than the WT (27.27 µg g^{-1} DON) (Figure. 4.5).

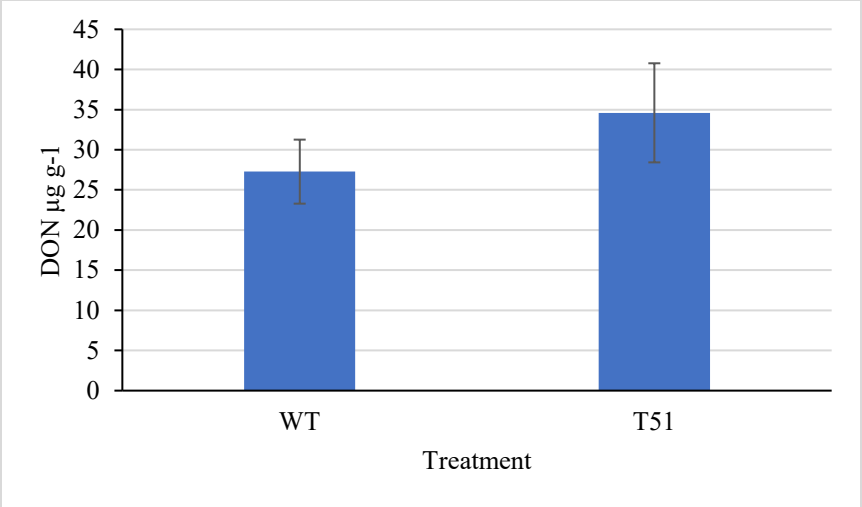

Figure 4.5. DON measurement. Data was represented by the mean ± SE of three biological replicates. Statistical significance differences among treatment were calculated using Student's t-test at 0.05 level.

Expression Profile of the Target Gene *FgGCN5* Post Infection

To test if in planta-derived silencing affected the target gene *FgGCN5* in *F. graminearum*, the transcript level of *FgGCN5* was evaluated in both WT and transgenic line T51. Comparing infected barley spike samples from WT and T51 at 4 and 14 dpi revealed no significant differences between the two lines at both time points based on absolute quantification of the target gene. The transgenic line T51 had less quantities of the target gene transcript than the WT line only at 14 dpi, but the difference was not statistically significant (Figure 4.6).

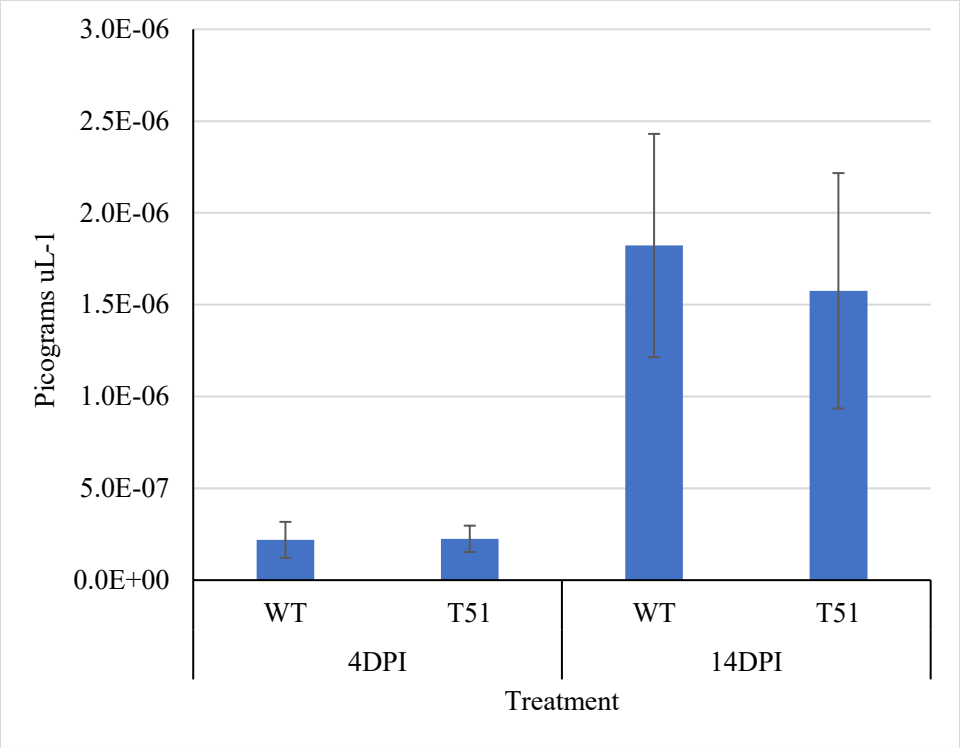

Figure 4.6. Absolute quantification of the target gene *FgGCN5* at 4 and 14 dpi. Data represents the mean ± SE of three biological replicates. Statistically significant differences among treatments per each time point were calculated using ANOVA, Pr > F = 0.871.

Discussion

Fusarium head blight is a devastating disease that reduces crop yield and grain quality. Breeding for disease resistance to FHB is the most efficient method of controlling the disease. However, due to the limited availability of disease-resistant germplasm and the rapid deterioration of resistance by new virulent races, there are no effective means to enhance FHB resistance in barley (Wegulo et al., 2015; Machado et al., 2017). Recently, HIGS has been used as novel method for the effective management of plant pathogens including *F. graminearum,* which also provided a new strategy for the safe, pesticide-free, potentially sustainable protection of plants from plant pathogens (Koch et al., 2013; Cheng et al., 2015; Chen et al., 2016). The purpose of this research was to identify a new HIGS target gene *FgGCN5* within the *F.*

graminearum genome and determine whether it influences the pathogen's pathogenicity, disease severity, DON accumulation, and fungal biomass.

RNAi is a biological phenomenon capable of inhibiting gene expression at the transcriptional, post-transcriptional, or translational levels (Chang et al., 2012). Plants contain RNAi, which is highly conserved and essential for the development and growth of organisms. HIGS uses the plant's RNAi system to produce silencing molecules (dsRNA and siRNAs) that can be translocated into fungus by an unidentified mechanism, and then uses the fungus's RNAi system to downregulate the expression of fungal genes (Qi et al., 2019; Cai et al., 2018). It has been proposed that host-derived mobile silencing signals may enter the cytosol of the target fungus and result in gene downregulation. This was demonstrated by planta-generated siRNAs directed against GFP mRNA in GFP-expressing transgenic *F.verticillioides*, which were able to translocate to fungal cytosol and diminish GFP signal (Tinoco et al., 2010).

In this study, small RNA sequencing results showed that the transgenic line T51 produced siRNAs which were specifically mapped to different locations of the target gene *FgGCN5*. It was suggested that the transgenic line T51 did generate dsRNAs through transcription which were then transformed into siRNAs by the plant RNAi system. However, there was no significant differences in the gene expression levels of the target gene *FgCNG5* at 4 and 14 dpi between the transgenic line T51 and the WT. The possible explanation is that *FgCNG5*-specific siRNAs were not sufficiently produced, or were ineffective at silencing the gene, or were not absorbed by the pathogen at all. As a result, there was no significant differences based on the disease severity, fungal biomass, and DON measurements between the WT and T51.

The precise siRNA sequence and concentration produced by the transgenic plant, affects how effectively it silences the target gene (Baldwin et al., 2018). The length of the siRNAs that mapped with *FgGCN5* specificity were varied, with 21 nt being the most redundant; however, only a small fraction was produced between 0.06-0.08%. Wang et al. (2020) showed that two independent transgenic wheat plants with *FgSGE1-STE12-PP1*-RNAi construct expressed greater amounts of siRNA to knock down three critical genes in *F.graminearum* upon infection: a regulator gene for DON biosynthesis (*FgSGE1*), a transcription factor gene for penetration structure formation (*STE12*), and a phosphatase gene (*PP1*). The derived target-specific small RNAs attained up to 1.38 - 3.90% of total small RNAs, resulting in an increase in FHB resistance and a decrease in DON biosynthesis. In addition, transgenic banana lines containing separate vector constructs producing *ERG6*-siRNAs and *ERG11*-siRNAs exhibited suppressed ergosterol biosynthesis, and the produced target-specific siRNAs were approximately 2.02-2.38% and 3.35-5.22 of the total sRNA, respectively. The *ERG11*-RNAi construct generated more siRNAs than *ERG6*-RNAi because of the presence of multiple copies of T-DNA insertions. Nonetheless, both mutant banana lines demonstrated increased resistance to fusarium wilt disease (Dou et al., 2020). In comparison with these positive precedents, the amount of *FgGCN5*-siRNA produced in the T51 line were deemed negligible, and therefore an even smaller amount of *FgGCN5*-siRNA were delivered to the pathogen. Consequently, the severity of the disease and other indicators were not significantly affected.

Although the mutation of *FgSCN5*-deletion displayed negative effects on pathogen virulence, pathogenicity, and DON contents (Kong et al., 2018), some undesirable effects can be trigged by HIGS of *FgGCN5*. Cheng et al. (2015) demonstrated that different RNAi constructs targeting the *Chs3b* gene in *F.graminearum* transgenic strains had varying silencing efficacy

under the same genetic background. Furthermore, the strain carrying the Chs3bRNAi-4 construct had higher virulence and chitin content than the WT, possibly as a result of compensation for the down-regulation of this *Chs3b* gene by the other eight *Chs* gene members (Chen et al., 2015). Although these mutation effects were caused by the stable transformation in *F.graminearum*, it could be the same if HIGS was used to target the same gene (Chen et al., 2015). Therefore, the slight increase in the disease severity and DON contents present in the transgenic line T51 could be due to the gene compensation by other HATs genes in *F.graminearum*. Alternatively, the transgenic line was less resilient to diseases due to the possible regeneration-induced mutations during tissue culture for barley transformation.

Based on the exogenous application of dsRNA to silence *CYP51* of *F. graminearum*, this necrotrophic fungal pathogen responds more efficiently to dsRNA than to siRNA, and thus spray-induced gene silencing (SIGS) was more powerful than HIGS in suppression of the *F. graminearum* infection (Koch et al., 2019). SIGS was found to be 50% and 30% in more effective in the controlling of two tomato pests *Tuta absoluta* (leaf miner) and *Tetranychus urticae* (two-spotted spider mite) than HIGS (Camargo et al., 2016; Suzuki et al., 2017). However, both strategies, HIGS and SIGS, achieved similar effects when they were used to control the biotrophic fungal pathogen of Asian soybean rust, *Phakopsora pachyrhizi* (Hu et al., 2020). Therefore, the effect of HIGS-trigged disease restriction is associated with lifestyle and feeding behavior of the pathogen.

To conclude, we investigated the effect of HIGS targeting *FgGCN5* in barley for FHB resistance. Despite the production of the *FgGCN5*-siRNA, there was no significant silencing effect in the target gene, and the transgenic line T51 did not show the improved resistance according to the analysis of disease severity, DON accumulation, and fungal biomass. I admit

that the HIGS effect may be biased because only one transgenic line was used in this study. More independent transgenic lines will be included in the follow-up study to identify if higher number of *FgSCN5*- specific siRNAs are produced in other lines. Spray-induced gene silencing (SIGS) will also be used to determine the efficacy of delivering dsRNA for silencing *FgGCN5*. Therefore, additional efforts are needed to systematically characterize the effect of HIGS targeting *FgGCN5* on barley FHB resistance.

Literature Cited

Baldwin, T., Islamovic, E., Klos, K., Schwartz, P., Gillespie, J., Hunter, S., and Bregitzer, P. (2018). Silencing efficiency of dsRNA fragments targeting *Fusarium graminearum TRI6* and patterns of small interfering RNA associated with reduced virulence and mycotoxin production. *PLoS One* 13**,** e0202798.

Baldwin. T., Baldwin. S. A., Kress. E., Mndolwa. E,. Klos. K. E., Marshall. J., Bregitzer. P. (unpublished 2020). A dip inoculation protocol for measuring resistance 3 to deoxynivalenol accumulation in barley. Unpublished manuscript.

Bartlett, J.G., Alves, S.C., Smedley, M., Snape, J.W., and Harwood, W.A. (2008). High-throughput *Agrobacterium*-mediated barley transformation. *Plant Methods* 4**,** 22.

Brownell, J.E., Zhou, J., Ranalli, T., Kobayashi, R., Edmondson, D.G., Roth, S.Y., and Allis, C.D. (1996). Tetrahymena histone acetyltransferase A: a homolog to yeast Gcn5p linking histone acetylation to gene activation. *Cell* 84**,** 843-851.

Cai, Q., Qiao, L., Wang, M., He, B., Lin, F. M., Palmquist, J., Huang, S. D., and Jin, H. (2018). Plants send small RNAs in extracellular vesicles to fungal pathogen to silence virulence genes. Science (New York, N.Y.), 360(6393), 1126–1129.

Cainong J.C., Bockus W.W., Feng Y., Chen P., Qi L., Sehgal S.K., Danilova T.V., Koo D.H., Friebe B., Gill B.S. Chromosome engineering, mapping, and transferring of resistance to Fusarium head blight disease from Elymus tsukushiensis into wheat. Appl. Genet. 2015;128:1019–1027. doi: 10.1007/s00122-015-2485-1.

Camargo RA, Barbosa GO, Possignolo IP, Peres LEP, Lam E, Lima JE, Figueira A, Marques-Souza H. (2016). RNA interference as a gene silencing tool to control *Tuta absoluta* in tomato (*Solanum lycopersicum*). *PeerJ*. doi:10.7717/peerj.2673.

Chang, S. S., Zhang, Z., and Liu, Y. (2012). RNA Interference Pathways in Fungi: Mechanisms and Functions. Annual Review of Microbiology, 66(1), 305–323. https://doi.org/10.1146/annurev-micro-092611-150138

Chen, W., Kastner, C., Nowara, D., Oliveira-Garcia, E., Rutten, T., Zhao, Y., Deising, H. B., Kumlehn, J., and Schweizer, P. (2016). Host-induced silencing of Fusarium culmorumgenes protects wheat from infection. Journal of Experimental Botany, 67(17), 4979–4991.

Cheng, W., Song, X. S., Li, H. P., Cao, L. H., Sun, K., Qiu, X. L., Xu, Y. B., Yang, P., Huang, T., Zhang, J. B., Qu, B., and Liao, Y. C. (2015). Host-induced gene silencing of an essential chitin synthase gene confers durable resistance to Fusarium head blight and seedling blight in wheat. Plant Biotechnology Journal, 13(9), 1335–1345.

Cuthbert P.A., Somers D.J., Brulé-Babel A. (2007). Mapping of Fhb2 on chromosome 6BS: A gene controlling Fusarium head blight field resistance in bread wheat (Triticum aestivum L.) Theor. Appl. Genet. 114:429–437. doi: 10.1007/s00122-006-0439-3.

Cuthbert P.A., Somers D.J., Thomas J., Cloutier S., Brule-Babel A. (2006). Fine mapping Fhb1, a major gene controlling fusarium head blight resistance in bread wheat (Triticum aestivum L.) Appl. Genet. 112:1465–1472. doi: 10.1007/s00122-006-0249-7

Dou, T., Shao, X., Hu, C., Liu, S., Sheng, O., Bi, F., ... and Yi, G. (2020). Host-induced gene silencing of Foc TR4 ERG6/11 genes exhibits superior resistance to Fusarium wilt of banana. Plant biotechnology journal, 18(1), 11.

Evans, C. K., Xie, W., Dill-Macky, R., and Mirocha, C. J. (2000). Biosynthesis of deoxynivalenol in spikelets of barley inoculated with macroconidia of Fusarium graminearum. *Plant Disease*, *84*(6), 654-660.

Harwood, W.A. (2014). A protocol for high-throughput *Agrobacterium*-mediated barley transformation. *Methods Mol Biol* 1099**,** 251-260.

Hu D, Chen ZY, Zhang C, Ganiger M. (2020). Reduction of *Phakopsora pachyrhizi* infection on soybean through host- and spray-induced gene silencing. *Molecular Plant Pathology* 21: 794–807.

Jeon, J., Kwon, S., and Lee, Y.H. (2014). Histone acetylation in fungal pathogens of plants. *Plant Pathol J* 30**,** 1-9.

Koch A, Höfle L, Werner BT, Imani J, Schmidt A, Jelonek L, Kogel KH. (2019). SIGS vs HIGS: a study on the efficacy of two dsRNA delivery strategies to silence Fusarium FgCYP51 genes in infected host and non-host plants. Molecular Plant Pathology 20: 1636–1644.

Koch, A., Kumar, N., Weber, L., Keller, H., Imani, J., and Kogel, K. H. (2013). Host-induced gene silencing of cytochrome P450 lanosterol C14α-demethylase–encoding genes confers strong resistance to Fusarium species. Proceedings of the National Academy of Sciences, 110(48), 19324–19329.

Kong, X., Van Diepeningen, A.D., Van Der Lee, T.a.J., Waalwijk, C., Xu, J., Xu, J., Zhang, H., Chen, W., and Feng, J. (2018). The *Fusarium graminearum* histone acetyltransferases are Important for morphogenesis, DON biosynthesis, and pathogenicity. *Front Microbiol* 9**,** 654.

Livak, K. J., and Schmittgen, T. D. (2001). Analysis of relative gene expression data using real-time quantitative PCR and the $2^{-\Delta\Delta CT}$ method. methods, 25(4), 402-408.

Machado, A. K., Brown, N. A., Urban, M., Kanyuka, K., and Hammond-Kosack, K. E. (2017). RNAi as an emerging approach to control Fusarium head blight disease and mycotoxin contamination in cereals. Pest Management Science, 74(4), 790–799.

Mann, D.G., Lafayette, P.R., Abercrombie, L.L., King, Z.R., Mazarei, M., Halter, M.C., Poovaiah, C.R., Baxter, H., Shen, H., Dixon, R.A., Parrott, W.A., and Neal Stewart, C., Jr. (2012). Gateway-compatible vectors for high-throughput gene functional analysis in switchgrass (*Panicum virgatum* L.) and other monocot species. *Plant Biotechnol J* 10**,** 226-236.

McMullen, M., Jones, R., and Gallenberg, D. (1997). Scab of wheat and barley: a re-emerging disease of devastating impact. Plant Dis. 81, 1340–1348. doi: 10.1094/PDIS.1997.81.12.1340

Mutlu, B., and Puigserver, P. (2021). GCN5 acetyltransferase in cellular energetic and metabolic processes. *Biochim Biophys Acta Gene Regul Mech* 1864**,** 194626.

Qi L.L., Pumphrey M.O., Friebe B., Chen P.D., Gill B.S. (2008). Molecular cytogenetic characterization of alien introgressions with gene Fhb3 for resistance to Fusarium head blight disease of wheat. Appl. Genet. 117:1155–1166. doi: 10.1007/s00122-008-0853-9.

Qi, T., Guo, J., Peng, H., Liu, P., Kang, Z., and Guo, J. (2019). Host-Induced Gene Silencing: A Powerful Strategy to Control Diseases of Wheat and Barley. International Journal of Molecular Sciences, 20(1), 206.

Qi, T., Guo, J., Peng, H., Liu, P., Kang, Z., and Guo, J. (2019). Host-induced gene silencing: a powerful strategy to control diseases of wheat and barley. *Int J Mol Sci* 20.

Schwarz, P.B. (2017). Fusarium head blight and deoxynivalenol in malting and brewing: successes and future challenges. Trop. plant pathol. 42, 153–164.

Strahl, B.D., and Allis, C.D. (2000). The language of covalent histone modifications. *Nature* 403**,** 41-45.

Suzuki, T., Nunes, M. A., España, M. U., Namin, H. H., Jin, P., Bensoussan, N., ... and Grbic, M. (2017). RNAi-based reverse genetics in the chelicerate model Tetranychus urticae: A comparative analysis of five methods for gene silencing. *PLoS One*, *12*(7), e0180654.

Tinoco, M. L. P., Dias, B., Dall'Astta, R. C., Pamphile, J. A., and Aragão, F. J. (2010). In vivo trans-specific gene silencing in fungal cells by in planta expression of a double-stranded RNA. BMC biology, 8(1), 1-11.

Verdone, L., Caserta, M., and Di Mauro, E. (2005). Role of histone acetylation in the control of gene expression. *Biochem Cell Biol* 83**,** 344-353.

Wang, H., Sun, S., Ge, W., Zhao, L., Hou, B., Wang, K., ... and Kong, L. (2020). Horizontal gene transfer of Fhb7 from fungus underlies Fusarium head blight resistance in wheat. *Science*, *368*(6493), eaba5435.

Wang, M., Wu, L., Mei, Y., Zhao, Y., Ma, Z., Zhang, X., and Chen, Y. (2020). Host-induced gene silencing of multiple genes of Fusarium graminearum enhances resistance to Fusarium head blight in wheat. Plant Biotechnology Journal, 18(12), 2373.

Wegulo, S. N., Baenziger, P. S., Hernandez Nopsa, J., Bockus, W. W., and Hallen-Adams, H. (2015). Management of Fusarium head blight of wheat and barley. Crop Protection, 73, 100–107.

Xue, S., Li, G., Jia, H., Xu, F., Lin, F., Tang, M., ... and Ma, Z. (2010). Fine mapping Fhb4, a major QTL conditioning resistance to Fusarium infection in bread wheat (Triticum aestivum L.). *Theoretical and Applied Genetics*, *121*(1), 147-156.

Xue, S., Xu, F., Tang, M., Zhou, Y., Li, G., An, X., ... and Ma, Z. (2011). Precise mapping Fhb5, a major QTL conditioning resistance to Fusarium infection in bread wheat (Triticum aestivum L.). *Theoretical and applied genetics*, *123*(6), 1055-1063.

Xue-Franzen, Y., Henriksson, J., Burglin, T.R., and Wright, A.P. (2013). Distinct roles of the Gcn5 histone acetyltransferase revealed during transient stress-induced reprogramming of the genome. *BMC Genomics* 14**,** 479.

APPENDIX A: CHAPTER 2 SUPPLEMENTARY MATERIALS

Table A1. The average seedling disease scores for the CI97_CI92 population with the *Ptm* 13IM8.3 isolate using a 1-5 rating scale.

RIL #	Average score
CI97_CI92-1	2.4
CI97_CI92-2	2.4
CI97_CI92-3	2.8
CI97_CI92-4	2.4
CI97_CI92-5	2.1
CI97_CI92-6	2.3
CI97_CI92-7	2.2
CI97_CI92-8	2.2
CI97_CI92-9	3.2
CI97_CI92-10	2.2
CI97_CI92-11	2.2
CI97_CI92-12	2.5
CI97_CI92-13	3
CI97_CI92-14	3.9
CI97_CI92-15	2.4
CI97_CI92-16	2.3
CI97_CI92-17	2.2
CI97_CI92-18	2.6
CI97_CI92-19	2
CI97_CI92-20	2.7
CI97_CI92-21	2
CI97_CI92-22	3
CI97_CI92-23	2.7
CI97_CI92-24	1.5
CI97_CI92-25	2.3
CI97_CI92-26	2.8
CI97_CI92-27	2
CI97_CI92-28	2
CI97_CI92-29	2.7
CI97_CI92-30	1.9
CI97_CI92-31	1.7
CI97_CI92-32	2.4
CI97_CI92-33	2
CI97_CI92-34	2.7

Table A1. The average seedling disease scores for the CI97_CI92 population with the *Ptm* 13IM8.3 isolate using a 1-5 rating scale (Continued).

RIL #	Average score
CI97_CI92-35	1.7
CI97_CI92-36	3
CI97_CI92-37	3.6
CI97_CI92-38	2.4
CI97_CI92-39	2.1
CI97_CI92-40	2.3
CI97_CI92-41	2.3
CI97_CI92-42	2.5
CI97_CI92-43	2.6
CI97_CI92-44	2
CI97_CI92-45	2.4
CI97_CI92-46	2.8
CI97_CI92-47	2.3
CI97_CI92-48	3.1
CI97_CI92-49	2.1
CI97_CI92-50	2.3
CI97_CI92-51	1.9
CI97_CI92-52	2.7
CI97_CI92-53	1.8
CI97_CI92-54	2.3
CI97_CI92-55	2.3
CI97_CI92-56	2.7
CI97_CI92-57	3.8
CI97_CI92-58	2.7
CI97_CI92-59	2.2
CI97_CI92-60	1.7
CI97_CI92-61	2.4
CI97_CI92-62	2.2
CI97_CI92-63	2.3
CI97_CI92-64	2.8
CI97_CI92-65	3.5
CI97_CI92-66	2.9
CI97_CI92-67	2.5
CI97_CI92-68	2.8
CI97_CI92-69	3.6
CI97_CI92-70	2.7

Table A1. The average seedling disease scores for the CI97_CI92 population with the *Ptm* 13IM8.3 isolate using a 1-5 rating scale (Continued).

RIL #	Average score
CI97_CI92-71	3.8
CI97_CI92-72	3.1
CI97_CI92-73	2
CI97_CI92-73	2
CI97_CI92-74	2.5
CI97_CI92-75	2
CI97_CI92-76	2.8
CI97_CI92-77	2.8
CI97_CI92-78	3.8
CI97_CI92-79	2.9
CI97_CI92-80	3
CI97_CI92-81	2.6
CI97_CI92-82	2.6
CI97_CI92-83	2.4
CI97_CI92-84	1.6
CI97_CI92-85	2.5
CI97_CI92-86	2.5
CI97_CI92-87	2.8
CI97_CI92-88	1.3
CI97_CI92-89	2.8
CI97_CI92-90	1.8
CI97_CI92-91	3
CI97_CI92-92	2.3
CI97_CI92-93	1.5
CI97_CI92-94	2.3
CI97_CI92-95	2.4
CI97_CI92-96	2.8
CI97_CI92-97	2
CI97_CI92-98	2.7
CI97_CI92-99	2.6
CI97_CI92-100	2.8
CI97_CI92-101	1.5
CI97_CI92-102	1.8
CI97_CI92-103	2.5
CI97_CI92-104	2.9
CI97_CI92-105	2.9

Table A 1. The average seedling disease scores for the CI97_CI92 population with the *Ptm* 13IM8.3 isolate using a 1-5 rating scale (Continued).

RIL #	Average score
CI97_CI92-106	2.9
CI97_CI92-107	2.7
CI97_CI92-108	2.5
CI97_CI92-109	2.1
CI97_CI92-110	2.5
CI97_CI92-111	2.8
CI97_CI92-112	1.7
CI97_CI92-113	2.2
CI97_CI92-114	2.2
CI97_CI92-115	2.9
CI97_CI92-116	3
CI97_CI92-117	1.8
CI97_CI92-118	2.3
CI97_CI92-119	2.8
CI97_CI92-120	2.4
CI97_CI92-121	3.3
CI97_CI92-122	2.7
CI97_CI92-123	2
CI97_CI92-124	2.4
CI97_CI92-125	3.1
CI97_CI92-126	2.4
CI97_CI92-127	1.5
CI97_CI92-128	2.6
CI97_CI92-129	2.5
CI97_CI92-130	3.1
CI97_CI92-131	2.3
CI97_CI92-132	2.3
CI97_CI92-133	1.8
CI97_CI92-134	2.9
CI97_CI92-135	1.9
CI97_CI92-136	2
CI97_CI92-137	2.4
CI97_CI92-138	1.9
CI97_CI92-139	2.8
CI97_CI92-140	2.6
CI97_CI92-141	2.8

Table A1. The average seedling disease scores for the CI97_CI92 population with the *Ptm* 13IM8.3 isolate using a 1-5 rating scale (Continued).

RIL #	Average score
CI97_CI92-142	2.4
CI97_CI92-143	2

Table A2. The average seedling disease scores for the CT population with the *Ptm* 13IM8.3 isolate using a 1-5 rating scale.

RIL #	Average score
CT-1	2.9
CT-2	1.4
CT-3	2.3
CT-4	2.4
CT-5	3
CT-6	1.6
CT-7	1.8
CT-8	2.6
CT-9	2.3
CT-10	1.6
CT-11	1.4
CT-12	2.1
CT-13	2.7
CT-14	1.5
CT-15	1.5
CT-16	2.2
CT-17	2.3
CT-18	1.9
CT-19	1.3
CT-20	1.4
CT-21	1
CT-22	2.3
CT-23	1.4
CT-24	2.2
CT-25	2.3
CT-26	2.3
CT-27	2
CT-28	2.1

Table A2. The average seedling disease scores for the CT population with the *Ptm* 13IM8.3 isolate using a 1-5 rating scale (Continued).

RIL #	Average score
CT-29	1
CT-30	2
CT-31	1.4
CT-32	2.3
CT-33	2
CT-34	2.8
CT-35	1.5
CT-36	1.7
CT-37	1.2
CT-38	1.9
CT-39	2.7
CT-40	2.6
CT-41	2.8
CT-42	1.6
CT-43	2.1
CT-44	2.3
CT-45	1.5
CT-46	2
CT-47	2.5
CT-48	2
CT-49	2.5
CT-50	2.2
CT-51	2.1
CT-52	2.1
CT-53	1.1
CT-54	1
CT-55	3.1
CT-56	2.5
CT-57	1.9
CT-58	1.1
CT-59	1.6
CT-60	1.8
CT-61	1.3
CT-62	2
CT-63	2.4

Table A2. The average seedling disease scores for the CT population with the *Ptm* 13IM8.3 isolate using a 1-5 rating scale (Continued).

RIL #	Average score
CT-64	2.3
CT-65	2.9
CT-66	2
CT-67	1.6
CT-68	1.8
CT-69	1.3
CT-70	2.1
CT-71	1.4
CT-72	1.7
CT-73	3.1
CT-74	1.1
CT-75	1.3
CT-76	1.8
CT-77	1.9
CT-78	2.3
CT-79	2.5
CT-80	1.3
CT-81	2.6
CT-82	1.2
CT-83	1.9
CT-84	1.9
CT-85	1.3
CT-86	1.7
CT-87	2.6
CT-88	2.8
CT-89	2.1
CT-90	2.5
CT-91	2.1
CT-92	1.5
CT-93	1.4
CT-94	1.8
CT-95	1.6
CT-96	2.3
CT-97	1.3
CT-98	1.6

Table A2. The average seedling disease scores for the CT population with the Ptm 13IM8.3 isolate using a 1-5 rating scale (Continued).

RIL #	Average score
CT-99	1
CT-100	1.8
CT-101	1.8
CT-102	2.5
CT-103	2.9
CT-104	1.1
CT-105	1.4
CT-106	2.6
CT-107	2.2
CT-108	1.7
CT-109	1.2
CT-110	1.1
CT-111	2.4
CT-112	2.5
CT-113	1.8
CT-114	1.4
CT-115	2.1
CT-116	1.4
CT-117	1.1

Table A3. Summary of seven genetic linkage groups for the CI97_CI92 population.

Chromosome	No. of markers	Length (cM)	Marker density (cM/locus)
1H	217	122.7	0.57
2H	263	144.47	0.55
3H	280	143.38	0.51
4H	223	107.18	0.48
5H	300	154.87	0.52
6H	221	110.23	0.50
7H	246	137.7	0.56
Total	1750	920.53	0.53

Table A4. Summary of seven genetic linkage groups for the CT population described by Koladia et al., (2017).

Chromosome	No. of markers	Length (cM)	Marker density (cM/locus)
1H	90	133.5	1.5
2H	143	161.2	1.1
3H	122	156.7	1.3
4H	91	115.3	1.3
5H	146	184.6	1.3
6H	103	113.6	1.1
7H	132	147.3	1.1
Total	827	1012.2	1.2

Table A5. QTL detected in the CI97_CI92 population.

QTLs	Ch	SNPs[a]	Physical position (bp)[b]	Support interval (cM)	LOD value	R^2 (%)	Additive effect[c]	QTL donor	Infrared Locus[d]
QRptm-1H-108-122	1H	JHI-Hv50k-2016-55796	516668348	108-122	5.556	16.4	0.2	CI9776	*QRptms1* (Grewal et al., 2012), *Qns-1H QTL* (Daba et al., 2019)
		SCRI_RS_165434	517300519						
		SCRI_RS_175218	520656756						
QRptm-3H-45-52	3H	BOPA1_10126_999	446718447	45-52	6.97	20.1	0.15	CI9214	*QTL_Tamang_3H_65.16* (Tamang et al., 2015), *QRptms3-2* (Wang et al., 2015), *Qns-3H.2* (Duba et al., 2019), *SFNB-3H-58.64* (Burlakoti et al., 2017), *QRptm-3H-56-65* (Tamang et al., 2019)
		SCRI_RS_152172	447867326						
		SCRI_RS_222102	476003071						
QRptm-4H-43-57	4H	SCRI_RS_188822	87623430	43-57	12.65	33.5	0.21	CI9776	*Rpt7* (Williams et al., 2003), *QRpts4* (Grewal et al., 2008), *QTL_Tamang_4H_47.17* (Tamang et al., 2015), *QTL_Tamang_4H_53.67-59.22* (Tamang et al., 2019)
		BOPA1_3193-671	396185414						
		SCRI_RS_10607	457888731						
QRptm-4H-93-109	4H	JHI-Hv50k-2016-268933	609391481	93-109	14.24	36.8	0.23	CI9776	*Rpt8* (Franckowiak and Platz 2013), *QRptm-4H-58-64* (Tamang et al., 2019), *QTL_Friesen/Rpt8* (Friesen et al., 2006), *QRptm4-2* (Wang et al., 2015), *QRpts4* (Grewal et al., 2008), *Qns-4H.2* (Daba et al., 2019)
		SCRI_RS_151357	615823408						
		JHI-Hv50k-2016-272270	616555836						
QRptm-5H-12-21	5H	JHI-Hv50k-2016-278862	4663752	12-21	4.478	13.4	0.12	CI9214	*Rpt6* (Manninen et al., 2006)
		JHI-Hv50k-2016-280523	6916305						
		JHI-Hv50k-2016-281470	9353471						
QRptm-7H-96-107	7H	JHI-Hv50k-2016-500801	597294111	96-107	7.174	20.6	0.15	CI9776	*Rpt4* (Williams et al., 1999, 2003), *QRpt7* (Grewal et al., 2008, Tamang et al., 2015), *QTL_Tamang_7H_133.84* (Tamang et al., 2015), *QRptm-7H-119-137* (Tamang et al., 2019), *QRptm7-6* (Wang et al., 2015)
		JHI-Hv50k-2016-501312	598670417						
		SCRI_RS_130990	602198212						

[a] SNPs flanking the QTL interval and the peak SNP in between were listed for marker development and position determination.
[b] Physical position of linked SNPs were based on the Morex genome assembly V3.
[c] Additive effect was used to represent QTL effect size.
[d] Infrared locus was probably reported previously.

Table A6. QTL detected in the CT population.

QTLs	Ch	SNPs[a]	Physical position (bp)[b]	Support interval (cM)	LOD value	R^2 (%)	Additive effect[c]	QTL donor	Infrared Locus[d]
QRptm-4H-4-8 (Allelic to *QRptm-4H-93-109*)	4H	SCRI_RS_235762	624215195	4-8	31.95	71.64	0.4	CI5791	*QTL_Tamang_4H_117.13* (Tamang et al., 2015), *QRptm-4H-120-125* (Tamang et al., 2019), *QRptm-4H-58-64* (Tamang et al., 2019)
		SCRI_RS_188829	616364353						
		SCRI_RS_216855	612295812						
QRptm-5H-81-88	5H	SCRI_RS_231239	519318035	81-88	5.38	19.1	0.12	Tifang	Novel
		SCRI_RS_106306	516074168						
QRptm-6H-60-64	6H	SCRI_RS_88710	514858623	60-64	7.36	25.1	0.15	Tifang	*QTL_Tamang* (Tamang et al., 2015), *QRptm-6H-55-64* (Tamang et al., 2019), *QRpt6* (Grewal et al., 2008)
		SCRI_RS_5787	481349544						
		SCRI_RS_209210	483149579						
		SCRI_RS_217187	522956072						
QRptm-7H-34-38 (Allelic to *QRptm-7H-96-107*)	7H	SCRI_RS_1383	607325324	34-38	8.24	28.8	0.16	CI5791	*Rpt4* (Williams et al., 1999, 2003), *QRpt7* (Grewal et al., 2008, Tamang et al., 2015), *QTL_Tamang_7H_133.84* (Tamang et al., 2015), *QRptm-7H-119-137* (Tamang et al., 2019), *QRptm7-6* (Wang et al., 2015),
		SCRI_RS_146324	605845045						
			604624987						
		SCRI_RS_152144							

[a] SNPs flanking the QTL interval and the peak SNP in between were listed for marker development and position determination.
[b] Physical position of linked SNPs were based on the Morex genome assembly V3.
[c] Additive effect was used to represent QTL effect size.
[d] Infrared locus was probably reported previously.

Table A7. Primer sequences designed for the STARP markers linked to QTL identified in the present study.

Marker name	CH	Population	Forward primer 1	Forward primer 2	Revers primer
SCRI_RS_165434	1H	CI97_CI92	GCAACAGGAACCAGCT-ATGACATTTGCAGGATCAACAACTC	GACGCAAGTGAGCAGTATGACATTTGCAGGATCAACAGTTT	CCAGGTCAACATGGCATTTGG
SCRI_RS_152172	3H	CI97_CI92	GACGCAAGTGAGCAGTATGACTGCCACACGTGCTCA	GCAACAGGAACCAGCTATGACTGCCACACGTGACCG	TCCGGTCACAATTTAGGATGACC
BOPA1_3193-671	4H	CI97_CI92	GACGCAAGTGAGCAGTATGACATGCAACTGCTCCAGCCTT	GCAACAGGAACCAGCTATGACATGCAACT-GCTCCAGACCC	TGCACATAGCAGCAGCTGT
SCRI_RS_151357	4H	CI97_CI92	GACGCAAGTGAGCAGTATGACATTTGCAATACTTAATCTTCATTCT	GCAACAGGAACCAGCTATGACATTTGCAATACTTAATCTTCATCT-G	AGAAGCTCACCGATGTCTACG
JHI-Hv50k-2016-280523	5H	CI97_CI92	GACGCAAGTGAGCAGTATGACATCAACTGACATGTATCACATGCTT	GCAACAGGAACCAGCTATGACATCAACTGACATGTATCACATGTCC	AGATGTTCCCAACGTCGTATGG
JHI-Hv50k-2016-501312	7H	CI97_CI92	GCAACAGGAACCAGCTATGACACAGTCAAGGAGAAGATTACCT	GACGCAAGTGAGCAGTATGACACAGTCAAGGAGAAGATTCACA	GCACATCTTGCGCATGTTCC
SCRI_RS_188829	4H	CT	GCAACAGGAACCAGCTATGACGACAATTAGACGCGAG	GACGCAAGTGAGCAGTATGACGACAATTAGACGCAGA	GTGTGCAACGCCCTGTTG
SCRI_RS_106306	5H	CT	GACGCAAGTGAGCAGTATGACGTAATAGAACCCGGAAGTAAATACCG	GCAACAGGAACCAGCTATGACGTAATAGAACCCGGAAGTAAATCACC	CGGCTACAGCCAATAGTTCTT
SCRI_RS_209210	6H	CT	GCAACAGGAACCAGCTATGACCAACATTTACATGGCACTC	GACGCAAGTGAGCAGTATGACCAACATTTACATGGCATCA	AGATACCGATTGTATGCTGCTGG
SCRI_RS_146324	7H	CT	GCAACAGGAACCAGCTATGACAATGGCGTCGAGAAACC	GACGCAAGTGAGCAGTATGACAATGGCGTCGAGAAGTG	TGCCACACCCGATGAATGATG

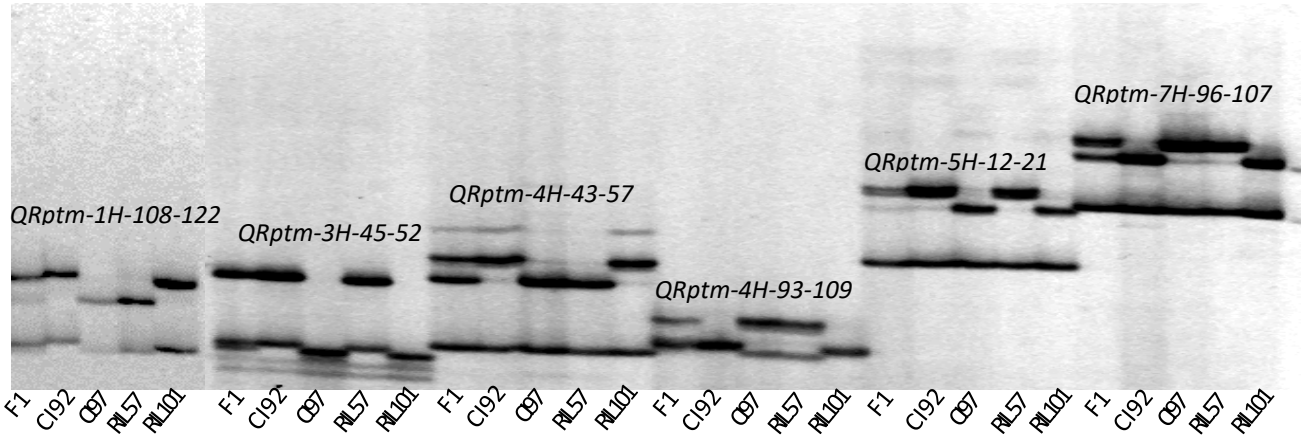

Figure A1. STARP markers designed based on the SNPs linked to QTL detected in the CI97_CI92 mapping population. RIL57 and RIL101 are susceptible and resistant RILs, respectively. F1, hybrid; CI92, CI9214; CI97, CI9776.

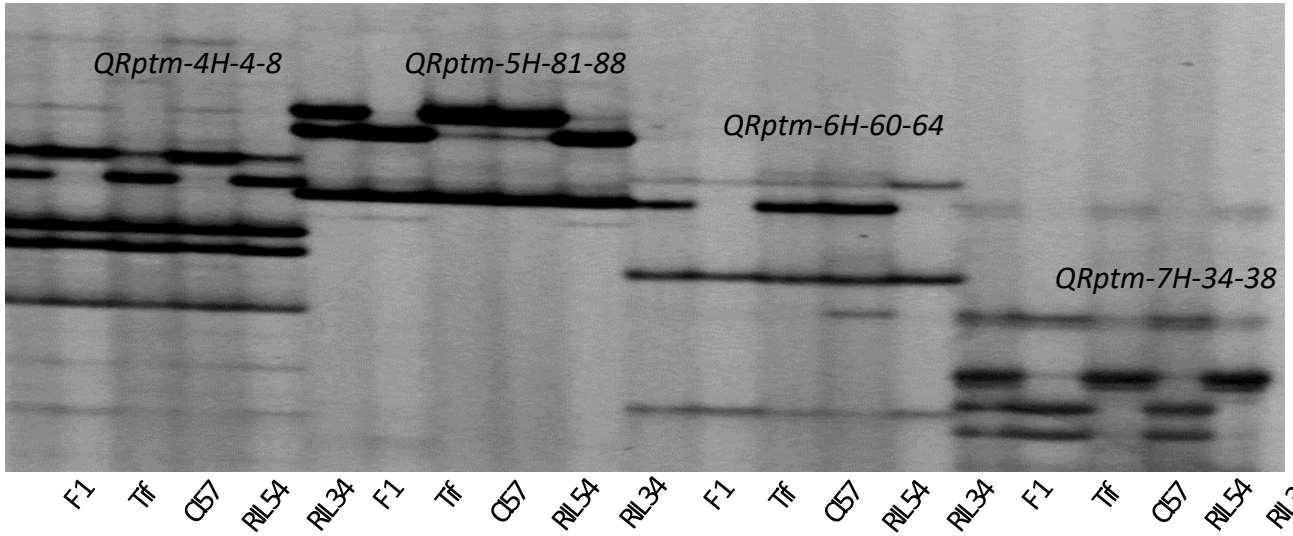

Figure A2. STARP markers designed based on the SNPs linked to QTL detect-ed in the CT mapping population. RIL54 and RIL34 are resistant and susceptible RILs, respectively. F1, hybrid; Tif, Tifang; CI57, CI5791.

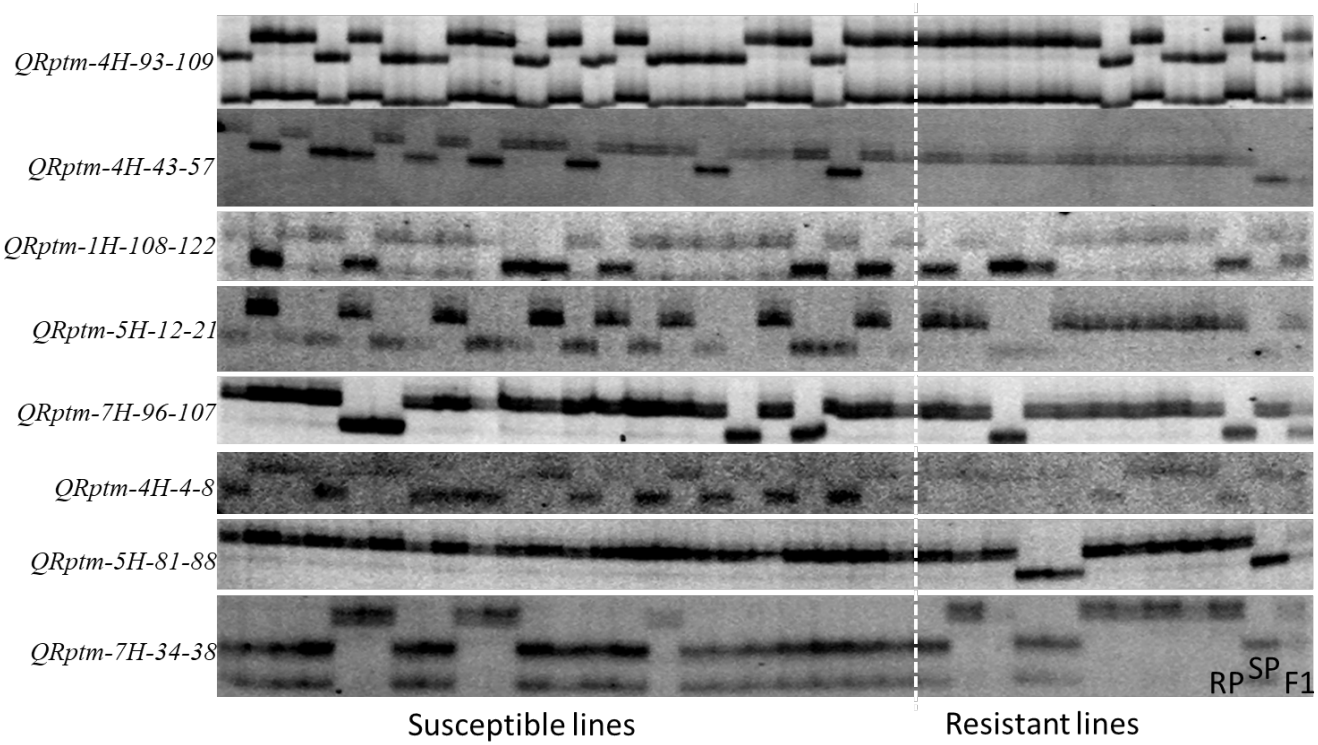

Figure A3. Genotyping survey of 31 differential lines with 8 peak markers. Lines on the left of the dashed were categories as susceptible, and they were loaded onto the gel in the following order (from left to right): Pinnacle, 81-82/033, Arimont, Chebec, Skiff, CI3576, CIho3694, Ciho4050, MXB468, PI269151, PI369731, PI392501 PI467375, PI467729, PI485524, PI498434, PI573662, TR250, TR326, Golden Promise, and Tradition. Ten resistant lines were arranged in the following order on the right of the dashed line (from left to right): Keel, Kombar, CI9819, CI7584, CI14219, CI2353, PI513205, PI565826, PI67381, PI84314. The last three lines are resistant parent (RP), susceptible parent (SP) and F1.

APPENDIX B: CHAPTER 3 SUPPLEMENTARY MATERIALS

Table B1. Markers used to select F_2s which carry heterozygous *Sptm1* on 7H but homozygous recessive alleles on 2H and 3H.

Marker	Chr	Type	Forward primer 1	Forward primer 2	Revers primer
11_21377	2H	STARP	GCAACAGGAACCAGCTATGACGCAAACT GGCCTTATGAGG	GACGCAAGTGAGCAGTATGACGCAAACT GGCCTTATAGGA	ACCACTACGCCAGTCCTTTG
12_30631	2H	STARP	GACGCAAGTGAGCAGTATGACCGCGTGA TCTTCTGAATTGTT	GCAACAGGAACCAGCTATGACCGCGTGA TCTTCTGAATCATC	TGATAGCGGGGAGAACTGGA
SCRI_RS_159340	3H	STARP	GCAACAGGAACCAGCTATGACGATTGGG ATCCAAAGTCGCC	GACGCAAGTGAGCAGTATGACGATTGGG ATCCAAAGTTACT	ACTGCAAAGTCATTGGTGGC
12_31018	3H	STARP	GCAACAGGAACCAGCTATGACCCAGACG CGTTCTTTTCC	GACGCAAGTGAGCAGTATGACCCAGACG CGTTCTCCTCT	CCGAAAACAGGCTTGCACTC
12_30368	7H	STARP	GCAACAGGAACCAGCTATGACATTTCCTC TCTCCTGATG	GACGCAAGTGAGCAGTATGACATTTCCTC TCTCCTAGTA	TCAAGTTTGGCACCGTCGA
11_11243	7H	STARP	GACGCAAGTGAGCAGTATGACTTCCTCGT TATAACTTCAGCGTA	GCAACAGGAACCAGCTATGACTTCCTCGT TATAACTTCAGAGCG	TGCAGATGATCCATCCGACA

Table B2. Markers used for genetic mapping of *Sptm1* in this study.

Marker ID	Source	Type	Forward primer 1	Forward primer 2	Revers primer
M24	JHI-Hv50k-2016-500174	STARP	GACGCAAGTGAGCAGTATGACCCCAAAGAGACATCTTCA	GCAACAGGAACCAGCTATGACCCCAAAGAGACATCCTTG	CCAGGCATGTGTTGCACA
M25	JHI-Hv50k-2016-500418	STARP	GACGCAAGTGAGCAGTATGACAAATGTGAAGTACCTGTCAGCCAA	GCAACAGGAACCAGCTATGACAAATGTGAAGTACCTGTCAGCTCT	CAGGTTCACAGTAGACCAAGGT
M27	JHI-Hv50k-2016-500744	STARP	GACGCAAGTGAGCAGTATGACTTCGTATCACTGATGGAACT	GCAACAGGAACCAGCTATGACTTCGTATCACTGATGGAGTG	GACAGTTTCGGTCTGCACA
M28	JHI-Hv50k-2016-500794	STARP	GACGCAAGTGAGCAGTATGACGCACTTGTTATTGCCTTTGT	GCAACAGGAACCAGCTATGACGCACTTGTTATTGCCTCTAG	TTGCATGGTACATGGGTAAACA
SSR3	Morex V3 genome	SSR	AACAACCACATACCGAAATC		AAGAAAAGATATCCTGCTGCT
M50	owbGBS37491	STARP	GCAACAGGAACCAGCTATGACTGAGAGAATGGTACGGAG	GACGCAAGTGAGCAGTATGACTGAGAGAATGGTACGAGT	TCAAACTTCATGCATGTCATGC
M57	3_HID_SNP1	STARP	GACGCAAGTGAGCAGTATGACCAGACAAGGTTTTGGAAAATAACTA	GCAACAGGAACCAGCTATGACCAGACAAGGTTTTGGAAAATAAACC	AAGAGATGCAGATCGGTACCT
M69	Schr7H_592631221	STARP	GCAACAGGAACCAGCTATGACAGTATCCACTACGATGAAGTG	GACGCAAGTGAGCAGTATGACAGTATCCACTACGATGAAACA	CACTTGTTACGGGGACAGAATC
M77	Schr7H_592807876	STARP	GACGCAAGTGAGCAGTATGACTTCCCTTTCCTTGCATCA	GCAACAGGAACCAGCTATGACTTCCCTTTCCTTGCACTG	CAGACGACTGGAGGTTCTGAT
k1	Kinase coding gene	STARP	GCAACAGGAACCAGCTATGACAGGCATTCGATTCAAGCAATCC	GACGCAAGTGAGCAGTATGACAGGCATTCGATTCAAGCAACAT	GCCGTGGAAACATGCCAT
M29	JHI-Hv50k-2016-501140	STARP	GACGCAAGTGAGCAGTATGACGCTAGAAGAACTTATTTTGAAATGT	GCAACAGGAACCAGCTATGACGCTAGAAGAACTTATTTTGAAGTAC	AACCGTCTGTGTGGCCAAT
M30	JHI-Hv50k-2016-501103	STARP	GACGCAAGTGAGCAGTATGACGCATAAGCATTGGCATGT	GCAACAGGAACCAGCTATGACGCATAAGCATTGGCGTAG	GGTTGACGACCAGTTGCTACT
M46	mbGBS19440	STARP	GCAACAGGAACCAGCTATGACTATGGACTAGAAATACTCTGCAGCG	GACGCAAGTGAGCAGTATGACTATGGACTAGAAATACTCTGCCGTA	CTGTCACGGACTGAATTGACCAT
M33	JHI-Hv50k-2016-501301	STARP	GACGCAAGTGAGCAGTATGACGTGGAACACGCTCAGCTA	GCAACAGGAACCAGCTATGACGTGGAACACGCTCAGTCG	TGCTTGCGAGAAAATCTAGAGTTG
12_30368	Barley 50K SNP chip	STARP	GCAACAGGAACCAGCTATGACATTTCCTCTCTCCTGATG	GACGCAAGTGAGCAGTATGACATTTCCTCTCTCCTAGTA	TCAAGTTTGGCACCGTCGA
SSR32	Morex V3 genome	SSR	ATCTGAAGCATGTGATGTGTA		AGCAGATGCTTTGTTAATTTG
M87	Schr7H_593037317	STARP	GACGCAAGTGAGCAGTATGACATTTATACCCACCAAAAATGTCCAA	GCAACAGGAACCAGCTATGACATTTATACCCACCAAAAATGTTCCG	TGAATGGCGATCAACTTCACATG

APPENDIX C: CHAPTER 4 SUPPLEMENTARY MATERIALS

Table C1. Mapping summary report for Small RNA targeting *FgGCN5* produced by T51 replicates.

Category	Line	Count	Percentage of reads (%)	Average length	Number of bases	Percentage of bases (%)
References	T51-1	1	-	385	385	-
Mapped reads		6,889	0.06	21.35	147,085	0.06
Not mapped reads		10,760,672	99.94	21.44	230,671,316	99.94
Total reads		10,767,561	100	21.44	230,818,401	100
References	T51-2	1	-	385	385	-
Mapped reads		4,330	0.03	21.6	93,521	0.03
Not mapped reads		13,319,495	99.97	22.9	304,995,160	99.97
Total reads		13,323,825	100	22.9	305,088,681	100
References	T51-3	1	-	385	385	-
Mapped reads		11,692	0.08	21.45	250,782	0.07
Not mapped reads		14,361,867	99.92	23.67	339,952,030	99.93
Total reads		14,373,559	100	23.67	340,202,812	100

Table C2. Mapping summary report for Small RNA produced by WT replicates.

Category	Line	Count	Percentage of reads (%)	Average length	Number of bases	Percentage of bases (%)
References		1	-	385	385	-
Mapped reads		1	0	27	27	0
Not mapped reads		12,377,346	100	18.94	234,424,527	100
Total reads	WT-1	12,377,347	100	18.94	234,424,554	100
References		1	-	385	385	-
Mapped reads		8	0	24.12	193	0
Not mapped reads		20,445,666	100	21.49	439,474,527	100
Total reads	WT-2	20,445,674	100	21.49	439,474,720	100
References		1	-	385	385	-
Mapped reads		7	0	24.14	169	0
Not mapped reads		15,559,013	100	27.47	427,361,773	100
Total reads	WT-3	15,559,020	100	27.47	427,361,942	100

Table C3. Results of small RNA sequencing for WT and T51 lines, total reads from three biological replicates.

Sample	Total reads	N% > 10%	Low quality	5_adapter contamine	3_adapter_null or insert_null	With ployA/T/G/C	Clean reads
WT_3	15892699 (100.00%)	256 (0.00%)	0 (0.00%)	67541 (0.42%)	240835 (1.52%)	25047 (0.16%)	15559020 (97.90%)
WT_1	12854811 (100.00%)	211 (0.00%)	0 (0.00%)	23443 (0.18%)	446506 (3.47%)	7304 (0.06%)	12377347 (96.29%)
WT_2	21121676 (100.00%)	15 (0.00%)	0 (0.00%)	85279 (0.40%)	579729 (2.74%)	10979 (0.05%)	20445674 (96.80%)
T51_3	14624830 (100.00%)	11 (0.00%)	0 (0.00%)	33005 (0.23%)	198483 (1.36%)	19772 (0.14%)	14373559 (98.28%)
T51_1	10952663 (100.00%)	0 (0.00%)	0 (0.00%)	23540 (0.21%)	147877 (1.35%)	13685 (0.12%)	10767561 (98.31%)
T51_2	13890683 (100.00%)	12 (0.00%)	0 (0.00%)	117646 (0.85%)	434225 (3.13%)	14975 (0.11%)	13323825 (95.92%)

Table C4. Small RNA sequencing quality reads for WT and T51 lines from three biological replicates.

Sample	Raw reads	Raw data(G)	Error(%)	Q20(%)	Q30(%)	GC(%)
WT_3	15892699	0.795	0.01	99.22	97.35	52.1
WT_1	12854811	0.643	0.01	99.31	97.76	51.93
WT_2	21121676	1.056	0.01	99.44	98.07	51.17
T51_3	14624830	0.731	0.01	98.87	96.92	52.1
T51_1	10952663	0.548	0.01	99.12	96.91	51.76
T51_2	13890683	0.695	0.01	99.44	98.13	51.93